Norfolk Vanguard Offshore Wind Farm

Stage 3 Geoarchaeological Sampling and Assessment

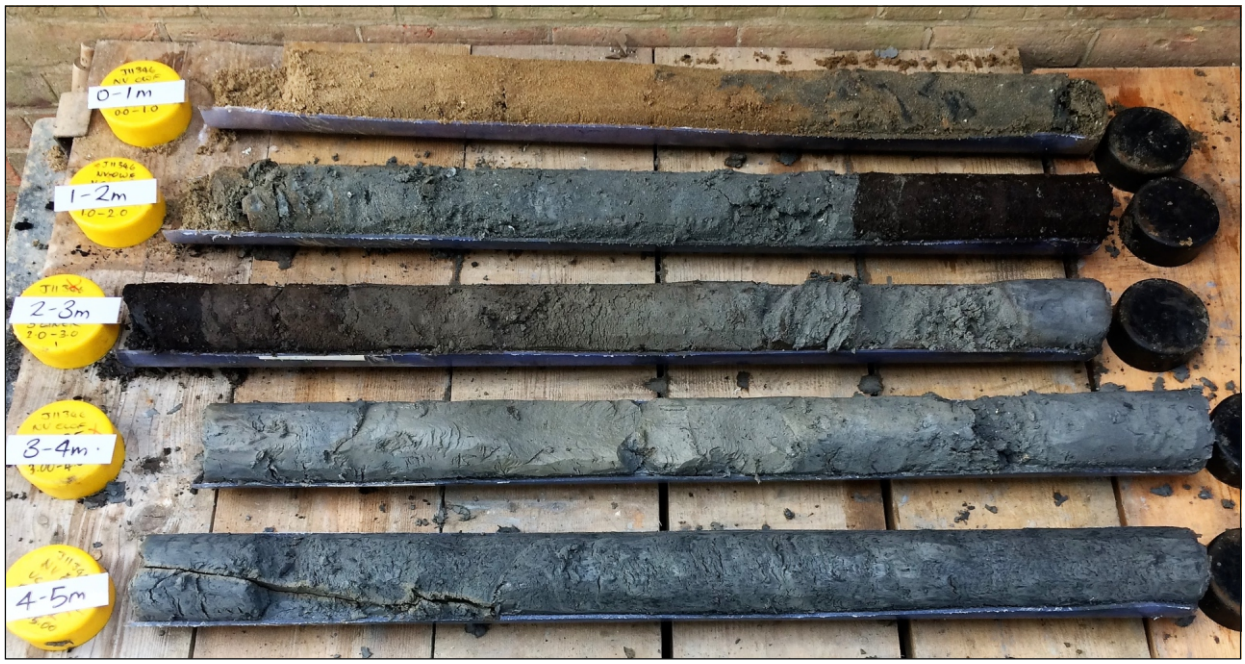

Ref: 114843.01
March 2018

wessexarchaeology

Portway House
Old Sarum Park
Salisbury
Wiltshire
SP4 6EB

www.wessexarch.co.uk

Wessex Archaeology Ltd is a Registered Charity no. 287786 (England & Wales) and SC042630 (Scotland)

Document Information

Document title	Norfolk Vanguard Offshore Wind Farm:
Document subtitle	Stage 3 Geoarchaeological Sampling and Assessment
Document reference	114843.01
Client name	Royal HaskoningDHV
Address	2 Abbey Gardens Great College Street, Westminster London SW1P 3NL
Site location	Southern North Sea
County	
National grid reference	
Statutory designations	
Planning authority	
Planning reference	
Museum name	
Museum accession code	
WA project code(s)	114843
Date(s) of fieldwork	
Fieldwork directed by	
Project management by	David Norcott
Document compiled by	Claire Mellett and Alexander Brown
Contributions from	
Graphics by	Nancy Dixon

Quality Assurance

Issue and date	Status	Author	Approved by
1	External draft	CLM & ADB	DRN
2	External draft	CLM	DRN

Contents

List of Figures

List of Tables

Summary

Wessex Archaeology (WA) were commissioned by Royal HaskoningDHV to undertake Stage 3 paleoenvironmental assessment of geotechnical vibrocores in support of the proposed Norfolk Vanguard Offshore Wind Farm development, located in the southern North Sea.

During Stage 2 geoarchaeological recording, three geological units were identified as having geoarchaeological potential: Upper Brown Bank Formation (**Unit 5**), comprising fine-grained sediments deposited in a shallow/intertidal lagoon during the early to late Devensian; wind-blown sands of the Twente Formation (**Unit 6**) corresponding to a time during the late Devensian when the southern North Sea was a periglacial terrestrial landscape; and early Holocene pre-transgression terrestrial peats and minerogenic deposits (**Unit 7**) that formed prior to post glacial sea-level rise.

Five vibrocores were subject to Stage 3 palaeoenvironment assessment (**VC074**, **VC076**, **VC079**, **VC085** and **VC107**). Deposits corresponding to Upper Brown Bank (**Unit 5**) were targeted in **VC079** and **VC107** for OSL dating and accompanying foraminifera, ostracod and diatom assessment to determine age and palaeoenvironment. To help confirm the presence or absence of Twente Formation (**Unit 6**), samples from **VC076** were targeted for particle size distribution analysis. Holocene pre-transgression peat deposits (**Unit 7**) in **VC074**, **VC076** and **VC085** were selected for radiocarbon dating as they showed the greatest potential for preservation of pollen and plant macrofossils which would provide information on landscape development. Diatoms, foraminifera and ostracod analysis was also undertaken on these cores across transitions between over/underlying minerogenic and organic sediments.

Brown Bank Formation (**Unit 5**) are the oldest deposits recovered in vibrocores. Six sub-samples (**VC074**, **VC079**, **VC085** and **VC107**) were submitted for OSL dating. Of these, three passed validity acceptance testing whereas three were considered tentative due to analytical behaviour. Accepted OSL results place deposition between 82.4 ± 8.5 ka and 57.2 ± 6.4 ka spanning Marine Isotope Stage (MIS) 5a to 3 (late Middle to Upper Palaeolithic). A rich and diverse assemblage of foraminifera and ostracods were preserved within Brown Bank sediments. Observed species are typical of marine embayment to outer estuarine environments suggesting Brown Bank across Norfolk Vanguard was deposited in a more open marine setting than previously thought. Several observed foraminifera and ostracod species are indicative of a subarctic climate. Diatoms were not preserved within Brown Bank sediments.

Sediments interpreted as possible Twente Formation (**Unit 6**) (wind-blown sands) were sub-sampled for particle size distribution analysis from **VC076**. Results are more indicative of sediments transported by water rather than wind. Therefore, it is suggested these sediments were deposited within or near the margins of a palaeochannel or floodplain. Given these findings, Twente Formation is considered to be absent in vibrocores from Norfolk Vanguard.

Six sub-samples from early Holocene pre-transgression (**Unit 7**) deposits were submitted for radiocarbon dating (two dates each from cores **VC074**, **VC076** and **VC085**). The dates from **VC085** are inverted suggesting erroneous ages in these cores. Dates from the top of the peat in **VC074** and **VC076** are 10226-9918 cal. BP and 10208-9911 cal. BP respectively, they are broadly conformable dating to the Early Mesolithic. A date of 13781-13556 cal. BP was returned from the base of the peat in **VC076**. Such an early date for peat development is unlikely given vegetation history suggesting another potential erroneous age, possibly due to reworking or a hard/soft water effects.

Pollen is moderately well preserved in all three peat sequences with moderate concentrations in **VC074** and **VC085**. Pollen assessment from peat deposits in **VC074** and **VC076** suggests an open woodland flora dominated by pine and hazel with sedges and reeds derived from local tall-herb swamps. The pollen assessment from **VC085** suggests a wooded rather than open woodland, although again dominated by pine and hazel with nearby areas of tall-herb swamp. In **VC074**,

foraminifera and ostracod assessments show inclusion of marine species indicative of reworking in the uppermost peat. These were likely washed into the peat during local storm events.

Underlying the peat in **VC074** is a clayey sand comprising freshwater diatom assemblages reinforcing the original interpretation as a palaeochannel deposit. In **VC085**, organic silty clay underlies the peat. Initial interpretations suggested a possible saltmarsh environment. However, diatom assemblages comprise freshwater species and the sediments are now interpreted as floodplain deposits close the margins of a palaeochannel. The peat is overlain by sediments comprising marine ostracod and foraminifera species in **VC076** and **VC085**. These deposits reflect marine inundation of Norfolk Vanguard.

The results of the Stage 3 palaeoenvironmental assessment are considered in terms of the archaeological and geoarchaeological significance of deposits. Upper Brown Bank Formation (**Unit 5**) across Norfolk Vanguard has low archaeological potential in terms of the preservation of *in situ* or derived artefacts as the unit represents deposition in an outer estuary or open marine embayment. Upper Brown Bank does however have high geoarchaeological potential in terms of palaeolandscape development as it dates to period when humans were absent, and then reappeared in Britain. Establishing if this embayment/estuary was a permanent fixture in the landscape, or whether it periodically became subaerially exposed opening migration pathways through the southern North Sea, is a key archaeological question.

Early Holocene pre-transgressive deposits (**Unit 7**) can be subdivided into palaeochannel/floodplain deposits overlain by terrestrial peats. There is potential for preservation of *in situ* and derived artefacts associated with these paleochannel and floodplain environments as they date to the Early Mesolithic when the southern North Sea was an extensive terrestrial landscape, although targeting finds is extremely difficult in offshore settings. Preservation of pollen in peat deposits is moderate and there is potential to reconstruct vegetation history, and final marine inundation of Norfolk Vanguard.

To further assess the geoarchaeological potential of Brown Bank Formation (**Unit 4**) and early Holocene pre-transgression deposits (**Unit 7**), it is recommended targeted Stage 4 analysis is undertaken on four vibrocores (**VC074**, **VC079**, **VC084** and **VC107**). Full pollen analysis, supported by two additional radiocarbon dates, is proposed for **VC074** which comprises the thickest peat deposit recovered from NV West. This will provide a high-resolution record of vegetation development and palaeolandscape change during the early Holocene. It is also recommended additional sub-samples are assessed for foraminifera and ostracods from **VC074** and **VC085**, along with two additional OSL dates (**VC079** and **VC107**). The results will help address questions about the persistence and configuration of a large open embayment/estuary within the southern North Sea landscape during the late Middle Palaeolithic.

Acknowledgements

This work was commissioned by Royal HaskoningDHV. The report was compiled by Dr Claire Mellett and Dr Alex Brown. Diatom assessment was undertaken by Dr Nigel Cameron of University College London. Foraminifera and ostracod assessment was carried out by Dr John Whittaker. Optical stimulated luminescence dating was undertaken at University of Gloucestershire by Dr Phil Toms. Pollen assessment was carried out by Dr Alex Brown and macrofossil assessment by Dr Ines Lopez Doriga, both of Wessex Archaeology. Nicki Mulhall carried out sub-sampling. Illustrations were prepared by Nancy Dixon. The project was managed on behalf of Wessex Archaeology by David Norcott.

Norfolk Vanguard Offshore Wind Farm

Stage 3 Palaeoenvironmental Assessment

1 INTRODUCTION

1.1 Project background

1.1.1 Wessex Archaeology (WA) have been commissioned by Royal HaskoningDHV to undertake Stage 3 paleoenvironmental assessment of five vibrocores within the proposed Norfolk Vanguard Offshore Wind Farm development (**Figure 1**).

1.1.2 The Norfolk Vanguard Project Area is located in the southern North Sea (**Figure 1**). It comprises two separate tranches, Norfolk Vanguard West (NV West) and Norfolk Vanguard East (NV East) which lie 47 km and 89 km respectively, east of Bacton, north Norfolk. An Offshore Cable Corridor joins the Norfolk Vanguard site to the landfall at Happisburgh South on the Norfolk coast.

1.1.3 The location of the proposed Norfolk Vanguard Project Area is of particular prehistoric archaeological interest, located in an area that at the height of the last ice age formed part of a vast habitable plain connecting Britain with the rest of the European continent. This landscape was then progressively drowned by rising post-glacial sea levels with full marine conditions occurring across the southern North Sea basin by ca. 7,000 yrs before present (BP) (**Figure 2**).

1.1.4 An initial Stage 1 geoarchaeological review of vibrocore logs from 65 locations identified twenty-three vibrocore sequences with very high (**VC074, VC076 VC085**), high (**VC079, VC089, VC095, VC101, VC107 and VC116**) and medium (**VC070, VC075, VC080, VC081, VC084, VC086, VC088, VC092, VC97 VC103, VC104, VC117, VC118 and VC119**) geoarchaeological potential (Wessex Archaeology 2017a).

1.1.5 Vibrocores identified in the Stage 1 review were subject to subsequent Stage 2 geoarchaeological recording and deposit modelling (Wessex Archaeology 2018). Three units of geoarchaeological interest were recovered in vibrocores, including; Upper Brown Bank Formation (**Unit 5**), possible Twente Formation (**Unit 6**) and early Holocene pre-transgression peats and minerogenic deposits (**Unit 7**) that were in places associated with palaeochannels identified in geophysical data. Stage 3 palaeoenvironmental assessment was recommended on five vibrocores **VC074**, **VC076**, **VC079**, **VC085** and **VC107**, focusing on deposits from **Units 5**, **6** and **7** which have greatest geoarchaeological potential.

1.1.6 This report presents the results of Stage 3 palaeoenvironmental assessments on five vibrocores from Norfolk Vanguard.

1.2 Scope of report

1.2.1 To help frame geoarchaeological investigations of this nature, WA has developed a five-stage approach, encompassing different levels of investigation appropriate to the results obtained, accompanied by formal reporting of the results at the level achieved. The stages are summarised below (**Table 1**).

Table 1 Stages of geoarchaeological assessment and recording.

Stage	Method	Description
1	Review	A desk-based archaeological review of the borehole, vibrocore and CPT logs generated by geotechnical contractors. Aims to establish the likely presence of horizons of archaeological interest and broadly characterise them, as a basis for deciding whether and what Stage 2 archaeological recording is required. The Stage 1 report will state the scale of Stage 2 work proposed**.**
2	Geoarchaeological recording and deposit modelling	Archaeological recording of selected retained or new core samples will be undertaken. This will entail the splitting of the cores, with each core being cleaned and recorded. The Stage 2 report will state the results of the archaeological recording and will indicate whether any Stage 3 work is warranted.
3	Sampling and assessment	Dependent upon the results of Stage 2, sub-sampling and palaeoenvironmental assessment (pollen, diatoms and foraminifera) may be required. Subsamples will be taken if required. Assessment will comprise laboratory analysis of the samples to a level sufficient to enable the value of the palaeoenvironmental material surviving within the cores to be identified. Subsamples will also be taken and/or retained at this stage in case scientific dating is required during Stage 4. Some scientific dating (e.g. radiocarbon or Optically Stimulated Luminescence (OSL)) may be undertaken at this stage to provide chronological context. The Stage 3 report will set out the results of each laboratory assessment together with an outline of the archaeological implications of the combined results, and will indicate whether any Stage 4 work is warranted.
4	Analysis and dating	Full analysis of pollen, diatoms and/or foraminifera assessed during Stage 3 will be undertaken. Typically, Stage 4 will be supported by scientific dating (e.g. radiocarbon or OSL) of suitable subsamples. Stage 4 will result in an account of the successive environments within the coring area, a model of environmental change over time, and an outline of the archaeological implications of the analysis.
5	Final report	If required Stage 5 will comprise the production of a final report of the results of the previous phases of work for publication in an appropriate journal. This report will be compiled after the final phase of archaeological work, whichever phase that is.

2 AIMS AND OBJECTIVES

2.1.1 The principal aims of the Stage 3 palaeoenvironmental assessment were to:

- Determine the nature, depositional history and age of accumulated deposits;
- Determine the preservation potential and concentration of palaeoenvironmental remains (pollen, plant macrofossils, diatoms, foraminifera and ostracods) within the deposits;

- Interpret the results to inform reconstructions of past environmental and landscape change (e.g. vegetation and sea level), and to asses archaeological and geoarchaeoogical potential of deposits.

2.1.2 A series of research questions were proposed in the Stage 2 report (Wessex Archaeology 2018) which underpin the Stage 3 palaeoenvironmental assessment, taking into account the regional research framework (Medlycott 2011) and the national maritime research framework (Ransley et al. 2013).

2.1.3 Specific research questions include:

- What is the depositional history of the Brown Bank Formation? Did it form relatively quickly in the early Devensian or accumulate as a more gradual deposit?

- Do the preserved peats represent a contemporary phase of peat formation across the entire site, or separate phases of peat formation within discrete environmental niches?

3 GEOARCHAEOLOGICAL BACKGROUND

3.1.1 The geology of the area has been outlined as part of an earlier palaeogeographic assessment of Norfolk Vanguard (Wessex Archaeology 2017b), combining a review of the, geotechnical, geophysical and known geological data. This identified a series of geological units across the broader area, outlined in **Table 2,** and shown in **Figures 3 and 4**.

3.1.2 The geological units identified by Wessex Archaeology are listed against the corresponding units identified by Fugro (2017a). It should be noted that Fugro used deeper digital seismic data which will have aided interpretation of deeper units such as the Westkapelle Ground Formation; the Wessex stratigraphic units by comparison were interpreted using shallow analogue sub-bottom profiler data and as such there was less confidence in interpreting those deeper units identified by Fugro.

3.1.3 Geotechnical investigations, comprising both Cone Penetrometer Tests (CPT) and vibrocore (VC) operations, were undertaken by Fugro EMU Limited, with onshore laboratory and reporting undertaken by Fugro GeoConsulting Limited (Fugro 2017b).

3.1.4 Geophysical survey data was acquired in 2012 by Emu Limited (Emu Ltd, 2013), and in 2016 by Fugro Survey B. V. (Fugro 2016; 2017a; 2017c), and subsequently reviewed by Wessex Archaeology as part of a palaeogeographic assessment of geophysical data within Norfolk Vanguard (Wessex Archaeology 2017b).

3.1.5 Where age estimates are available these are expressed in millions of years (MA), thousands of years (ka), and within the Holocene epoch as years before present (BP). These dates are supplemented, where known, with the comparable Marine Isotope Stages (MIS) where odd numbers indicate an interglacial period and even numbers a glacial period.

3.1.6 The Pleistocene geological history of the North Sea basin is dominated by repeated glacial/interglacial cycles, resulting in rising and falling sea levels and deposition of terrestrial, marine and glacially-derived sediments (**Figure 2**).

3.1.7 Despite repeated episodes of ice advance and retreat throughout the Middle-Late Pleistocene, only one major glacial episode shows evidence of extending as far south as Norfolk Vanguard, this was during the Anglian period (ca. 480–423 ka). Subsequent glacial episodes will have affected the region indirectly as a result of changing climate, sediment

input and sea level. The exact southern extent of the Anglian glaciation, particularly offshore, is debated, although bathymetric data suggests part of the Anglian ice sheet may have extended as far south as offshore Felixstowe (Emu 2009).

Table 2 Geological units identified within Norfolk Vanguard (after Wessex Archaeology 2017b and Fugro 2017a). Units shaded grey were too deep to be recovered in vibrocores.

WA Unit	Fugro Unit	Geological Unit	Age	Geoarchaeological potential
8	A1	Holocene seabed sediments	Post-transgression (MIS 1)	Gravelly sand with shell fragments, sand waves and ripples indicate sediment is mobile. Low potential in areas of mobile sediment: basal contact may cover old land surfaces.
7	A2	Holocene sediments	Pre-transgression (MIS 2–1)	Fluvial, estuarine and terrestrial (including peat) deposits. Shallow infilled depressions or channels with potential for preserved organic material of palaeoenvironmental significance.
6	B	Twente Formation	Upper Devensian (MIS 2)	Thin layer of aeolian periglacial sand. Potential to contain in-situ and derived archaeological and palaeoenvironmental material
5	C	Upper Brown Bank Formation	Early/Mid Devensian (MIS 5d–3)	Clayey silty sand infilling channels or hollows and deposited in an intertidal/lagoon environment. Potential for *in-situ* Lower Palaeolithic artefacts. Middle Palaeolithic artefacts may be associated with channel edges dependent on age of infill. Basal contact may cover old land surface
4	C / D	Lower Brown Bank Formation / Eem Formation	Ipswichian or Lower Devensian (MIS 5e–5d)	Silty sand and sandy silt. Possible intertidal or shallow marine deposit. In-situ Lower Palaeolithic artefacts may be protected. Middle Palaeolithic artefacts may be associated with channel edges dependent on age of infill. Basal contact may cover old land surface
3	E	Swarte Bank Formation	Anglian (MIS 12)	Silty sandy clays associated with the Anglian glaciation. Unlikely to contain archaeological material.
2	F	Yarmouth Formation	Lower to Middle Pleistocene (MIS >13)	Silty sand with occasional shell fragments, deposited as part of marine delta complex. Low potential, unlikely to contain archaeology or deposits of palaeoenvironmental significance.
1	I	Westkapelle Ground Formation	Pliocene – Lower Pleistocene (MIS 103-63)	Deltaic silty clays and sands. Pre-date earliest occupation; of no archaeological interest

3.1.8 Palaeolandscape features have higher preservation potential off the East Anglian coast when compared to areas of the seabed further North. This is because the last two major ice ages dating to the Saalian and Devensian did not extend as far south as East Anglia

therefore protecting former land surfaces from the highly erosive processes associated with ice sheets. The last major ice advance across the southern North Sea offshore of East Anglia occurred during the Anglian ice age approximately 450 thousand years ago. Therefore, offshore East Anglia there is potential to preserve any palaeolandscape features that formed when the southern North Sea was periodically subaerially exposed during the last ~450 ka.

3.1.9 Geophysical and geotechnical data have been used to devise a basic stratigraphy for Norfolk Vanguard, comprising eight units covering the Pleistocene and Holocene (**Table 2**). These comprise both terrestrial and fluvial sediments associated with palaeochannels, floodplains, periglacial aeolian deposits, lagoon and lacustrine environments.

3.1.10 **Unit 1** pre-dates the earliest human occupation of Britain and is unlikely to contain archaeological or palaeoenvironmental remains, and is therefore of limited geoarchaeological relevance. **Unit 2** is a shallow marine deltaic deposit that is contemporary with the terrestrial Cromer Forest Bed Formation (> MIS 13) which has produced some of the earliest evidence for the hominin occupation of Britain (Parfitt *et al*. 2010, Ashton *et al*. 2014). **Unit 3** deposits are associated with the Anglian glaciation and therefore unlikely to contain archaeological material. **Unit 3** has not been definitively recognised on geophysical data within Norfolk Vanguard (Fugro 2017a; WA 2017b).

3.1.11 **Unit 4** is of uncertain age, but may contain either the Eem Formation, dating to the Ipswichian, or Lower Brown Bank Formation deposits of Lower Devensian age (Cameron *et al.* 1992). The Eem Formation is described as shelly and muddy sands representing a shallow marine/intertidal environment, whilst the Lower Brown Bank Formation comprises clayey silts and sands infilling channels and/or hollows, interpreted to have been deposited within an intertidal/lagoon environment. **Unit 4** has only been sporadically identified in NV West compared to NV East (**Figures 3 and 4**).

3.1.12 Humans were absent from the area during the development of the Eem and Lower Brown Bank Formations (**Unit 4**), although the geoarchaeological potential of the Upper Brown Bank Formation (**Unit 5**) is considered to be higher, although variable, dependent on the presence/absence of suitable features. **Unit 5** is present as a blanket deposit across the whole of NV East and NV West, and is provisionally interpreted as a shallow lagoon environment, comprising clayey silty sands. The presence of organic material within the sediment has been suggested in places by accumulations of shallow gas revealed during geophysical surveys. A number of internal features have been identified within **Unit 5** that have been interpreted as possible internal erosion surfaces. It is possible that the lagoon may have periodically dried up, exposing previously submerged sediment as dryland resulting in the observed internal erosion surfaces.

3.1.13 The geophysical surveys hint at a complex deposition history for **Unit 5**, suggesting a multi-period, multi-phase unit rather than continuous deposition of lagoon sediment, which has implications for the archaeological potential of the deposits. This multi-phase history likely relates to changing water levels and there is potential the lagoon dried out periodically creating environments suitable for human exploitation, and a pathway for migration through the southern North Sea.

3.1.14 The Upper Brown Bank Formation is overlain across NV East by recent post-transgression sea bed sediments (**Unit 8**), varying in thickness from a thin veneer to sand banks up to 15 m thick.

3.1.15 Overlying the Upper Brown Bank Formation within NV West is the Twente Formation (**Unit 6**), comprising a thin deposit of sand up to 1 m thick, provisionally interpreted as a periglacial aeolian (windblown) sand deposit of Upper Devensian age. **Unit 6** has been tentatively identified in vibrocores **VC075**, **VC076** and **VC088** but has not been identified along the Offshore Cable Corridor. The extent of the Twente Formation shown on **Figure 4** is based on BGS data as it could not be confidently identified on the seismic data (Fugro, 2017a).

3.1.16 **Unit 6** would have formed after the retreat of the Devensian ice sheet, with wind transporting loose sediment southward across the largely unvegetated periglacial landscape. Similar windblown sands (also called coversands) have been found across East Anglia and continental Europe (Crombe *et al.* 2012). In places these form small dune ridges within low-lying wetland landscapes that would have been favourable locations for settlement with potential for recovery of *in situ* archaeological material.

3.1.17 Overlying the Pleistocene sediments is a sequence of early Holocene deposits (**Unit 7** and **Unit 8**). Geophysical surveys and coring in this area have identified terrestrial deposits, including peat, which are thought to have been deposited prior to and during the early-mid Holocene marine transgression of the southern North Sea basin. According to geophysical interpretations, the peat deposits form either on the top of Upper Brown Bank deposits, on top of windblown sands, or within Holocene channels (**Figure 3**). Where peat overlies Upper Brown Bank or Twente Formation, a high amplitude reflector marks the presence of peat in geophysical data. Geophysical interpretations identified 12 pre-transgression shallow channel features. Some of these channels can be correlated to high amplitude reflectors. One of the cores appears to show a gradual upward transition from saltmarsh to peat (**VC085**), in turn sealed by muds (classified together as **Unit 7**), providing evidence of the progressive inundation of terrestrial landscapes as a result of rising post-glacial sea levels (Cooper *et al.* 2008). Where peat deposits are preserved on the top of the Upper Brown Bank these may equally indicate peat formation during the Late Devensian. These deposits, and particularly the peat, have high palaeoenvironmental potential.

3.1.18 The progressive inundation of North Sea palaeolandscapes occurred over an extended time scale, with particularly rapid sea-level rise occurring during the early Holocene (11,500–7000 cal. BP) and fully marine conditions across the North Sea by probably around 6000 cal. BP (Ward *et al.* 2006). Marine sediments deposited since the Holocene transgression typically comprise sands, gravels and muds (**Unit 8**).

4 METHODS

4.1 Stage 3 assessment

4.1.1 Five vibrocores were subject to Stage 3 palaeoenvironment assessment (**VC074**, **VC076**, **VC079**, **VC085** and **VC107**). Deposits corresponding to Upper Brown Bank (**Unit 5**) were targeted in **VC079** and **VC107** for OSL dating and accompanying foraminifera, ostracod and diatom assessment to determine palaeoenvironment. To help confirm the presence or absence of Twente Formation (**Unit 6**), samples from **VC076** were targeted for particle size analysis to help determine depositional environment. Holocene pre-transgression peat and over/underlying minerogenic deposits (**Unit 7**) in **VC074**, **VC076** and **VC085** were selected for radiocarbon dating as they showed the greatest potential for preservation of pollen within the peat. Diatoms, foraminifera and ostracod analysis was also undertaken on these cores across transitions between minerogenic and organic sediments.

4.1.2 Full analytical methods for each palaeoenvironmental and dating technique are described below. All sub-sample depths are quoted as metres below sea floor (mbsf). In some cases, the elevation of sub-samples has been corrected to Lowest Astronomical Tide (LAT). At this

stage depths have not been corrected to meters Ordnance Datum. A full list of sub-samples is presented in **Appendix 1**.

4.2 Radiocarbon dating

4.2.1 Six sub-samples were taken for radiocarbon dating, two each from vibrocores **VC074**, **VC076** and **VC085** (**Table 3**). Suitable material was identified under microscope, stored in glass tubes, and sent to the ^{14}CHRONO Centre at Queens University Belfast for dating. Calibrated age ranges were calculated with OxCal 4.1 (Bronk-Ramsey 2009) using the IntCal13 curve (Reimer *et al.* 2013). All radiocarbon dates are quoted as uncalibrated years before present (BP), followed by the lab code and the calibrated date-range (cal. AD and/or BP) at the 2σ (95.4%) confidence.

4.3 Optically stimulated luminescence dating

4.3.1 Six sub-samples from four cores were taken for optical stimulated luminescence (OSL) dating (**VC074**, **VC079**, **VC086** and **VC107)**. The cores had previously been opened and exposed to light as part of the Stage 2 geoarchaeological recording. Therefore, the location of sub-samples was chosen to target undisturbed sections of core with a sufficient sand component. All sub-samples were carefully wrapped and transported to the OSL laboratory at the University of Gloucestershire where they were opened and prepared under controlled laboratory illumination provided by Encapsulite RB-10 (red) filters. To isolate that material potentially exposed to daylight during sampling, sediment located within 10 mm of each core face was removed.

4.3.2 Equivalent dose (D_e) values were quantified using a single-aliquot regenerative-dose (SAR) protocol (Murray and Wintle 2000; 2003). Weighted (geometric) mean D_e values were calculated from 12 aliquots using the central age model outlined by Galbraith *et al*. (1999) and are quoted at 1σ confidence (**Table 4**). Lithogenic Dose Rate (D_r) values were defined through measurement of U, Th and K radionuclide concentration and conversion of these quantities into β and γ D_r values (Adamiec and Aitken, 1998), accounting for D_r modulation forced by grain size (Mejdahl, 1979) and present moisture content (Zimmerman, 1971) (**Table 4**). Cosmogenic D_r values were calculated on the basis of sample depth, geographical position and matrix density (Prescott and Hutton, 1994). Note, no *in situ* γ spectrometry was undertaken due to these samples being collected offshore, therefore the level of U disequilibrium was estimated by laboratory based Ge γ spectrometry.

4.3.3 The accuracy with which D_e equates to total absorbed dose and that dose absorbed since burial was assessed. The former can be considered a function of laboratory factors, including feldspar contamination, preheating, irradiation and internal consistency, the latter, one of environmental issues such as incomplete zeroing and the influence of turbation. Diagnostics were deployed to estimate the influence of these factors and criteria instituted to optimise the accuracy of D_e values. The analytical validity of each sample is presented in **Table 4**.

4.3.4 Ages reported in **Table 4** provide an estimate of sediment burial period based on mean D_e and D_r values and their associated analytical uncertainties. Full OSL results are presented in **Appendix 2**.

4.4 Plant macrofossils

4.4.1 Six sub-samples were processed for the assessment of plant macrofossils for recovery of suitable material for radiocarbon dating, two each from vibrocores **VC074**, **VC076** and **VC085**. The sub-samples were processed by standard methods for the recovery of waterlogged plant remains; the flots were retained on a 2.5 mm mesh. Flots were stored in

sealed containers with water. The flots were scanned under a x10 – x40 stereo-binocular microscope and the preservation and nature of the plant remains recorded in **Table 3**. Nomenclature follows Stace (1997).

4.5 Pollen and spores

4.5.1 Eighteen sub-samples of 1 ml volume were processed using standard pollen extraction methods (Moore *et al.* 1991), comprising eight sub-samples from **VC074** and five sub-samples each from **VC076** and **VC085**. Pollen was identified and counted using a Nikon eclipse E400 biological research microscope. A total of 150 pollen grains was counted for each sub-sample in addition to aquatics, fern spores and algal Pediastrum. Where 150 counts were not possible, all pollen and spores were counted from four transects. One Lycopodium tablet was added to enable calculation of pollen concentrations. Pollen and spores were identified to the lowest possible taxonomic level. Plant nomenclature followed Stace (1997) and Bennett et al. (1994). Pollen sums are based on total land pollen (TLP) excluding aquatics and fern spores which are calculated as a percentage of TLP plus the sum of the component taxa within the respective category. Identification of indeterminable grains was according to Cushing (1967).

4.5.2 At assessment stage the results are not presented as pollen diagrams, but are presented in tabular form as raw data (**Tables 5-7**). Plant taxa are assigned to one of the following groups (trees and shrubs, dwarf shrubs, cultivated, herbaceous open/ undefined, fern spores and aquatics) based on their most likely ecological affinity, although many plant taxa occur in a range of environmental niches (see Stace 1997 for specific plant taxa).

4.6 Diatoms

4.6.1 Thirty-eight sub-samples were prepared for diatom assessment, comprising ten sub-samples from both **VC079** and **VC107**, eight sub-samples from **VC074**, six sub-samples from **VC085** and four sub-samples from **VC076**.

4.6.2 Diatom preparation followed standard techniques (Battarbee et al. 2001). Two coverslips were made from each sample and fixed in Naphrax for diatom microscopy. A large area of the coverslips on each slide was scanned for diatoms at magnifications of x400 and x1000 under phase contrast illumination.

4.6.3 Diatom floras and taxonomic publications were consulted to assist with diatom identification; these include Hendey (1964), Werff and Huls (1957-1974), Hartley et al. (1996), Krammer and Lange-Bertalot (1986-1991) and Witkowski et al. (2000). Diatom species' salinity preferences are indicated using the halobian groups of Hustedt (1953; 1957), these salinity groups are summarised as follows:

1. Polyhalobian: >30g l^{-1}

2. Mesohalobian: 0.2-30g l^{-1}

3. Oligohalobian - Halophilous: optimum in slightly brackish water

4. Oligohalobian - Indifferent: optimum in freshwater but tolerant of slightly brackish water

5. Halophobous: exclusively freshwater

6. Unknown: taxa of unknown salinity preference

4.6.4 Diatom assessment results are summarised in **Table 8** with comments on potential for full diatom analyses. Where diatom preservation was suitable, more detailed assessment was undertaken and is presented in **Appendix 3**.

4.7 Foraminifera and Ostracods

4.7.1 Thirty-eight sub-samples were processed for foraminifera and ostracod analysis, comprising ten sub-samples from both **VC079** and **VC107**, eight sub-samples from **VC074**, six sub-samples from **VC085** and four sub-samples from **VC076**.

4.7.2 The sub-samples were weighed, then broken into small pieces by hand, placed into ceramic bowls, and dried in an oven. Boiling-hot water was then poured over them with a little sodium carbonate added to help disaggregate the clay fraction. Each was left to soak overnight. It was found that breakdown was aided, especially with the organic-rich samples, by re-heating the still soaking samples in the oven for several hours before attempting to wash them. The peats, however, needed processing twice and even then, breakdown was not entirely satisfactory.

4.7.3 Sub-samples were then washed through a 75 µm sieve with the remaining residue returned to the ceramic bowl for final drying in the oven. The residues were then stored in labelled plastic bags. For examination, each sample was placed in a nest of sieves (>50, >250, >150 µm, and base pan) and thoroughly shaken. Each grade was then sprinkled onto a picking tray, a little at a time, and viewed under a binocular microscope. “Contained material” were logged on a presence(x)/absence basis and is shown in the accompanying table (**Tables 9-13**).

4.7.4 The abundance of each foraminiferal and ostracod species was estimated semi-quantitatively (one specimen, several specimens, common and abundant/superabundant) by experience and by eye. Species identification comes from Murray (2006) for the foraminifera, Athersuch et al. (1989) for the brackish and marine ostracods, and Meisch (2000) for the freshwater ostracods, in addition to expert judgement.

4.8 Particle size distribution analysis

4.8.1 Particle size distribution analysis was undertaken by laser granulometry (range 0.01-2000 microns) using a Malven Mastersizer 3000 on 3 samples from **VC076**. Sub-samples were mixed with a spatula to form a homogenous ‘paste’. A subsample was then placed on a plastic watchglass and a weak dispersant solution (c. 0.5ml 3.3% Calgon) was added in order to aid dispersion of the material (Blott et al. 2004). Physical disaggregation on a clean watchglass with a rubber pestle was carried out. Any particles observed to be greater than 2 mm were removed. The sample was then washed with distilled water into the analyser. The results are reported as percentages of sand, silt and clay in **Table 14** and their respective frequency distribution histograms are presented in **Appendix 4**.

5 RESULTS

5.1 Radiocarbon dating

5.1.1 Six sub-samples were taken for radiocarbon dating, comprising two sub-samples each from peat deposits in **VC074**, **VC076** and **VC085**. The calibrated results implies peat deposition occurred from the Upper Palaeolithic into the early Mesolithic (late glacial-early Holocene) which suggests these relatively thin (0.36-0.80 m) peat deposits may represent up to ~4000 years of peat development across NV West. However, this age range assumes all radiocarbon dates are accurate and reliable which may not be the case as discussed below.

Table 3 AMS radiocarbon dates

Laboratory No	Material dated	Depth (mbsf)	Age B.P	Age range cal. BC (95.4%)	Age range cal. BP (95.4%)
UB-36846	Seeds (*Nuphar lutea* 2x, *Nymphaea alba* 2x, *Juncus* sp. 1x, Cyperaceae 1/2x) + leaves (*Sphagnum* sp. 25x)	0.90	8955 ± 46	8277- 7969	10226-9918
UB-36847	Seeds (*Betula* sp. 3x, *Solanum* sp. 2x, *Chenopodium* sp. 1x, Caryophyllaceae 1x, *Betula* sp. 5x, *Lycopus europaeus* 1x, *Potamogeton* sp. 1x, *Nymphaea alba* 1x, Cyperaceae 15x), *Betula* sp. 1x catkin scale	1.56	9122 ± 49	8467-8250	10416-10199
UB-36848	Seeds: *Lycopus europaeus* 1x, *Juncus* sp 2x, Asteraceae1x, *Carex* sp 2x, *Ranunculus* sp. 0.5	3.61-3.63	8936 ± 47	8259-7962	10208-9911
UB-36849	Seeds: *Potamogeton* sp. 5x	3.91-3.93	11863 ± 55	11832-11607	13781-13556
UB-36850	Seeds: Ceratophyllum sp. 1x, *Menyanthes trifoliata* 2x	1.75-1.77	10192 ± 47	10142- 9758	12091-11707
UB-36851	Seeds: *Menyanthes trifoliata* 2x	2.07-2.09	8856 ± 48	8220- 7795	10169-9744

VC074

5.1.2 Two sub-samples from **VC074** were taken for radiocarbon dating, located at the top (0.90 mbsf) and base (1.58 mbsf) of a 0.90 m peat deposit. The basal date is 10416-10199 cal. BP (UB-36847) and the overlying upper date is 10226-9918 cal. BP (UB-36846) indicating a conformable sequence of dates (**Table 3**). The dates suggest formation of the peat over a relatively short period of time during the Early Mesolithic.

VC076

5.1.3 Two sub-samples from **VC076** were taken for radiocarbon dating, located at the top (3.61 mbsf) and base (3.91 mbsf) of a 0.40 m peat deposit. The basal date is 13781-13556 cal. BP (UB-36849) while the upper date is 10208-9911 cal. BP (UB-36848) (**Table 3**) suggesting up to 3870 yrs of peat deposition across the Palaeolithic to Early Mesolithic transition is represented in this core. The likelihood of a 0.40 m thick deposit representing ~4000 yrs of peat development is low. Furthermore, such an early date (13781-13556 cal. BP) for peat formation has not been observed elsewhere across the southern North Sea suggesting the basal date is erroneous possibly due to reworking, contamination or local hard/soft water errors.

VC085

5.1.4 Two sub-samples from **VC085** were taken for radiocarbon dating, located at the top (1.75 mbsf) and the base (2.07 mbsf) of a 0.36 m peat deposit. The basal date is 10169-9744 cal. BP (UB-36851) while the upper date is 12091-11707 cal. BP (UB-36850) (**Table 3**). The ages suggest the peat was deposited during the Palaeolithic to Early Mesolithic transition. However, there is an inversion in the ages with the uppermost date ca. 1136 yrs older than the basal date. This implies one or both of these dates are unreliable.

5.2 Optically Stimulated Luminescence dating

VC074

5.2.1 One sub-sample from **VC074** at a depth of 5.00-5.36 mbsf was taken from deposits interpreted to be Upper Brown Bank for OSL dating (GL17081) (**Table 4**). Only one sub-sample was taken from this vibrocore due to the relatively thin (0.85 m) sequence of Upper

Brown Bank recovered at this location. Sample GL17081 satisfied validation tests resulting in an age estimate of 82.4 ± 8.5 ka which correlates to MIS 5a.

VC079

5.2.2 Two sub-samples from a 4.95 m thick sequence of Upper Brown Bank deposits in **VC079** were taken for OSL dating, one near the base of the core at 4.15-4.35 mbsf and one near the top at 0.75-1.00 mbsf.

5.2.3 The lowermost sub-sample (GL17079) gives an age of 57.6 ± 5.9 ka (**Table 4**) which marks the transition from MIS 4 to MIS 3. However, this age should be interpreted with caution as validity tests showed evidence of overdispersion in the regenerated signal which has an impact on the Equivalent Dose interpolation.

5.2.4 The uppermost sample (GL17080) gives an age of 66.8 ± 7.1 ka (**Table 4**) dating to MIS 4. However, this sub-sample showed evidence of Uranium disequilibrium which effects the calculation of dose rate. Therefore, this date has been tentatively accepted and must be interpreted with caution.

5.2.5 OSL ages from **VC079** are inverted whereby the uppermost, and supposedly younger date, is 9.2 ka older than the lower date. This inversion in ages could be explained by sediment reworking and/or bioturbation. During Stage 2 geoarchaeological recording, the deposit was described as 'marbled' with no clear laminations which may be evidence of reworking. However, given the analytical discrepancies in this sample, it is possible this inversion is due to inherent sample behaviour.

VC085

5.2.6 Two sub-samples from **VC085** were taken for OSL dating at depths of 4.60-4.80 mbsf and 5.10-5.30 mbsf near the base of a 2.76 m thick sequence of Upper Brown Bank. The samples were located 0.30 m apart to test repeatability.

5.2.7 The basal sub-sample (GL17076) returned an age of 57.2 ± 6.4 ka with the overlying sub-sample (GL17077) giving an age of 69.5 ± 7.7 ka (**Table 4**). Both dates passed validity tests and have been accepted. Ages are inverted but there is some overlap within error margins. The dates suggest deposition of Upper Brown Bank during MIS 4 transitioning into MIS 3. Given samples are located 0.30 m apart, the ages suggest low deposition rates assuming no periods of erosion or non-deposition.

VC107

5.2.8 One sub-sample from **VC107** was taken for OSL dating to test variability in the age of Upper Brown Bank between NV East and NV West. Sample GL17078 was taken at 1.00-1.25 mbsf near the top of a 5.2 m sequence of Upper Brown Bank deposits. The resulting age is 59.8 ± 6.2 ka (**Table 4**) which correlates to the transition from MIS 4 to MIS 3. This date should be interpreted as a minimum age estimate as it shows evidence of feldspar contamination which tends to underestimate age. Therefore, the sub-sample taken from **VC107** is at least 59.8 ± 6.2 ka but may be older.

Table 4 Dose Rate (D_r) and Equivalent Dose (D_e) and resulting OSL age estimates. Age estimates expressed in ka relative to year

of sampling. Uncertainties in age are quoted at 1σ confidence and include combined systematic and experimental variability.

Laboratory id	Core	Depth (mbsf)	Total D_r (Gy.ka-1)	D_e (Gy)	Age (ka)	Considerations and analytical validity
GL17076	VC085	5.10-5.30	2.43 ± 0.22	139.0 ± 8.7	57.2 ± 6.4	None, accept age
GL17077	VC085	4.60-4.80	2.19 ± 0.21	152.0 ± 8.7	69.5 ± 7.7	None, accept age
GL17078	VC107	1.00-1.25	2.37 ± 0.22	141.7 ± 6.6	59.8 ± 6.2	Significant feldspar contamination, accept as minimum age estimate
GL17079	VC079	4.15-4.35	2.42 ± 0.22	139.1 ± 6.3	57.6 ± 5.9	Overdispersion in the interpolated to applied regenerative-dose ratio, accept tentatively
GL17080	VC079	0.75-1.00	1.96 ±0.18	131.2 ± 7.4	66.8 ± 7.1	Potentially significant U disequilibrium, accept tentatively
GL17081	VC074	5.00-5.36	1.75 ± 0.16	144.3 ± 7.3	82.4 ± 8.5	None, accept age

5.3 Plant macrofossils

5.3.1 Plant macrofossils were assessed from 6 sub-samples to identify material suitable for radiocarbon dating. See **Tables 5-7** in **section 5.4**.

5.4 Pollen and spores

5.4.1 The results of pollen assessment of vibrocores **VC074**, **VC076** and **VC085** are presented here (**Tables 5-7**), accompanied by an outline interpretation (where results allow) of past vegetation environments and evidence for associated anthropogenic activity.

VC074

5.4.2 Pollen is well-preserved and present in moderate concentrations in all eight sub-samples through vibrocore **VC074**. The sequence is dominated by arboreal pollen (AP), in seven of the eight sub-samples ranging between 78.7% to 90.3% (0.88 mbsf) with a minimum of 68% AP in the basal sub-sample (1.58 mbsf). Non-arboreal pollen (NAP) frequencies are highest within the basal sub-sample (32%), thereafter ranging between 9.7 (0.88 mbsf) to 21.3% (1.08 mbsf).

5.4.3 Woodland is characterised initially by a mix of *Betula* (birch) (23.3%) and *Pinus sylvestris* (pine) (34%) with lesser frequencies for *Corylus avellana* type (hazel) (6.0%). *Betula* frequencies decline through **VC074** (4.7 to 12%), with values for *Pinus sylvestris* increasing up to 62.7% (1.38 mbsf), and *Corylus avellana* type peaking at c. 32.5% (1.08 mbsf) and 33.3% (0.88 mbsf) respectively. Small quantities of other arboreal taxa are recorded, including *Quercus* (oak) (1.3 to 3.3%), *Ulmus* (elm) (0.7 to 5.3%) and *Salix* (0.7 to 2.7%).

5.4.4 Herbaceous taxa are dominated by Poaceae (grasses), varying from 6.7% (1.38 mbsf) to 19.3% (1.58%), with smaller quantities of Cyperaceae (sedges) (1.3 to 4%) and typically single grains of a restricted range of herbs (e.g. Chenopodiaceae–goosefoots; Caryophyllaceae–pinks; Rosaceae–roses; *Artemisia*–mugworts), with the most diversity in pollen types at 1.58 mbsf.

5.4.5 Fern spores are present in moderate and increasing quantities from 1.46 mbsf, largely Pteropsida (undifferentiated fern spores) (8.8 to 20.7%), along with smaller quantities of *Thelypteris palustris* (marsh fern) (maximum 7.1%, 1.28 mbsf) and *Dryopteris filix-mas* (male fern) (≤1.6%).

5.4.6 Aquatic pollen occurs in small but consistent quantities, largely *Potamogeton natans* type (pondweed) (2.5 to 6%), *Sparganium emersum* type (unbranched bur-reed) (0.6 to 3%) and *Typha latifolia* (bulrush) (0.6 to 5.6%). Occasional *Sphagnum* spores were recorded along with consistent but small quantities of Pediastrum (green algae).

5.4.7 The pollen assemblage from **VC074** suggests a relatively open woodland canopy dominated by *Pinus sylvestris* and *Corylus avellana* type with smaller quantities of other trees such as Ulmus and *Quercus*. The herbaceous taxa, dominated by Poaceae and Cyperaceae, probably derive from the local environment, most likely reflecting wetland flora growing within the peat-infilling channel (e.g. reeds and sedges forming tall herb swamp) as well the ground flora component of woodland and more open areas.

5.4.8 Slow or still water is suggested by pollen of aquatic plants (*Potamogeton natans* type and *Sparganium emersum* type), with stands of *Typha latifolia* likely growing along with sedges and reeds within the channel. The presence of algal Pediastrum suggests a freshwater environment.

5.4.9 Very occasional flecks of microscopic charcoal were present in sub-samples through **VC074**, particularly at 1.18 mbsf. Microscopic charcoal was <5 µm in size, displaying no cellular structure.

Table 5 Pollen assessment, vibrocore VC074 (percentages are followed in parenthesis by the number of grains counted for each taxon)

Taxa / **Depth (mbsf)**	**0.88**	**0.98**	**1.08**	**1.18**	**1.28**	**1.38**	**1.46**	**1.58**
Deposit								
Betula (Birch)	9.1 (14)	6.7 (10)	5.3 (8)	7.3 (11)	12.0 (18)	4.7 (7)	6.6 (10)	23.3 (35)
Pinus sylvestris (Pine)	41.6 (64)	47.3 (71)	35.3 (53)	36.7 (55)	46.7 (70)	62.7 (94)	54.3 (82)	34.0 (51)
Corylus avellana type (Hazel)	32.5 (50)	14.7 (22)	33.3 (50)	28.0 (42)	18.7 (28)	16.0 (24)	20.5 (31)	6.0 (9)
Quercus (Oak)	1.3 (2)	3.3 (5)	3.3 (5)	2.0 (3)	1.3 (2)	3.3 (5)	2.0 (3)	1.3 (2)
Ulmus (Elm)	3.2 (5)	5.3 (8)	0.7 (1)	3.3 (5)	2.7 (4)	0.7 (1)	0.7 (1)	1.3 (2)
Salix (Willow)	2.6 (4)	2.0 (3)	-	2.7 (4)	2.0 (3)	2.0 (3)	0.7 (1)	2.0 (3)
Cornus (Dogwood)	-	-	0.7 (1)	-	-	-	-	-
Poaceae (Grasses)	8.4 (13)	16.0 (24)	18.7 (28)	16.0 (24)	12.7 (19)	6.7 (10)	13.2 (20)	19.3 (29)
Cyperaceae (Sedges)	1.3 (2)	4.0 (6)	2.0 (3)	1.3 (2)	3.3 (5)	3.3 (5)	2.0 (3)	5.3 (8)
Chenopodiaceae (Goosefoots)	-	0.7 (1)	-	0.7 (1)	-	-	-	2.7 (4)
Caryophyllaceae (Pinks)	-	-	-	-	-	0.7 (1)	-	-
Rumex acetosa (Common sorrel)	-	-	-	-	-	-	-	0.7 (1)
Rosaceae	-	-	-	1.3	0.7	-	-	-

Taxa	Depth (mbsf)	0.88	0.98	1.08	1.18	1.28	1.38	1.46	1.58
Deposit									
(Roses)					(2)	(1)			
Filipendula (Meadowsweet)		-	-	-	0.7 (1)	-	-	-	0.7 (1)
Apiaceae (Carrots)		-	-	-	-	-	-	-	2.0 (3)
Rubiaceae (Bedstraws)		-	-	-	-	-	-	-	0.7 (1)
Artemisia type (Mugwort)		-	-	0.7 (1)	-	-	-	-	0.7 (1)
Pteropsida undiff. (Undiff. fern spore)		20.7 (42)	14.4 (27)	16.5 (31)	11.1 (20)	10.3 (19)	10.5 (18)	8.8 (15)	1.3 (2)
Thelypteris palustris (Marsh fern)		3.4 (7)	3.7 (7)	3.7 (7)	5.0 (9)	7.1 (13)	1.8 (3)	2.3 (4)	2.5 (4)
Dryopteris filix-mas (Male fern)		-	1.6 (3)	-	-	1.1 (2)	-	0.6 (1)	0.6 (1)
Polypodium (Polypody)		-	-	-	0.6 (1)	-	-	-	-
Potamogeton natans type (Pondweed)		5.4 (9)	5.5 (9)	-	4.4 (7)	3.1 (5)	6.1 (10)	5.0 (8)	2.5 (4)
Sparganium emersum type (Unbranched bur-reed)		1.2 (2)	1.8 (3)	1.9 (3)	0.6 (1)	3.1 (5)	3.0 (5)	1.2 (2)	3.1 (5)
Typha latifolia (Bulrush)		0.6 (1)	0.6 (1)	5.6 (9)	1.3 (2)	1.8 (3)	-	-	1.2 (2)
Sphagnum (Bog moss)		0.6 (1)	0.7 (1)	-	-	-	-	-	0.7 (1)
Pediastrum (Green algae)		-	4.5 (7)	8.0 (13)	3.2 (5)	8.5 (14)	6.3 (10)	2.6 (4)	5.7 (9)
Indeterminables		2.4 (4)	2.5 (4)	3.0 (5)	-	0.5 (1)	3.5 (7)	-	-
Total Land Pollen		154	150	150	150	150	150	151	150

VC076

5.4.10 Pollen is moderately well-preserved through sequence **VC076**, but generally present in low concentrations. The pollen assemblages show a significant degree of variation through the sequence. Arboreal pollen forms an important component within the basal sub-sample (3.95 mbsf) (63.2%), is dominant at 3.7 mbsf and 3.6 mbsf (82.7 to 89.3%), but forms a minor component of the pollen assemblage from 3.87-3.8 mbsf (19.9 to 36.7%) where non-arboreal pollen dominates (63.3 to 80.1%).

5.4.11 Woodland within the base of **VC076** (3.95 mbsf) is dominated by *Betula* (53.9%) with only a minor contribution of other arboreal taxa including Salix (willow) (4.6%), *Pinus sylvestris* (2.6%) and *Corylus avellana* type (2%). Values for arboreal pollen decline at 3.87-3.8 accompanied by a significance increase in Cyperaceae (max. 76.8%), but with *Betula* remaining the key arboreal pollen taxa.

5.4.12 Cyperaceae values decline sharply from 3.8-3.7 mbsf (58.5 to 1.3%), with arboreal pollen increasing, particularly *Pinus sylvestris* (up to 50.7%) and *Corylus avellana* type (up to 29.3%) along with large quantities of undifferentiated fern spores (60 to 70%).

5.4.13 Non-arboreal pollen is also represented by small quantities of a limited diversity of herbaceous taxa including Apiaceae (carrots), Rubiaceae (bedstraws), Lactuceae (lettuces) and Aster type (daisies) (<1%).

5.4.14 Aquatic plants are indicated by small quantities of pollen, largely of *Potamogeton natans* type, along with *Sparganium emersum* type, *Typha latifolia* and *Menyanthes trifoliata* (bogbean).

5.4.15 The pollen assemblage suggests an open woodland flora within the base of **VC076** dominated by *Betula*. The subsequent dominance of Cyperaceae and Poaceae from 3.87-3.8 mbsf most likely reflects the local presence of a tall herb swamp expanding within the wetland, although Betula woodland is still indicated within the surrounding environment. The dominance of this reedswamp is short-lived, rapidly declining from 3.7 mbsf with the pollen instead indicating the presence of a *Pinus sylvestris–Corylus* avellana dominated woodland, with smaller quantities of *Betula*, *Ulmus* and *Quercus*. The large quantities of Pteropsida spores at 3.7-3.6 mbsf could reflect the ground flora of the forest floor, or represent grains of *Thelypteris palustris* that have lost their outer coating, growing as a component of the wetland flora, or a combination of the two. Patches of slow or still water, including boggy pools are suggested by aquatic plants, likely occurring as components of the Poaceae-Cyperaceae dominated herb swamp.

Table 6 Pollen assessment, vibrocore VC076 (percentages are followed in parenthesis by the number of grains counted for each taxon)

Taxa	Depth (mbsf)	3.6	3.7	3.8	3.87	3.95
Deposit						
Betula (Birch)		9.3 (14)	12.7 (19)	24.5 (36)	11.9 (18)	53.9 (82)
Pinus sylvestris (Pine)		50.7 (76)	33.3 (50)	3.4 (5)	2.6 (4)	2.6 (4)
Corylus avellana type (Hazel)		22.7 (34)	29.3 (44)	4.8 (7)	1.3 (2)	2.0 (3)
Quercus (Oak)		2.0 (3)	3.3 (5)	-	-	-
Ulmus (Elm)		3.3 (5)	3.3 (5)	0.7 (1)	0.7 (1)	-
Salix (Willow)		1.3 (2)	0.7 (1)	3.4 (5)	3.3 (5)	4.6 (7)
Ericaceae (Heathers)		-	2.0 (3)	-	-	-
Calluna vulgaris (Heather)		-	0.7 (1)	-	-	-
Poaceae (Grasses)		4.0 (6)	12.0 (18)	2.0 (3)	2.6 (4)	12.5 (19)
Cyperaceae (Sedges)		6.0 (9)	1.3 (2)	58.5 (86)	76.8 (116)	19.7 (30)
Filipendula (Meadowsweet)		-	-	2.0 (3)	-	2.0 (3)
Apiaceae (Carrots)		0.7 (1)	0.7 (1)	-	-	-

Taxa / Depth (mbsf)	3.6	3.7	3.8	3.87	3.95
Deposit					
Rubiaceae (Bedstraws)	-	-	-	0.7 (1)	-
Lactuceae (Lettuces)	-	-	-	-	0.7 (1)
Aster type (Daisies)	-	0.7 (1)	-	-	-
Artemisia type (Mugworts)	-	-	0.7 (1)	-	0.7 (1)
Anthemis (Chamomile)	-	-	-	-	1.3 (2)
Pteropsida undiff. (Undiff. fern spores)	70.6 (369)	60.3 (237)	1.3 (2)	-	-
Thelypteris palustris (Marsh fern)	0.6 (3)	1.5 (6)	-	-	-
Dryopteris filix-mas (Male fern)	0.2 (1)	-	-	0.7 (1)	-
Potamogeton natans type (Pondweed)	2.6 (4)	1.3 (2)	0.7 (1)	0.7 (1)	3.1 (5)
Sparganium emersum type (Unbranched bur-reed)	-	-	-	-	1.9 (3)
Typha latifolia (Bulrush)	0.6 (1)	0.6 (1)	-	-	-
Menyanthes trifoliata (Bog bean)	-	1.9 (3)	-	-	-
Sphagnum (Bog moss)	0.7 (1)	-	-	-	-
Pediastrum (Green algae)	4.5 (7)	-	-	-	-
Indeterminables	2.0 (3)	2.0 (3)	2.0 (3)	1.9 (3)	-
Total Land Pollen	150	150	147	151	152

VC085

5.4.16 Pollen is moderately well preserved through sequence **VC085** and present in moderate concentrations, apart from at 2.16 mbsf where pollen concentrations were very poor; a full assessment count was not possible at this depth.

5.4.17 The remaining four pollen samples (2.06 to 1.76 mbsf) are dominated by arboreal pollen taxa (82 to 89%), primarily *Pinus sylvestris* (29.3 to 43.3%) and *Corylus avellana* type (27.3 to 34%) with smaller quantities of *Quercus* (0.7 to 6.7%), *Ulmus* (0.6 to 4.7%) and *Salix* (1.3 to 3.3%). Small quantities of shrub (Rosa) type and dwarf shrub taxa (Ericaceae) were also recorded.

5.4.18 Non-arboreal pollen values are correspondingly lower, between 9 to 18% and primarily comprising Poaceae (5.3 to 12.7%) and Cyperaceae (2.7 to 4.7%) with smaller quantities of a restricted range of herbaceous taxa ≤1.3% (Rosaceae. Filipendula, *Potentilla*, Apiaceae, *Aster* type).

5.4.19 Significant quantities of fern spores were recorded from 2.06 mbsf and 1.96 mbsf, particularly undifferentiated fern spores (Pteropsida) (25.7 to 53.1%), declining to 13.7% at 1.76 mbsf, with moderate quantities of Thelypteris palustris (13.7% at 2.06 mbsf, declining to 3.8% at 1.76 mbsf).

5.4.20 Aquatic plants are represented by small quantities of pollen of *Potamogeton natans* type, *Sparganium emersum* type, *Typha latifolia* and *Myriophyllum* (watermilfoil). Small quantities of Pediastrum were recorded from 1.76-2.06 mbsf, but with significant quantities present in the basal sample at 2.16 mbsf.

5.4.21 The pollen assemblages are indicative of a predominantly wooded environment (*Pinus* and *Corylus*) with the herbaceous pollen most probably reflecting nearby areas of tall herb swamp including a mix of reeds, sedges and other herbs, and small open areas within the adjoining woodland. The large quantities of fern spores likely reflect both the flora of the woodland as well as the wetland. Patches of still and slow-moving water are suggested by the small quantities of aquatic pollen.

Table 7 Pollen assessment, vibrocore VC085 (percentages are followed in parenthesis by the number of grains counted for each taxon)

Taxa / Depth (mbsf)	1.76	1.86	1.96	2.06	2.16
Deposit					
Betula (Birch)	13.3 (20)	18.2 (29)	9.3 (14)	11.3 (17)	- (17)
Pinus sylvestris (Pine)	29.3 (44)	31.4 (50)	43.3 (65)	33.3 (50)	- (4)
Corylus avellana type (Hazel)	32.0 (48)	30.2 (48)	27.3 (41)	34.0 (51)	- (3)
Quercus (Oak)	6.7 (10)	2.5 (4)	0.7 (1)	2.7 (4)	-
Ulmus (Elm)	4.7 (7)	0.6 (1)	-	2.0 (3)	-
Salix (Willow)	3.3 (5)	1.9 (3)	1.3 (2)	1.3 (2)	-
Rosa type (Rose)	-	0.6 (1)	-	-	-
Ericaceae (Heathers)	1.3 (2)	-	-	-	-
Poaceae (Grasses)	5.3 (8)	9.4 (15)	12.7 (19)	9.3 (14)	(9)
Cyperaceae (Sedges)	2.7 (4)	4.4 (7)	4.7 (7)	4.0 (6)	-
Rosaceae (Roses)	-	-	-	-	(1)
Filipendula (Meadowsweet)	1.3 (2)	-	-	0.7 (1)	(1)
Potentilla (Cinquefoil)	-	0.6 (1)	-	-	-

Taxa / Depth (mbsf)	1.76	1.86	1.96	2.06	2.16
Deposit					
Apiaceae (Carrots)	-	-	0.7 (1)	1.3 (2)	-
Aster type (Daisies)	-	0.6 (1)	-	-	-
Pteropsida undiff. (Undiff. fern spores)	13.7 (25)	14.4 (27)	35.1 (92)	25.7 (64)	-
Thelypteris palustris (Marsh fern)	3.8 (7)	-	7.6 (20)	13.7 (34)	-
Pteridium (Bracken)	-	0.5 (1)	-	0.4 (1)	-
Potamogeton natans type (Pondweeds)	2.6 (4)	1.2 (2)	0.7 (1)	-	-
Sparganium emersum type (Unbranched bur-reed)	1.3 (2)	1.2 (2)	0.7 (1)	0.7 (1)	(2)
Myriophyllum (Watermilfoil)	0.0	0.0	0.0	0.7 (1)	(1)
Typha latifolia (Bulrush)	-	-	-	-	(1)
Pediastrum (Green algae)	14.3 (25)	6.5 (11)	6.8 (11)	4.5 (7)	(371)
Indeterminables	1.8 (3)	1.8 (3)	0.6 (1)	2.4 (4)	-
Total Land Pollen	150	159	150	150	35

5.5 Diatoms

5.5.1 Diatom assessment was undertaken on thirty-eight sub-samples, comprising ten sub-samples from both **VC079** and **VC107**, eight sub-samples from **VC074**, six sub-samples from **VC085** and four sub-samples from **VC076**. A summary of the assessment results is presented in **Table 8** with comments on potential for full diatom analyses. Where diatom preservation was suitable, more detailed assessment was undertaken and is presented in **Appendix 3**.

Table 8 Summary of diatom assessment results

Sample No	Depth (mbsf)	Diatoms	Abundance	Quality of preservation	Diversity	Assemblage type	Potential for % count
VC074							
D1	0.80	+	low	ex poor	low	fw with bk & mar	low/some
D2	0.85	+	mod	mod to poor	mod	fw	good
D3	1.24	+	mod	mod to poor	mod	fw	good
D4	1.30	+	ex low	ex poor	v low	fw	v low/none
D5	1.40	+	low	poor to v poor	mod	fw	low
D6	1.50	+	ex low	v poor	low	fw (hal)	v low
D7	1.61	+	low	v poor	mod	fw	v low

Sample No	Depth (mbsf)	Diatoms	Abundance	Quality of preservation	Diversity	Assemblage type	Potential for % count
D8	1.76	+	ex low	ex poor	v low	fw	v low
VC076							
D9	3.40	-	-	-	-	-	none
D10	3.50	-	-	-	-	-	none
D11	3.98	-	-	-	-	-	none
D12	4.08	-	-	-	-	-	none
VC079							
D13	0.40	+	ex low	ex poor	1 sp.	mar	none
D14	0.70	+	ex low	ex poor	low	mar	none
D15	1.40	+	ex low	ex poor	low	mar	none
D16	1.90	-	-	-	-	-	none
D17	2.10	-	-	-	-	-	none
D18	2.90	-	-	-	-	-	none
D19	3.40	-	-	-	-	-	none
D20	3.90	-	-	-	-	-	none
D21	4.40	-	-	-	-	-	none
D22	4.90	-	-	-	-	-	none
VC085							
D23	1.58	-	-	-	-	indet frag	none
D24	1.70	+	ex low	ex poor	ex low	mar fw	none
D25	2.14	-	-	-	-	-	none
D26	2.26	+	ex low	ex poor	1 sp.	aero	none
D27	2.38	+	ex low	ex poor	v low	fw aero hal	none
D28	2.50	+	ex low	ex poor	v low	fw hal	none
VC107							
D29	1.33	-	-	-	-	-	none
D30	1.80	-	-	-	-	-	none
D31	2.10	-	-	-	-	-	none
D32	2.50	-	-	-	-	-	none
D33	3.05	-	-	-	-	-	none
D34	3.50	-	-	-	-	-	none
D35	4.05	-	-	-	-	-	none
D36	4.50	-	-	-	-	-	none
D37	5.05	-	-	-	-	-	none
D38	5.50	-	-	-	-	-	none

Key: + = present; - = absent; mod = moderate; ex = extremely; bk = brackish; mar = marine; fw = freshwater; aero = aerophilous; hal = halophilous; acid = acidophilous; oligtr = oligotrophic; non-planktonic = non-pk; indet frag = indeterminant fragment

VC074

5.5.2 Eight sub-samples from **VC074** were assessed for diatoms at ~10 cm intervals from 0.80-1.76 mbsf. The location of the sub-samples was chosen to capture the transition through a peat deposit into underlying minerogenic deposits potentially deposited in a palaeochannel. Diatoms were present in all eight sub-samples.

5.5.3 Diatoms are poorly preserved and present in very low numbers in the lowermost five samples (D8 to D4 **Table 8**) (1.76 mbsf to 1.30 mbsf). The species diversity in these samples varies from very low to moderately high. However, the low diatom numbers and poor quality of valve preservation means there is low potential for further diatom analysis of samples D8 to D4. Diatom assemblages in samples D8 to D4 are composed of freshwater diatom taxa such as *Synedra ulna, Fragilaria pinnata, Cocconeis placentula, Amphora pediculus, Amphora libyca, Achnanthes kolbei, Navicula cari, Navicula elginensis, Navicula laterostrata* and *Aulacoseira ambigua*. Marine diatoms are absent from these samples.

5.5.4 In samples D3 and D2 (1.24 m and 0.85 mbsf), there are moderately high numbers of diatoms. The quality of diatom preservation varies from moderate to poor. Species diversity is moderately high and there is good potential to carry out percentage diatom analysis of these two samples. Again, the diatom assemblages are comprised of freshwater taxa; in particular the centric planktonic diatoms *Aulacoseira ambigua* and *Aulacoseira granulata* are common. These planktonic diatoms form filaments and represent freshwater habitats of moderate water depth and having moderate to low nutrient levels. Also present in samples D2 and D3 are non-planktonic diatoms from shallow water benthic, epiphytic and other attached habitats, including *Synedra parasitica*, *Amphora pediculus*, *Fragilaria brevistriata*, *Fragilaria construens*, *Epithemia turgida*, *Epithemia adnata*, *Navicula scutelloides* and *Sellaphora pupula*.

5.5.5 In the top sample from **VC074** (D1 0.80 m) there are low numbers of very poorly preserved diatoms which form an assemblage composed mainly of freshwater diatoms with some marine and brackish-marine taxa also present. The most common freshwater diatoms in D1 are, as for samples D2 and D3, the planktonic species *Aulacoseira granulata* and *Aulacoseira ambigua*. The benthic species *Navicula scutelloides* is present. Marine taxa are represented by the coastal planktonic species *Paralia sulcata* and girdle bands from *Grammatophora sp*. The brackish-marine species *Cyclotella striata* is also present. The poor preservation in sample D1 means that there is low potential for percentage diatom counting of this sample.

VC076

5.5.6 Four sub-samples from **VC076** were assessed for diatoms. These samples span the transition from peat to underlying fine sand deposits interpreted as possible Twente Formation. Diatoms were absent from all samples (**Table 8**).

5.5.7 The absence of diatom valves from this sequence can be attributed to taphonomic processes (Flower 1993, Ryves et al. 2001). This may be the result of diatom silica dissolution and breakage caused by factors such as extremes of sediment alkalinity or acidity, the under-saturation of sediment pore water with dissolved silica, cycles of prolonged drying and rehydration, movement of water, or physical damage to diatom valves from abrasion or wave action.

VC079

5.5.8 Ten sub-samples from Upper Brown Bank deposits in **VC079** were taken for diatom assessment (0.40-4.90 mbsf). Diatoms were absent from the lowermost seven samples (D16-D22; 1.90-4.9 mbsf). Again, this absence can be attributed to taphonomic processes (Flower 1993, Ryves et al. 2001).

5.5.9 An extremely low number of very poorly preserved diatoms are present in the top three samples (D13-D15; 0.40-1.40 mbsf). The diatom assemblages in these samples are of extremely low diversity and have no further potential for percentage diatom counting. However, the diatoms that are present are all polyhalobous (marine) taxa. The coastal

marine planktonic diatom *Paralia sulcata* is present and relatively common in all three samples. In addition, girdle bands of *Grammatophora sp*. are present in D14 and D15, with *Rhaphoneis surirella* in D14 and undifferentiated *Rhaphoneis sp*. in D14 and D15. Brackish and freshwater diatoms are absent from these samples.

VC085

5.5.10 Six sub-samples were assessed from core **VC085** for diatoms. The sub-samples span depths of 1.58-2.50 mbsf capturing a peat deposit and associated underlying and overlying minerogenic deposits of possible saltmarsh or intertidal origin. Diatoms were absent from sample D25 (2.14 mbsf) (**Table 8**) which lies at the top of the organic minerogenic saltmarsh deposits, in which possible higher plant fragments and *Pediastrum* sp. were recorded. An indeterminate diatom fragment was recorded in sample D23 (1.58 mbsf) which is located in the overlying intertidal deposit.

5.5.11 Extremely low numbers of extremely poorly preserved diatoms are present in samples D24, and D26 to D28 within the peat and underlying salt marsh. In samples D28, D27 and D26 the diatoms are freshwater, halophilous to freshwater or aerophilous (semi-terrestrial) species. These include *Epithemia sp*., *Epithemia turgida* and *Pinnularia* major. Marine and brackish water diatom taxa are absent from these samples. In sample D24 possible marine (*Paralia sulcata*) and freshwater (*Fragilaria pinnata*) diatom fragments were recorded along with a fragment of *Diploneis sp*. The poor quality of diatom preservation and extremely low diatom numbers of valves in the samples from **VC085** means that there is no further potential for percentage diatom analysis of this sequence.

VC107

5.5.12 Ten sub-samples from Upper Brown Bank deposits were taken from **VC107** (1.33-5.50 mbsf). Diatoms were absent from all sub-samples and there is no further potential for diatom analyses.

5.6 Foraminifera and Ostracods

5.6.1 The results of foraminifera and ostracod assessment of vibrocores **VC074**, **VC076**, **VC079**, **VC085** and **VC107** are presented here (**Table 9-13**), accompanied by an outline interpretation of past climatic and environmental conditions. Foraminifera and ostracods are recorded on a presence (x) or absence (-) basis, either as (o) one specimen, several specimen (x), abundant (xx) or superabundant (xxx). Where other palaeoenvironmental material (e.g. plant fragments) was observed within the sample residue, this was also noted in the assessment.

VC074

5.6.2 Eight sub-samples were investigated for formainifera and ostracods from **VC074** (**Table 9**). These sub-samples span the transition from lower minerogenic sediments interpreted to have been deposited within an early Holocene palaeochannel, into overlying peat deposits that show evidence of fluctuating water levels, or storm/flood events in the form of sand laminations.

5.6.3 No formainifera or ostracods were preserved in the lower minerogenic palaeochannel deposits (**Table 9**). However, the presence of plant debris and seeds/megaspores along with freshwater fish remains and opercula of *Bithynia* which is a freshwater gastropod, were noted. This material is easily reworked so may have been washed in, but does suggest a freshwater environment.

5.6.4 The peat deposit contains marine molluscs, echinoderm fragments (including whole small sea-urchins), marine foraminifera and ostracods, and freshwater ostracods. The microfauna is of a low diversity and generally uncommon. The deposit shows indications of reworking as the foraminifera, principally *Ammonia batavus* and miliolids, are very robust and of the same size and shape as the sediment grains. There are also reworked Crag Formation (Pliocene age) foraminifera within the samples. The peat contains the occasional specimen of *Sarsicytheridea bradii* which is a northern, cool/cold climate indicator species possibly suggesting the peat formed in a cooler climate. However, there is potential these specimens are also the result of reworking.

Table 9 Foraminifera and ostracod assessment, vibrocore VC074.

Depth in core (mbsf)	**0.80**	**0.85**	**1.24**	**1.30**	**1.40**	**1.50**	**1.61**	**1.76**
Deposit	**Peat**						**Palaeochannel**	
Micro/macro fossils preserved								
Peat/plant debris/seeds/megaspores	**x**	**x**	**x**	**x**	**x**	**x**	**x**	**x**
Molluscs	**x**	**x**	**x**	**x**	**x**			
Echinoderm fragments	**x**	**x**						
Marine foraminifera	**x**	**x**	**x**	**x**				
Freshwater ostracods	**x**	**x**		**x**				
Marine ostracods				**x**				
Reworked Crag foraminifera	**x**	**x**						
Bithynia opercula			**x**	**x**	**x**		**x**	
Fish remains			**x**	**x**	**x**		**x**	**x**
Insect remains			**x**	**x**		**x**		
Marine foraminifera								
Ammonia batavus	**x**	**x**	**x**	**xx**				
Miliolids	**x**							
Elphidium excavatum		**o**						
Freshwater ostracods								
Candona neglecta	**x**							
Limnocythere inopinata		**o**						
Darwinula stevensoni		**o**						
*Limnocytherina sanctipatricii**				**o**				
Marine ostracods								
*Sarsicytheridea bradii**				**o**				

* Cool/cold indicator species

VC076

5.6.5 Four sub-samples were assessed for foraminifera and ostracods from **VC076** (**Table 10**). One sub-sample was taken within the lowermost sands tentatively interpreted as possible Twente Formation deposited by periglacial aeolian processes. One sub-sample was taken near the base of the peat to capture the transition between the peat and underlying sands. Two sub-samples were taken in the overlying shelly sands interpreted to be marine.

5.6.6 No formainifera or ostracods were recorded in the sub-samples taken across the lower sand to peat transition. However, plant debris, seeds/megaspores and Charophyte oogonia (the reproductive organ of stonewort plants) were recorded. This indicates a freshwater environment, either a palaeochannel or shallow waterbody infilling depressions in the landscape.

5.6.7 Marine sands overlying the peat deposit contain molluscs, echinoderm fragments including whole small sea-urchins), and marine foraminifera and ostracods. Again, foraminifera of the Crag Formation (Pliocene age) are recorded and species diversity is low and dominated by *Ammonia batavus,* both suggestive of reworking.

Table 10 Foraminifera and ostracod assessment, vibrocore VC076.

Depth in core (mbsf)	**3.40**	**3.50**	**3.98**	**4.08**
Deposit	**Marine sands**		**Peat**	**Aeolian sands**
Micro/macro fossils preserved				
Molluscs (white)	**x**			
Molluscs (brown and polished)	**x**	**x**		
Echinoderm fragments	**x**			
Marine foraminifera	**x**	**x**		
Marine ostracods	**x**			
Reworked Crag foraminifera	**x**			
Peat/plant debris/seeds			**x**	**x**
Charophyte oogonia			**x**	**x**
Marine foraminifera				
Miliolids	**x**	**x**		
Ammonia batavus	**x**	**x**		
Marine ostracods				
*Sarsicytheridea bradii**	**o**			

* Cool/cold indicator species

VC079

5.6.8 Ten sub-samples were investigated for foraminifera and ostracods from **VC079** (**Table 11**). These samples span the breadth of clayey silt becoming clayey sand deposits interpreted as Upper Brown Bank.

5.6.9 All sub-samples show a rich and diverse microfauna of both foraminifera and ostracods (**Table 11**). Foraminifera are characterised as “marine and outer estuarine” species, these being largely marine but able to penetrate, and are frequently found in, large open estuaries and embayments. Certain species, for example *Elphidium williamsoni* and *Haynesina germanica* amongst the foraminfera, and *Leptocythere psammophila* amongst the ostracods can be found in brackish water with low salinity. This suggests deposition of the clayey silts of the Upper Brown Bank occurred in a shallow protected embayment or open estuary with a slightly lower than expected salinity for this setting, possibly due to a local freshwater influence.

5.6.10 Of noted interest is the occurrence of four species of ostracods (*Elofsonella concinna, Semicytherura undata, Robertsonites tuberculatus and Sarsicytheridea bradii*), particularly the common *Elofsonella concinna,* which are cool/cold climate indicators found today in Scandinavia whose southern limit is in northern Britain. A further two species of interest, *Hemicytherura clathrate* and *Finmarchinella angulate*, are also cold indicator species that have been extinct since the early Holocene.

5.6.11 The lowermost sample at a depth of 4.90 mbsf, was taken within a shelly sand deposit interpreted as Lower Brown Bank/Eem Formation. The sample shows the same diversity and presence of cool/cold indicator species as the overlying Upper Brown Bank. The age of this deposit is unknown. However, if it dates the Ipswichian interglacial (MIS 5e), it would imply this interglacial is characterised by subarctic conditions in the southern North Sea (Jones & Whittaker, 2010).

5.6.12 The foraminifera and ostracod assemblages suggest deposition in a cool/cold brackish, but low salinity, environment prior to the early Holocene. Establishing the age of these brown Bank Formation deposits is a necessity to understand the palaeogeographic configuration of the North Sea from the Ipswichian to early Devensian.

Table 11 Foraminifera and ostracod assessment, vibrocore VC079. LBK= Lower Brown Bank/Eem Formation)

Depth in core (mbsf)	**0.40**	**0.70**	**1.40**	**1.90**	**2.10**	**2.90**	**3.40**	**3.90**	**4.40**	**4.90**
Deposit	**Upper Brown Bank**									**LBK**
Micro/macro fossils preserved										
Marine molluscs	x	x	x	x	x	x			x	x
Marine and outer estuarine foraminifera	x	x	x	x	x	x	x	x	x	x
Marine and outer estuarine ostracods	x	x	x	x	x	x	x	x	x	x
Plant debris/peat/megaspores		x	x	x	x	x			x	
Insect remains					x					
Iron, iron tubes							x		x	
Freshwater ostracods							x			
Reworked Crag foraminifera									x	
Marine and outer estuarine foraminifera										
Ammonia batavus	xxx	xxx	xxx	xxx	xxx	xxx			xx	xxx
Miliolids	xx	xx	x	xx	x	xx	x	x		x
Elphidium williamsoni	x	xx	xx	x	x	x	x		o	
Elphidium exavatum	x	x	x		x	xx	x	x	x	
Elphidium margaritaceum	x			o			o			
Haynesina germanica	x		x	x			x	x		
Elphidium macellum	o				o					x
Lagenids		x	o			o		o		
Discorbids							o	x	o	
Marine and outer estuarine ostracods										

Depth in core (mbsf)	0.40	0.70	1.40	1.90	2.10	2.90	3.40	3.90	4.40	4.90
Deposit	**Upper Brown Bank**									**LBK**
*Elofsonella concinna**	xxx	xx	x	x	xx	xxx			o	o
Letocythere pellucida	x				o	x	o		x	
Pontocythere elongata	x		o	o		x				
Leptocythere psammophila	x	xx	xx	x	x	o				
Sclerochilusspp.	x	x	x	x		o			o	
Cytheropteron latissimum	x		o		o		o			
Cythere lutea	x	x				o	o		x	
*Hemicytherura clathrate***	x		x	x		x	x	x		o
Eucythere argus	x				o		o	o		
*Semicytherura undata**	x	o	x							
Semicytherura spp.	x	x	x	x	x	x	x			
Hirschmannia viridis	x	x	o	x	o	x				
Paradoxostomasp.	o	x	o	o						
Hemicythere villosa	o		o	x	o	x	x	x	x	x
Leptocythere tenera		x	x	x	x	o		x		
*Finmarchinella angulate***					o					
Leptocythere lacertosa						o		o		
*Robertsonites tuberculatus**						x			x	o
*Sarsicytheridea bradii**						o		o	x	x
Freshwater ostracods										
Cytherissa lacustris							o			

* Cool/cold indicator species ** Cold indicator, extinct in Britain since early Holocene

VC085

5.6.13 Six sub-samples were assessed for foraminifera and ostracods from **VC085** (**Table 12**). Four sub-samples were taken from an organic silty clay deposit, interpreted as a possible saltmarsh environment, underlying a peat deposit. Two sub-samples were located within a clayey sand deposit that overlies the peat.

5.6.14 Sub-samples taken below the peat do not contain any marine or brackish foraminifera and ostracods but do comprise freshwater ostracods, plant debris and charophyte oogonia (the reproductive organ of stonewort plants). These are interpreted to represent deposition in a spring-fed waterbody (Meisch, 2000), either a stream or channel associated with a larger river. The occurrence of charophyte oogonia suggests the water was shallow and clean.

5.6.15 Overlying the peat, the clayey sand preserves marine molluscs, echinoderm fragments, and a quite restricted marine foraminifera and ostracod assemblage (**Table 12**). One species of brackish ostracod *Cyprideis torosa* was recorded. It is not possible to determine if these species are *in situ*, thus indicating deposition in a marine environment, or if they have been reworked.

Table 12 Foraminifera and ostracod assessment, vibrocore VC085

Depth in core (mbsf)	1.58	1.70	2.14	2.26	2.38	2.50
Deposit	**Clayey sand (palaeochannel?)**		**Organic silty clay (saltmarsh?)**			
Micro/macro fossils preserved						
Molluscs	x	x				
Echinoderm fragments	x	x				
Marine foraminifera	x	x				
Marine ostracods	x	x				
Brackish ostracods	x	x				
Freshwater ostracods	x	x			x	x
Reworked Crag foraminifera	x				x	x
Peat/plant debris+seeds/megaspores			x	x	x	x
Charophyte oogonia				x	x	x
Marine foraminifera						
Ammonia batavus	xx	xx				
Miliolids	xx	xx				
Elphidium macellum	x	x				
Marine ostracods						
Pontocythere elongata	xx	xx				
Leptocythere pellucida	x	x				
*Elofsonella concinna**	x	o				
Heterocythereis albomaculata	x	o				
Hemicythere villosa	x	o				
Cythere lutea	o					
*Semicytherura undata**		o				
Brackish ostracods						
Cyprideis torosa	x	x				
Freshwater ostracods						
Ilyocypris bradyi	x	x			xx	xx
Herpetocypris reptans					xx	xx
Candona neglecta					xx	xx
Limnocythere inopinata					xx	xx
Cyclocypris ovum					x	x
Candona candida					x	
Potamocypris zschokkei						x
Eucypris pigra						x

* Cool/cold indicator species

VC107

5.6.16 Ten sub-samples were assessed for foraminifera and ostracods from **VC107** (**Table 13**). These samples span 5.2 m of Upper Brown Bank deposits within NV East.

5.6.17 As with **VC079**, these sub-samples show a rich and diverse microfauna of both foraminifera and ostracods (**Table 13**). The foraminifera and ostracods are characterised as "brackish outer estuarine" species, being potentially more brackish than those recorded in **VC079**. This interpretation is supported by the occurrence of such foraminifera as *Haynesina germanica, Elphidium williamsoni* and a small brackish *Ammonia* (undifferentiated). Ostracod preservation is low, possibly due to decalcification through weathering.

5.6.18 In terms of climatic conditions, the foraminifera contain cold/cool indicators (**Table 13**), including *Elphidium clavatum* and *Pseudopolymorphina novanangliae,* which have not been recorded in any other cores at NV West. Ostracods include the cool/cold water species *Finmarchinella angiulata* and *Sarsicytheridea bradii*. Ostracod preservation is low, possibly due to decalcification which can occur through weathering when tidal flats/banks are exposed.

5.6.19 The assemblages suggest deposition of the Upper Brown Bank in an outer estuarine brackish environment in a cooler than present-day climate. The relationship between Upper Brown Bank at **VC079** and **VC107** will depend on the age and elevation of the deposits relative to one another.

Table 13 Foraminifera and ostracod assessment, vibrocore VC107

Depth in core (mbsf)	**1.33**	**1.80**	**2.10**	**2.50**	**3.05**	**3.50**	**4.05**	**4.50**	**5.05**	**5.50**
Deposit	**Upper Brown Bank**									
Micro/macro fossils preserved										
Plant debris + seeds	x	x	x	x	x	x	x	x	x	x
Brackish/outer estuarine foraminifera	x	x	x	x	x	x	x	x	x	x
Brackish/outer estuarine ostracods	x	x	x	x	x		x	x		x
Insect remains		x	x							
Freshwater ostracods							x			
Brackish/outer estuarine foraminifera										
Haynesina germanica	x	xx	x	x	x	xx	x	o	x	x
Elphidium williamsoni	x	x	o		x	o	x			x
*Elphidium excavatum/clavatum**	x	x		x	x	x	x	x	x	x
Ammoniasp. (small)	o	o								
Miliolids			o	o	o		xx	x	x	x
*Pseudopolymorphina novangliae**				x	o	o	o			
Ammonia batavus								o		
Elphidium macellum									o	
Brackish/outer estuarine ostracods										
Ssmicytherura nigrescens	x									

Depth in core (mbsf)	1.33	1.80	2.10	2.50	3.05	3.50	4.05	4.50	5.05	5.50
Deposit	**Upper Brown Bank**									
Hirschmannia viridis	x	x								
Leptocythere psammophila	x				x					
Hemicythere villosa	x						o			
Cytheropteronsp.			x							
*Finmarchinella angiulata**				o						
Eucythere argus					o					
Leptocythere pellucida							o			
Sclerochilussp.							o			
*Sarsicytheridea bradii**							o	o		o
Freshwater ostracods										
Limnocythere inopinata							o			

* Cool/cold indicator species

5.7 Particle size distribution analysis

5.7.1 Three sub-samples for particle size distribution (PSD) analysis from vibrocore **VC076** were taken from the lowermost fine sand deposit interpreted as possible periglacial blown sands of the Twente Formation. The sub-samples were taken at depths of 3.99-4.01 mbsf, 4.13-4.15 mbsf and 4.20-4.24 mbsf. The results are presented in **Table 14** with their respective frequency histogram distributions given in **Appendix 4**.

Table 14 Results of particle size distribution analysis

Core	Depth (mbsf)	% Clay (0.01-2 µ)	% Silt (2-63 µ)	Sand (63-2000 µ)
VC076	3.99-4.01	1.56	28.24	70.21
	4.13-4.15	1.22	10.98	87.81
	4.20-4.24	1.18	11.29	87.53

5.7.2 The results of particle size distribution analysis confirm that all three sub-samples are fine sand and support qualitative descriptions made during Stage 2 recording. The results show there is a very minor clay component (1.58%) which may be related to organic matter along root traces from the overlying peat. The lowermost two sub-samples comprise ~11% silt whereas the upper sample comprises ~28% silt possibly reflecting the transition into overlying peat deposits.

5.7.3 Frequency distributions (**Appendix 4**) show all three samples are characterised by unimodal distributions which can be typical of wind-blown sediments (Ujvari et al. 2016). However, these distributions can also be seen in sediments deposited by river processes. The dominant grain size is fine sand which is coarser than would be expected for a periglacial wind-blown deposit. Furthermore, assessment of the grains under a binocular microscope showed they were transparent and well-rounded which is more typical of water-lain sediment as grains transported by wind tend to be more angular and opaque due to abrasion on their surface.

6 DISCUSSION

6.1 Introduction

6.1.1 The results from the vibrocores are considered collectively for each of the stratigraphic units highlighted as being of archaeological interest in the Stage 2 report, namely the pre-transgressive early Holocene peats and over/underlying minerogenic deposits, and Brown Bank Formation deposits. Deposits tentatively interpreted as periglacial aeolian sand of the Twente Formation were also targeted for Stage 3 assessment. Consideration is given to how the data addresses key research questions raised in the Stage 2 report (Wessex Archaeology 2018), regional research agendas (Medlycott 2011) and the national maritime research framework (Ransley et al. 2013), with recommendations for further analysis presented in **Section 7** below.

6.2 Brown Bank Formation

6.2.1 Brown Bank Formation was identified as having geoarchaeological potential during Stage 2 recording (WA 2018) as it comprises fine-grained deposits interpreted to have been deposited in a lagoon to intertidal environment, indicating shallow water in close proximity to a coast which may have been suitable for human exploitation. Brown Bank Formation is considered to have the potential to preserve *in situ* Lower Palaeolithic artefacts depending on its age. However, chronological information from these deposits is rare; and those dates that do exist suggest deposition during the Early/Middle Devensian (MIS 5d-MIS 3), potentially extending into the Late Devensian (Limpenny *et al.,* 2011). It is unknown if these dates represent continuous deposition, and thus continuous presence of a shallow lagoon in the southern North Sea over a long period of time, or if they represent punctuated shorter phases of deposition where the lagoon dried out periodically. The palaeogeography of the lagoon is also unknown making it difficult to locate or target the margins which would have greater potential for occupation and thus preservation of *in situ* artefacts. Therefore, to fully assess the archaeological potential of this Formation we need greater age control by way of absolute dating, and a stronger understanding of the paleogeographic configuration of this landscape, particularly as it corresponds to a time when humans were absent from Britain.

6.2.2 Variable thickness sequences of Brown Bank Formation were recovered in **VC074** (0.85 m), **VC079** (4.95 m), **VC085** (3.24 m) and **VC107** (5.48 m). **VC107** is the only vibrocore subject to Stage 3 assessment from NV East (**Figure 3**), all other Stage 3 vibrocores comprising Brown Bank Formation are located in NV West (**Figure 4**). **VC085** is located in the north-eastern part of NV West whereas **VC074** and **VC079** are located to the south (**Figure 4**).

6.2.3 According to interpretations of geophysical data (Wessex Archaeology 2017b), Brown Bank deposits in **VC074** have been eroded by a later phase of paleochannel development, and the vibrocore lies on the margin of a feature interpreted to represent erosion during the Devensian. The upper surface of Brown Bank Formation lies at elevations of -43.25 m LAT at **VC074**, -41.10 m LAT at **VC079** and -38.01 m LAT at **VC085** in NV West. At NV East, the elevation of the top of Brown Bank is shallower at -37.22 m LAT (**VC107)**.

6.2.4 Brown Bank Formation has been subdivided into an Upper Brown Bank (**Unit 5**) which is characterised by clayey silts and sands (**Table 2**), and a Lower Brown/Eem Formation (**Unit 4**) which is typically coarser grained and can comprise frequent shell fragments (**Table 2**). Deposits recovered from vibrocores in NV East and NV West predominantly recovered sediments interpreted as Upper Brown Bank with the exception of **VC079** where deposits from 4.55-5.25 mbsf showed characteristics of Lower Brown Bank/Eem deposits. These

sediments were deemed unsuitable for OSL dating as they had been exposed to light and showed evidence of core disturbance which meant it could not be guaranteed that the inner core used for OSL dating was undisturbed.

6.2.5 However, foraminifera, ostracod and diatom analyses were undertaken on a sub-sample (4.90 mbsf) from these potential Lower Brown Bank/Eem Formation deposits. Diatoms were absent from the sample but the presence of marine and outer estuarine foraminifera was recorded (**Table 11**) suggesting a shallow marine depositional environment. These assemblages did not differ significantly from overlying Upper Brown Bank deposits making it difficult to characterise between Upper and Lower Brown Bank using microfauna alone. To fully assess the geoarchaeological potential of Brown Bank Formation there is a need to determine whether the coarser-grained sediments at the base of Brown Bank were deposited during the Ipswichian (MIS 5e) interglacial or early Devensian (MIS 5d-5a) which can potentially be achieved by OSL dating undisturbed vibrocores recovered during future geotechnical campaigns.

6.2.6 During Stage 2 geoarchaeological recording, interpretation of depositional environment was based on sediment descriptions alone. The fine-grained nature of Upper Brown Bank deposits, coupled with rare organics, shell fragments and fine laminations led to the interpretation of a low energy shallow water environment potentially influenced by tidal currents. The landscape was thus interpreted as a lagoon. However, the configuration of this lagoon is unknown and there is no evidence preserved or mapped of a barrier system that would have afforded protection from the sea allowing the lagoon to form. The results of foraminifera, ostracod and diatom assessments can be used to test interpretations of palaeoenvironment.

6.2.7 Sub-samples were taken from Brown Bank Formation deposits in **VC079** and **VC107**. Diatoms were absent from all but three samples (**VC079** D13-D15; 0.40-1.40 mbsf) where poorly preserved, low diversity marine taxa are recorded. In contrast, a rich and diverse assemblage of foraminifera and ostracods was observed (**Table 11** and **Table 13**) in both cores. In NV West, **VC079** comprises formaminifera and ostracod species typical of marine and outer estuarine environments commonly found in large open estuaries or embayments close to a freshwater input (i.e. not fully marine). In NV East, **VC107** located 35 km east of **VC079** records brackish and outer estuarine species of foraminifera and ostracod, suggesting a more brackish setting than NV West. If these deposits are the same age, it would suggest freshwater input was to the east, although this is based on only two site locations and assessment of other vibrocores would be required to test this. Furthermore, the source of freshwater is unknown but could be related to drainage of large rivers such as the Rhine, or meltwater from ice, although ice margins are expected to be located further to the north.

6.2.8 Of significance, both **VC079** and **VC107** comprise species of ostracod and foraminifera that are indicative of cold/cool climates with temperatures lower than present-day (**Tables 11 and 13**). In **VC107**, foraminifera species *Elphidium clavatum* and *Pseudopolymorphina novanangliae* are also indicative of cool climates. In **VC079**, species *Hemicytherura clathrate* and *Finmarchinella angulate* are cold indicator species that have been extinct in southern Britain since the early Holocene.

6.2.9 Five OSL dates were obtained from Upper Brown Bank deposits from **VC074**, **VC079**, **VC085** and **VC107** (**Table 4**). The two ages from **VC079** have been tentatively accepted but should be interpreted with caution as they failed validity tests. The age from **VC107**, should be interpreted as a minimum age estimate due to feldspar contamination. **VC079** and **VC107** recovered the thickest sequences of Upper Brown Bank (4.95 m and 5.48 m

respectively) and they demonstrated high potential for preservation of foraminifera and ostracods. Therefore, additional dating of these key cores is recommended.

6.2.10 The OSL ages from **VC074** and **VC085** have been accepted with no limitations. However, these cores have not undergone foraminifera and ostracod assessment due to recovery of relatively thinner sequences. It is therefore, recommended sub-samples are taken from these cores for foraminifera and ostracod assessment.

6.2.11 Considering the three accepted OSL ages (**VC074** and **VC085**), deposition of Upper Brown Bank occurred between 82.4 ± 8.5 and 57.2 ± 6.4 ka spanning MIS 5a to MIS 3 which is a period during the early Devensian where temperatures and sea level started to fall towards the Last Glacial Maximum (LGM) of MIS 2. The three tentative OSL dates (GL17078, GL17079 and GL17080) fall within this age range and will be discussed accordingly.

6.2.12 The oldest date (GL17081 82.4 ± 8.5) comes from **VC074** at an elevation of -43.50 m LAT located in the south-west corner of NV West. An isopach map (or digital elevation model) showing the morphology of the topography filled in by Brown Bank Formation was created by Fugro (2017a). This map shows Brown Bank is thicker towards the west of NV West where it appears to fill large channels/depressions (possibly tunnel valleys). Brown Bank Formation thins both northwards and eastwards across NV West. Core **VC074** is located within this channel feature but shows evidence of post-depositional erosion by a later Early Holocene palaeochannel. This may explain why **VC074** is older than the more northerly deposits of Upper Brown Bank in **VC085**, whereby erosion removed the upper younger deposits exposing older sediment below. However, it is also possible sediments were deposited in the deeps (**VC074**) first and then as sea level continued to rise it would have flooded the higher ground (**VC085)** at a later date.

6.2.13 Considering all six OSL dates, of interest is five (including two tentative ages GL17079 and GL17080) out of the six dates correlated to the transition from MIS 4 to MIS 3. This period saw fluctuations in global sea level between approximately -90 m to -70 m (Lisiecki and Raymo 2005) (**Figure 2**). The elevation at which the OSL ages were obtained ranges from -43.50 m LAT to -37.98 m LAT which suggests locally relative sea level was higher than the global average if sediments across Norfolk Vanguard were being deposited in an open estuary to embayment type setting at the time. However, this interpretation is caveated given uncertainly surrounding relative sea level reconstructions and post-depositional changes in land level as a result of Devensian ice dynamics.

6.2.14 The remaining date (**VC074**) correlates to MIS 5a when relative sea levels are expected to be higher (-40 m) (**Figure 2**). At this location, the age (82.4 ± 8.5 ka) and elevation (-43.50 m LAT) of the sub-sample corresponds the expected sea level (-40 m; Lisiecki and Raymo 2005) at this time.

6.2.15 The dating evidence from Norfolk Vanguard suggests Brown Bank deposits accumulated over a period of ~25,000 years during the early Devensian. However, the ages do not provide enough chronological control to test if this was the result of continuous deposition, or punctuated phases of deposition during MIS 5a and MIS 4-3.

6.2.16 To summarise the results of this Stage 3 geoarchaeological assessment, Upper Brown Bank within NV East and NV West is the product of deposition of fine-grained sediments in an open estuary to embayment setting under sub-arctic climate conditions between MIS 5a and MIS 3.

6.3 Twente Formation deposits

6.3.1 Deposits associated with the Twente Formation were identified as having geoarchaeological potential as they are indicative of deposition by wind in a cold periglacial terrestrial environment. Twente Formation is stratigraphically younger than Brown Bank and thus marks a period during the early Devensian when the shallow embayment became dryland. The age of this event is important for understanding the timing of land connections between Britain and Europe when considering migration pathways through the southern North Sea.

6.3.2 In core **VC076**, sand rich deposits underlying a peat were tentatively interpreted as Twente Formation and sub-samples were submitted for particle size distribution analysis to corroborate interpretations of depositional environment. The results suggest the sand is coarser grained than would be expected for a wind-blown deposit, and observations of grain characteristics at microscopic level suggest the sand was transported by water rather than wind. Therefore, this sand more likely reflects deposition in a channel or floodplain environment prior to peat development in the early Holocene. Diatoms, foraminifera and ostracods were absent from this deposit making it difficult to corroborate interpretations. However, similar deposits are observed underlying the peat in **VC074**.

6.4 Early Holocene pre-transgression deposits

6.4.1 Early Holocene pre-transgressive deposits were identified as having geoarchaeological potential during Stage 2 geoarchaeological recording. These deposits comprise terrestrial peats and associated minerogenic deposits interpreted as being deposited in palaeochannels and saltmarsh environments. Preservation of palaeonvironmental material is expected to be high and these deposits have the potential to record the progressive inundation of terrestrial landscapes in the southern North Sea which can be used to inform paleogeographic reconstructions. Previous mapping of geophysical data suggests these deposits may be preserved within paleochannels which are of archaeological interest due to their potential to preserve derived or *in situ* Upper Palaeolithic to Early Mesolithic artefacts, particularly on channel margins or floodplains.

6.4.2 Early Holocene pre-transgressive deposits were recovered in **VC074**, **VC076** and **VC085** all of which are located within NV West. These deposits are thickest in **VC074** thinning to 1.61 m in **VC085** and 0.75 m in **VC076**. The thickest sequence of peat is 0.80 m in **VC074** which is located within a palaeochannel mapped from geophysical data (**Figure 4**) (Wessex Archaeology 2017b) in the southwest corner of NV West. **VC076** and **VC085** are located further north and cannot be definitively tied to palaeochannel features (**Figure 4**). However, they are located in an area underlain by an extensive high amplitude reflector observed on geophysical data interpreted to represent a blanket peat deposit (**Figure 4**).

6.4.3 Early Holocene pre-transgressive deposits (**Unit 7**) can be subdivided into lower palaeochannel deposits (**VC074**), lower saltmarsh deposits (**VC085**), terrestrial peat deposits (**VC074**, **VC079** and **VC085**) and upper intertidal channel deposits (**VC085**). The paleoenvironmental interpretation and age of each of these subunits will be discussed below.

6.4.4 In **VC074** a 3.17 m thick deposit of clayey, silty fine sand was recovered within a palaeochannel feature. Due to the non-organic nature of this deposit, sub-samples were taken for diatom, foraminifera and ostracod assessment near the boundary with the overlying peat. Foraminifera and ostracods were absent from the sub-samples (**Table 9**) and diatom preservation was very low (**Table 8**) making these sub-samples unsuitable for Stage 4 analysis. Of the diatom fragments identifiable, species assemblages are indicative

of a freshwater environment supporting the interpretation these sediments were laid down in a river channel.

6.4.5 Underlying the peat deposit in **VC085** lies a 0.51 m thick sequence of very organic silty clay that was tentatively interpreted as being deposited in a saltmarsh environment. Sub-samples were taken for diatom, foraminifera and ostracods assessment and a single sub-sample was taken for pollen assessment to test preservation potential in this organic clay. Foraminifera were absent from samples (**Table 12**) but freshwater species of ostracods (**Table 12**) and diatoms (**Table 8**) were observed, along with plant debris (**Table 12**). Pollen preservation was poor (**Table 7**). If this organic clay was deposited in a saltmarsh environment, brackish and potentially marine species of diatoms, foraminifera and ostracods would be expected. However, the palaeoenvironmental assessment has uncovered freshwater species suggesting a more terrestrial environment. The vibrocore is located close (300 m) to margins of a palaeochannel (**Figure 4**), therefore this organic clay (or gyttja) may represent a floodplain environment prior to peat development, as appose to a saltmarsh.

6.4.6 Sub-samples were taken from peat deposits in **VC074**, **VC076** and **VC085** for pollen assessment and two sub-samples from each core, taken at the top and base of the peat were submitted for radiocarbon dating (**Table 3**). In **VC074**, sub-samples were also taken for diatom, foraminifera and ostracod assessment due to the presence of thin beds of sand possibly washed in during flood or storm events.

6.4.7 The peat preserved in **VC074** which is located within a palaeochannel (**Figure 4**) has been radiocarbon dated to between 10416 and 9918 cal. BP (**Table 3**). Pollen assessment suggests an open woodland canopy dominated by pine and hazel with smaller quantities of elm and oak. Pollen of grasses and sedges most likely derive from the wetland flora growing within the peat-infilling channel where slow or standing water is suggested by pollen of pondweeds, bur-reeds and bulrushes.

6.4.8 Sub-samples taken for diatom, foraminifera and ostracod assessment of sandy laminations within the peat in **VC074** returned variable results. Diatoms were present in all samples but typically in low numbers (**Table 8**). The diatoms that were present indicated a freshwater environment with the exception of 0.80 mbsf where freshwater, brackish and marine species were observed, indicating an increasing marine influence before the peat was inundated by sea-level transgression. Foraminifera were absent from samples at depth but the marine species *Ammonia batavus* (**Table 9**) was identified in the upper four sub-samples. This species, along with miliods, are very robust and of the same size and shape as the sediment grains which is particularly indicative of reworking. This micro fauna was likely washed in with the sand lenses which are interpreted to represent storms events close to the coast.

6.4.9 The pollen assessment from **VC076** also suggests an open woodland flora, although initially dominated by birch, followed by an increase in pollen of sedges and reeds derived from local tall-herb swamp, and later by pine and hazel-dominated woodland similar to **VC074**.

6.4.10 The top of the peat in **VC076** dates to between 10208-9911 cal. BP (**Table 3**), broadly comparable to the top of the peat in **VC074**. However, the basal date of 13781-13556 cal. BP would place peat formation within the latter stages of the Windermere Interstadial (termed Bølling Allerød Interstadial on the Continent, approximately 15-13 ka). Such an early date for peat formation appears highly unlikely, suggesting an erroneous date, possibly due to reworking or intrusion of earlier material, or contamination due to hard and/or soft water errors.

6.4.11 The pollen assessment from **VC085** suggests a predominantly wooded rather than open woodland environment, although again comprising pine and hazel with nearby areas of tall herb swamp. The base of the peat dates to between 10169-9744 cal. BP (**Table 3**) which is comparable to the uppermost peat dates in **VC076** and **VC074**. However, the upper date is 12091-11707 cal. BP (**Table 3**), which is again older than expected given the vegetation history, but the dates are also inverted. It is unknown if this is due to reworking of the upper peat, hard/soft water contamination, or a combination of both.

6.4.12 Together these three peat sequences provide a comparable picture of the regional and local landscape, with areas of dry ground covered by pine-hazel dominated woodland with stands of birch. Both pine and birch are pioneer species and require relatively open conditions with limited species competition, aided by the production of large quantities of lightweight and buoyant seeds that are dispersed widely and grow fast. All three sequences including an increasing contribution of pollen from oak and elm towards the tops of the peat as these trees began to migrate into the southern North Sea basin from their glacial refugia to the south. Ferns and grasses are likely to have formed a component of the ground flora of this woodland, with other grass pollen and fern spores likely reflecting reeds and marsh ferns growing within adjacent areas of wetlands characterised by tall-herb swamp.

6.4.13 One of the key questions outlined in the Stage 2 works focused on determining whether the peat deposits present at NV West represent one broadly contemporary phase of peat formation or separate phases of peat formation in distinct ecological niches. The pollen suggests a degree of contemporaneity in the vegetation records (all containing pine-hazel dominated woodland), although the higher values for birch pollen in the base of **VC076** suggests this sequence may pre-date the peat in **VC074** at a time before birch is superseded by pine as the dominant woodland component.

6.4.14 However, the radiocarbon dates and pollen are not in complete agreement. The base of the peat in **VC076** dates to the Windermere Interstadial (13781-13556 cal. BP) which may reflect inclusion of reworked material of interstadial date into an early Holocene peat, or the influence of hard and/or freshwater errors that can produce erroneously old dates.

6.4.15 The two radiocarbon dates from **VC085** are inverted, with the upper date likewise of a spuriously earlier date within the Younger Dryas – a period of cold temperatures at the end of the last Ice Age when one would not expect conditions to favour peat formation.

6.4.16 The radiocarbon dates from **VC074** are however in close agreement with the vegetation signal for an early Holocene environment. It is very likely therefore that the peats collectively represent a contemporary phase of peat formation even though this is not conclusively demonstrated by the radiocarbon dates in **VC076** and **VC085**.

6.4.17 The peat deposits in **VC074** have significant further potential for investigating the physical evolution of the landscape during the early Holocene. Pollen is well-preserved and present in moderate concentrations. There is less potential for further analysis in **VC076** and **VC085** where pollen was more poorly preserved and present in lower pollen concentrations, with further concerns raised by spuriously early and inverted radiocarbon dates.

6.4.18 In **VC085**, the peat is overlain by a 0.74 m sequence of fine sand with clay laminations interpreted as being deposited in an intertidal channel. Two sub-samples were taken within this deposit for diatom, foraminifera and ostracod assessment. Diatoms were absent from the upper sub-sample and fragments of marine diatoms were recorded in the lower sample (**Table 8**). Foraminifera and ostracods were present in both sub-samples and species indicate a marine environment. More brackish species would be expected if this was an

intertidal channel deposit whereas the results suggest a marine dominated environment. These sediments were likely deposited in a shallow marine setting as NV West became inundated as sea levels rose. The timing of inundation in this core is unknown due to an erroneously old radiocarbon date at the top of the peat.

6.4.19 The peat deposit in **VC074** implies an increasing marine influence near the top demonstrated by the presence of storm inundation deposits and increasingly brackish and marine diatom assemblages. The peats are overlain by late Holocene marine sands (**Unit 8**) and the sharp boundary between the deposits likely represents sea-level transgression across Norfolk Vanguard. The date at the top of the peat is 10226-9918 cal. BP at -39.40 m LAT which is comparable to model predictions for the date of inundation in this part of the southern North Sea (Sturt *et al.* 2013). A similar age of 10208-9911 cal. BP was obtained for the top of the peat in **VC076** which is also overlain by marine sands (**Unit 8**), again supporting the model of inundation across Norfolk Vanguard during the early Holocene.

7 RECOMMENDATIONS

7.1 Introduction

7.1.1 Recommendations for Stage 4 analysis of geoarchaeological units of interest are discussed here, principally Brown Bank Formation (**Unit 5**), Twente Formation (**Unit 6**) and Early Holocene pre-transgression deposits (**Unit 7**). Recommendations are made to address outstanding research questions raised during this Stage 3 assessment (**Table 15**), taking into account the regional research agendas (Medlycott 2011) and the national maritime research framework (Ransley et al. 2013). Stage 4 recommendations are itemised in **Table 16**.

Table 15 Table 16 summary of progress against research questions proposed during Stage 2.

What is the depositional history of the Brown Bank Formation?	
Answer	Deposited in a marine embayment to open estuary type setting under subarctic climatic conditions during the early to mid-Devensian (MIS 5a to MIS 3)
Outstanding question(s)	What is the palaeogeographic configuration of this embayment and associated coastlines?
Archaeological importance	Preservation of in-situ or derived artefacts within Brown Bank deposits is expected to be low. The margins of the embayment/estuary may have been suitable for occupation and exploitation.
Further work	Foraminifera and ostracod assemblages were rich and diverse and results suggest the Brown Bank deposits were more brackish in NV East suggesting a palaeoshoreline was possibly located to the east. Additional foraminifera and ostracod assessment on Brown Bank deposits in **VC074** and **VC085**, which produced the most reliable OSL dates, may reinforce this interpretation.
Did Brown Bank Formation form relatively quickly in the early Devensian or accumulate as a more gradual deposit?	
Answer	OSL results suggest deposition occurred over a period of ~25 ka during the early to mid-Devensian.
Outstanding question(s)	Was deposition continuous over this time period or did deposition occur in phases punctuated by periods of subaerial exposure, non-deposition and/or erosion? Did the Brown Bank embayment create an obstacle for human migration through the southern North Sea during the early to mid-Devensian?
Archaeological importance	If deposition was continuous it suggests the Brown Bank embayment was persistent in the landscape for ~25 ka corresponding to a time period when humans were absent from Britain.

Further work	The resolution of chronological information acquired to date is not sufficient to address the outstanding questions. Therefore, additional dating is required.
Do the preserved peats represent a contemporary phase of peat formation across the entire site, or separate phases of peat formation within discrete environmental niches?	
Answer	Pollen assessments imply peat development was broadly contemporaneous across the site occurring during the early Holocene. However, radiocarbon dates were inconclusive due to three potentially erroneous ages making it difficult to fully address this question.
Outstanding question(s)	Was peat development contemporaneous across the site? What is the vegetation and landscape history?
Archaeological importance	This will provide a landscape context for any human activity in the area and enable assessments of the availability of resources and habitats for human settlement and exploitation.
Further work	Higher resolution pollen sample interval and statistically valid analysis, combined with higher resolution age control, which allow these questions to be addressed.

7.2 Brown Bank Formation

7.2.1 The most reliable OSL dates came from Upper Brown Bank deposits in **VC074** and **VC085**. However, assessments of diatoms, foraminifera and ostracods were not undertaken on these cores. Diatoms were absent from Upper Brown Bank in **VC079** and **VC107** so are not recommended for further assessment and analysis. However, foraminifera and ostracods were preserved.

7.2.2 It is recommended assessment of foraminifera and ostracods is undertaken on **VC074** and **VC085** a to provide a palaeonvironmental context to the OSL ages and help assess spatial variability in environmental conditions across NV East and NV West.

7.2.3 The results of foraminifera and ostracod assessments in **VC079** and **VC107** revealed a rich and diverse assemblage of marine, outer estuarine and brackish species suggesting Upper Brown Bank sediments were deposited in an embayment or open estuary. The potential for preservation of *in situ* or derived archaeological material in these deposits is expected to be low. However, the impact the palaeogeographic configuration of this embayment would have had on human migration pathways from North West Europe to Britain is significant.

7.2.4 OSL dates from Upper Brown Bank deposits across Norfolk Vanguard suggest this embayment was a fixture in the landscape from 82.4 ± 8.5 and 57.2 ± 6.4 ka spanning MIS 5a to MIS 3. These dates are significant as they correspond to in the late Middle Palaeolithic, and span a period of human absence, and then reappearance, in Britain. It remains unclear if this embayment was a permanent fixture in the southern North Sea landscape through the late Middle Palaeolithic, or if it periodically dried out creating pathways for migration from North West Europe.

7.2.5 Therefore, it is recommended an additional OSL date is obtained from the base of Upper Brown Bank in **VC107**, an a further OSL date from **VC079,** to help refine the chronology as initial ages have been only tentatively accepted due to experimental considerations.

7.3 Twente Formation

7.3.1 The results of particle size distribution analysis combined with an assessment of grain characteristics support an alternative interpretation for deposits identified as Twente Formation during Stage 2 geoarchaeological recording. It is suggested the minerogenic sand deposits underlying peat deposits in **VC076** are palaeochannel or floodplain deposits most likely deposited during the early Holocene. As diatoms, ostracods and foraminifera are absent from these deposits, no further analysis is recommended.

7.4 Early Holocene pre-transgression deposits

7.4.1 Diatoms preserved in **VC074** show potential for Stage 4 full analysis within early Holocene pre-transgression lower palaeochannel deposits. However, the assessment results have provided sufficient information to characterise depositional environment. Therefore, no additional diatom analyses of these deposits are recommended.

7.4.2 Diatoms were also preserved in newly interpreted floodplain deposits characterising the lowermost early Holocene pre-transgression deposits in **VC085**, However, abundance and quality of preservation is low and Stage 4 analysis is not recommended.

7.4.3 Foraminifera were absent from early Holocene pre-transgressive deposits in **VC085** but were present in the peat at **VC074** where marine reworked species were recorded. Due to the potential for reworking, no further foraminifera assessment or analysis is recommended on early Holocene pre-transgressive deposits.

7.4.4 The preservation of ostracods in early Holocene pre-transgressive deposits is typically higher than diatoms or foraminifera. However, the ostracods were used to determine depositional environment, particularly in relation to water quality (fresh vs marine). The results of Stage 3 assessment are sufficient for paleoenvironmental interpretation and no further analysis is recommended.

7.4.5 Pollen has been found to be moderately well preserved in **VC074**, **VC076** and **VC085**, with moderate pollen concentrations in **VC074** and **VC085.** Low pollen concentrations in **VC076** make it unsuitable for Stage 4 analysis. Radiocarbon dates in **VC085** are inverted. Therefore, **VC074** is the only core comprising early Holocene pre-transgression deposits considered suitable for Stage 4 analysis.

7.4.6 It is recommended the existing 8 assessment samples from **VC074** are taken to full analysis stage, and that an additional eight sub-samples are taken for full pollen analysis to provide a high-resolution record of vegetation development, and broader palaeolandscape change over the course of the early Holocene.

7.4.7 To provide a robust chronological framework for this early Holocene sequence, it is recommended an additional two sub-samples are submitted for radiocarbon dating and all chronological results analysed using Bayesian modelling techniques.

Table 16 Recommendations for Stage 4 paleoenvironmental analysis.

Core	OSL Dating	Radiocarbon dating	Pollen (analysis)	Foraminifera and ostracods
VC074	-	2	16	4
VC076	-	-	-	-
VC079	1	-	-	-
VC085	-	-	-	4
VC107	1	-	-	-
Total	**2**	**2**	**16**	**4**

8 BIBLIOGRAPHY

Adamiec, G. and Aitken, M.J. (1998) Dose-rate conversion factors: new data. *Ancient TL*, 16, 37-50.

Ashton, N., Lewis, S G., De Groote, I., Duffy, S M., Bates, M., Bates, R., Hoare, P., Lewis, M., Parfitt, S A., Peglar, S., Williams, C., and Stringer, C, (2014). Hominin Footprints from Early Pleistocene Deposits at Happisburgh, UK. In: *PLoS ONE*, 9 (2), e88329.

Athersuch, J., Horne, D.J. & Whittaker, J.E. 1989. Marine and brackish water ostracods. *In:* Kermack, D.M. and Barnes, R.S.K. (eds), *Synopsis of the British Fauna (New Series)*, no. 43. E.J. Brill, Leiden (for the Linnean Society of London and The Estuarine and Brackish-water Sciences Association), 359pp.

Battarbee, R.W., Jones, V.J., Flower, R.J., Cameron, N.G., Bennion, H.B., Carvalho, L. & Juggins, S. 2001. Diatoms. In (J.P. Smol and H.J.B. Birks eds.), *Tracking Environmental Change Using Lake Sediments Volume 3: Terrestrial, Algal, and Siliceous Indicators*, 155-202. Dordrecht: Kluwer Academic Publishers.

Bennett, K.D. Whittington, G. and Edwards, K.J., 1994, Recent plant nomenclatural changes and pollen morphology in the British Isles. *Quaternary Newsletter,* 73, 1–6.

Blott, S, Croft, D.J, Pye, K, Sayene, S.E, and Wilson, H.E. (2004) Particle Size Analysis by Laser Diffraction. *Forensic Geoscience: Principles, Techniques and Applications* **232**, 63-73

Bronk-Ramsay, C., 2009. *OxCal calibration programme version v4.10*. Radiocarbon accelerator Unit, University of Oxford.

Cameron, T D J., Crosby, A., Balson, P S., Jeffery, D H., Lott, G K., Bulat, J. and Harrison, D J, (1992). *The Geology of the Southern North Sea.* British Geological Survey United Kingdom Offshore Regional Report. London, HMSO.

Crombé, P., Van Strydonck, M., Boudin, M., Van den Brande, T., Derese, C., Vandenberghe, D A G., Van den Haute, P., Court-Picon, M., Verniers, J., Gelorini, V., Bos, J A A., Verbruggen, F., Antrop, M., Bats, M., Bourgeois, J., De Reu, J., De Maeyer, P., De Smedt, P., Finke, P A., Van Meirvenne, M., and Zwertvaegher, A, (2012). Absolute Dating (^{14}C and OSL) of the Formation of Coversand Ridges Occupied by Prehistoric Hunter-Gatherers in NW Belgium. *Radiocarbon*, 54(3-4), 715-726.

Cooper, W S., Townsend, I H., and Balson, P S, (2008). *A Synthesis of Current Knowledge on the Genesis of the Great Yarmouth and Norfolk Bank Systems*. The Crown Estate.

EMU Limited, (2009). *The Outer Thames Estuary Regional Environmental Characterisation*, London, GB ALSF/MEPF (DEFRA).

EMU Limited (2013). *East Anglia FOUR Offshore Wind Farm Geophysical Survey Report*. Unpublished Client Report, Ref: 12/J/1/02/2066/1346 FINAL.

Flower, R.J. 1993. Diatom preservation: experiments and observations on dissolution and breakage in modern and fossil material. *Hydrobiologia 269/270*: 473-484.

Fugro, (2016). *Measure and derived geotechnical parameters and final results. Annex 1 – vibrocore photographs. Norfolk Vanguard Offshore Windfarm Geotechnical investigation report, UK Continental Shelf, North Sea*. GEO50/R2/Rev.1

Fugro (Fugro Survey B.V.) (2017a). *Report 1 of 3: Geophysical Investigation Report. Volume 2 of 3: Geophysical Survey Report. Norfolk Vanguard Offshore Wind Farm*. Unpublished report, ref. GE050-R1.

Fugro, (2017b). Report 2 of 3: Geotechnical Investigation Report: *Measured and derived geotechnical parameters and final results.* Unpublished Report, ref. GEO50/R2/Rev.2

Fugro (Fugro Survey B.V.) (2017c). *Report 1 of 3: Geophysical investigation report. Volume 1 of 3: Operations & Calibrations. Norfolk Vanguard Offshore Wind Farm*. Unpublished report, ref. GE050-R1.

Újvári, G., Kok, J.F., Varga, G. & Kovács, J. 2016. The physics of wind-blown loess: Implications for grain size proxy interpretations in Quaternary paleoclimate studies, *Earth-Science Reviews*, 54: 247-278.

Hartley, B., H.G. Barber, J.R. Carter & P.A. Sims. 1996. *An Atlas of British Diatoms.* Biopress Limited. Bristol. pp. 601.

Hendey, N.I. 1964 *An Introductory Account of the Smaller Algae of British Coastal Waters. Part V. Bacillariophyceae (Diatoms)*. Ministry of Agriculture Fisheries and Food, Series IV. pp. 317.

Hustedt, F. 1953. Die Systematik der Diatomeen in ihren Beziehungen zur Geologie und Okologie nebst einer Revision des Halobien-systems. *Sv. Bot. Tidskr.*, 47: 509-519.

Hustedt, F. 1957. Die Diatomeenflora des Fluss-systems der Weser im Gebiet der Hansestadt Bremen. *Ab. naturw. Ver. Bremen* 34, 181-440.

Jones, R.W. and Whittaker, J.E. 2010. Palaeoenvironmental interpretation of the Pleistocene-Holocene of the British Isles, using proxy Recent benthonic foraminiferal distribution data. *In:* Whittaker, J.E. & Hart, M.B. *Micropalaeontology, Sedimentary Environments and Stratigraphy: A Tribute to Dennis Curry (1912-2001).* The Micropalaeontological Society, Special Publications. The Geological Society, London, 261-279.

Krammer, K. & H. Lange-Bertalot, 1986-1991. *Bacillariophyceae.* Gustav Fisher Verlag, Stuttgart.

Limpenny, S E., Barrio Froján, C., Cotterill, C., Foster-Smith, R L., Pearce, B., Tizzard, L., Limpenny,D L., Long, D., Walmsley, S., Kirby, S., Baker, K., Meadows, W J., Rees, J., Hill, J., Wilson,C., Leivers, M., Churchley, S., Russell, J., Birchenough, A C., Green, S L. and Law, R J,(2011). The East Coast Regional Environmental Characterisation. MEPF.

Lisiecki, L. E., and M. E. Raymo (2005), A Pliocene-Pleistocene stack of 57 globally distributed benthic d 18O records, *Paleoceanography*, 20, PA1003

Medlycott, M, (2011). Research and archaeology revisited: a revised framework for the East of England. *East Anglian Archaeology* 24.

Meisch, C. 2000. Freshwater Ostracoda of Western and Central Europe. *In:* Schwoerbel, J. & Zwick, P. (eds.), *Suβwasserfauna von Mitteleuropa, Band 8/3.* Spektrum Akadamischer Verlag, Heidelberg and Berlin. 522pp.

Mejdahl, V. (1979) Thermoluminescence dating: beta-dose attenuation in quartz grains. A*rchaeometry*, 21, 61-72.

Murray, A.S. and Wintle, A.G. (2000) Luminescence dating of quartz using an improved single-aliquot regenerative-dose protocol. *Radiation Measurements*, 32, 57-73.

Murray, A.S. and Wintle, A.G. (2003) The single aliquot regenerative dose protocol: potential for improvements in reliability. *Radiation Measurements*, 37, 377-381.

Murray, J.W. 2006. *Ecology and Applications of Benthic Foraminifera.* Cambridge University

Parfitt, S. A, Ashton, N M., Lewis, S G., Abel, R L., Coope, G R., Field, M H., Gale, R., Hoare, P G., Larkin, N R., Lewis, M D., Karloukovski, V., Maher, B A, Peglar, S M., Preece, R C., Whittaker, J E., and Stringer, C B, (2010). Early Pleistocene human occupation at the edge of the boreal zone in northwest Europe. *Nature*, 466 (7303), 229–33. Press. 426pp.

Prescott, J.R. and Hutton, J.T. (1994) Cosmic ray contributions to dose rates for luminescence and ESR dating: large depths and long-term time variations. *Radiation Measurements*, 23, 497-500.

Ransley, J., Sturt, F., Dix, J., Adams, J. and Blue, L, (2013). *People and the sea: a maritime archaeological research agenda for England*. York, Council for British Archaeology Research Report 171.

Reimer, P. J., Bard, E., Bayliss, A., Beck, J. W., Blackwell, P. G., Bronk Ramsey, C., Grootes, P. M., Guilderson, T. P., Haflidason, H., Hajdas, I., HattŽ, C., Heaton, T. J., Hoffmann, D. L., Hogg, A. G., Hughen, K. A., Kaiser, K. F., Kromer, B., Manning, S. W., Niu, M., Reimer, R. W., Richards, D. A., Scott, E. M., Southon, J. R., Staff, R. A., Turney, C. S. M. and van der Plicht, J. (2013). IntCal13 and Marine13 Radiocarbon Age Calibration Curves 0-50,000 Years cal BP. *Radiocarbon*, 55(4), 1869–1887.

Ryves, D. B., Juggins, S., Fritz, S. C. & Battarbee, R. W. 2001. Experimental diatom dissolution and the quantification of microfossil preservation in sediments. *Palaeogeography, Palaeoclimatology, Palaeoecology*, 172, 99-113

Stace, C, 1997, *New flora of the British Isles* (2nd edition), Cambridge, Cambridge University Press.

Sturt, F., Garrow, D. and Bradley, S., (2013) New models of North West European Holocene palaeogeography and inundation. *Journal of Archaeological Science*, 40 3963-3976.

Ward, I., Larcombe, P., and Lillie, M, (2006). The dating of Doggerland – Post-Glacial geochronology of the southern North Sea. *Environmental Archaeology* 11, 207-218.

Werff, A. Van Der & H. Huls. 1957-1974. *Diatomeenflora van Nederland*, 10 volumes

Witkowski, A, H. Lange-Bertalot & D. Metzeltin 2000. *Diatom Flora of Marine Coasts I.* Iconographia Diatomologica. Annotated Diatom Micrographs Ed. by H. Lange-Bertalot Vol. 7. A.R.G. Gantner Verlag. Koeltz Scientific Books. Königstein, Germany pp 925

Wessex Archaeology, (2017a). *Vanguard Offshore Wind Farm, Stage 1 geoarchaeological review.* Unpublished client report, ref: 11480.01.

Wessex Archaeology, (2017b). *Norfolk Vanguard Offshore Wind Farm, marine archaeological technical report*. Unpublished client report, ref: 112380.02.

Wessex Archaeology 2018. *Norfolk Vanguard Offshore Windfarm: Stage 2 Geoarchaeological Recording*. Unpublished client report ref: 112380.03.

Zimmerman, D. W. (1971) Thermoluminescent dating using fine grains from pottery. *Archaeometry*, 13, 29-52.

APPENDICES

APPENDIX 1

VC	Easting (m)	Northing (m)	Water Depth (m LAT)	Depth (m down core)		Depth (m LAT)		Assessment
				From	To	From	To	
VC074	464000.93	5853014.97	-38.50	0.80		-39.30		Foraminifera, ostracod and diatom
VC074	464000.93	5853014.97	-38.50	0.85		-39.35		Foraminifera, ostracod and diatom
VC074	464000.93	5853014.97	-38.50	0.88		-39.38		Pollen
VC074	464000.93	5853014.97	-38.50	0.90		-39.40		Radiocarbon and macros
VC074	464000.93	5853014.97	-38.50	0.98		-39.48		Pollen
VC074	464000.93	5853014.97	-38.50	1.08		-39.58		Pollen
VC074	464000.93	5853014.97	-38.50	1.18		-39.68		Pollen
VC074	464000.93	5853014.97	-38.50	1.24		-39.74		Foraminifera, ostracod and diatom
VC074	464000.93	5853014.97	-38.50	1.28		-39.78		Pollen
VC074	464000.93	5853014.97	-38.50	1.30		-39.80		Foraminifera, ostracod and diatom
VC074	464000.93	5853014.97	-38.50	1.38		-39.88		Pollen
VC074	464000.93	5853014.97	-38.50	1.40		-39.90		Foraminifera, ostracod and diatom
VC074	464000.93	5853014.97	-38.50	1.46		-39.96		Pollen
VC074	464000.93	5853014.97	-38.50	1.50		-40.00		Foraminifera, ostracod and diatom
VC074	464000.93	5853014.97	-38.50	1.56		-40.06		Radiocarbon and macros
VC074	464000.93	5853014.97	-38.50	1.58		-40.08		Pollen
VC074	464000.93	5853014.97	-38.50	1.61		-40.11		Foraminifera, ostracod and diatom
VC074	464000.93	5853014.97	-38.50	1.76		-40.26		Foraminifera, ostracod and diatom
VC074	464000.93	5853014.97	-38.50	5.00	5.50	-43.50	-44.00	OSL
VC076	458994.6	5863171.76	-34.00	3.40		-37.40		Foraminifera, ostracod and diatom
VC076	458994.6	5863171.76	-34.00	3.50		-37.50		Foraminifera, ostracod and diatom
VC076	458994.6	5863171.76	-34.00	3.60		-37.60		Pollen
VC076	458994.6	5863171.76	-34.00	3.61	3.63	-37.61	-37.63	Radiocarbon and macros
VC076	458994.6	5863171.76	-34.00	3.70		-37.70		Pollen
VC076	458994.6	5863171.76	-34.00	3.80		-37.80		Pollen
VC076	458994.6	5863171.76	-34.00	3.87		-37.87		Pollen
VC076	458994.6	5863171.76	-34.00	3.91	3.93	-37.91	-37.93	Radiocarbon and macros
VC076	458994.6	5863171.76	-34.00	3.95		-37.95		Pollen

VC	Easting (m)	Northing (m)	Water Depth (m LAT)	Depth (m down core)		Depth (m LAT)		Assessment
				From	To	From	To	
VC076	458994.6	5863171.76	-34.00	3.98		-37.98		Foraminifera, ostracod and diatom
VC076	458994.6	5863171.76	-34.00	3.99	4.01	-37.99	-38.01	PSD
VC076	458994.6	5863171.76	-34.00	4.08		-38.08		Foraminifera, ostracod and diatom
VC076	458994.6	5863171.76	-34.00	4.13	4.15	-38.13	-38.15	PSD
VC076	458994.6	5863171.76	-34.00	4.20	4.24	-38.20	-38.24	PSD
VC079	466749.74	5853859.05	-40.8	0.40		-41.20		Foraminifera and ostracod
VC079	466749.74	5853859.05	-40.8	0.70		-41.50		Foraminifera and ostracod
VC079	466749.74	5853859.05	-40.8	0.75	1.00	-41.55	-41.80	OSL
VC079	466749.74	5853859.05	-40.8	1.40		-42.20		Foraminifera and ostracod
VC079	466749.74	5853859.05	-40.8	1.90		-42.70		Foraminifera and ostracod
VC079	466749.74	5853859.05	-40.8	2.10		-42.90		Foraminifera and ostracod
VC079	466749.74	5853859.05	-40.8	2.90		-43.70		Foraminifera and ostracod
VC079	466749.74	5853859.05	-40.8	3.40		-44.20		Foraminifera and ostracod
VC079	466749.74	5853859.05	-40.8	3.90		-44.70		Foraminifera and ostracod
VC079	466749.74	5853859.05	-40.8	4.15	4.35	-44.95	-45.15	OSL
VC079	466749.74	5853859.05	-40.8	4.40		-45.20		Foraminifera and ostracod
VC079	466749.74	5853859.05	-40.8	4.90		-45.70		Foraminifera and ostracod
VC085	465321.16	5871195.82	-35.4	1.58		-36.98		Foraminifera and ostracod
VC085	465321.16	5871195.82	-35.4	1.70		-37.10		Foraminifera and ostracod
VC085	465321.16	5871195.82	-35.4	1.75	1.77	-37.15	-37.17	Radiocarbon and macros
VC085	465321.16	5871195.82	-35.4	1.76		-37.16		Pollen
VC085	465321.16	5871195.82	-35.4	1.86		-37.26		Pollen
VC085	465321.16	5871195.82	-35.4	1.96		-37.36		Pollen
VC085	465321.16	5871195.82	-35.4	2.06		-37.46		Pollen
VC085	465321.16	5871195.82	-35.4	2.07	2.09	-37.47	-37.49	Radiocarbon and macros
VC085	465321.16	5871195.82	-35.4	2.14		-37.54		Foraminifera and ostracod
VC085	465321.16	5871195.82	-35.4	2.16		-37.56		Pollen
VC085	465321.16	5871195.82	-35.4	2.26		-37.66		Foraminifera and ostracod
VC085	465321.16	5871195.82	-35.4	2.38		-37.78		Foraminifera and ostracod
VC085	465321.16	5871195.82	-35.4	2.50		-37.90		Foraminifera and ostracod
VC085	465321.16	5871195.82	-35.4	4.60	4.80	-40.00	-40.20	OSL
VC085	465321.16	5871195.82	-35.4	5.10	5.30	-40.50	-40.70	OSL
VC107	499791.68	5848922.33	-36.7	1.00	1.25	-37.70	-37.95	OSL

VC	Easting (m)	Northing (m)	Water Depth (m LAT)	Depth (m down core)		Depth (m LAT)		Assessment
				From	To	From	To	
VC107	499791.68	5848922.33	-36.7	1.33		-38.03		Foraminifera and ostracod
VC107	499791.68	5848922.33	-36.7	1.80		-38.50		Foraminifera and ostracod
VC107	499791.68	5848922.33	-36.7	2.10		-38.80		Foraminifera and ostracod
VC107	499791.68	5848922.33	-36.7	2.50		-39.20		Foraminifera and ostracod
VC107	499791.68	5848922.33	-36.7	3.05		-39.75		Foraminifera and ostracod
VC107	499791.68	5848922.33	-36.7	3.50		-40.20		Foraminifera and ostracod
VC107	499791.68	5848922.33	-36.7	4.05		-40.75		Foraminifera and ostracod
VC107	499791.68	5848922.33	-36.7	4.50		-41.20		Foraminifera and ostracod
VC107	499791.68	5848922.33	-36.7	5.05		-41.75		Foraminifera and ostracod
VC107	499791.68	5848922.33	-36.7	5.50		-42.20		Foraminifera and ostracod

APPENDIX 2

University of Gloucestershire

Luminescence dating laboratory

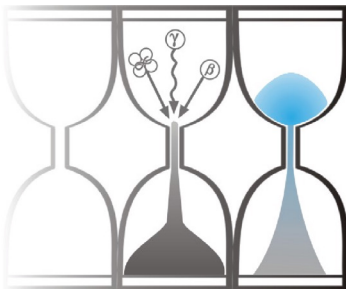

Optical dating of sediments: Vanguard Offshore Windfarm

to

Dr C. Mellett

Wessex Archaeology

Analysis & Reporting, Dr P.S. Toms
Sample Preparation & Measurement, Mr J.C. Wood
16 March 2018

Contents

Scope of Report

This is a standard report of the Luminescence dating laboratory, University of Gloucestershire. In large part, the document summarises the processes, diagnostics and data drawn upon to deliver Table 1. A conclusion on the analytical validity of each sample's optical age estimate is expressed in Table 2; where there are caveats, the reader is directed to the relevant section of the report that explains the issue further in general terms.

Copyright Notice

Field Code	Lab Code	Overburden (m)	Grain size (μm)	Moisture content (%)	NaI γ-spectrometry (*in situ*)			γ D_r ($Gy.ka^{-1}$)	Ge γ-spectrometry (*ex situ*)			β D_r ($Gy.ka^{-1}$)	Cosmic D_r ($Gy.ka^{-1}$)	Preheat (°C for 10s)	Low Dose Repeat Ratio	Interpolated:Applied Low Regenerative-dose D_e	High Dose Repeat Ratio	Interpolated:Applied High Regenerative-dose D_e	Post-IR OSL Ratio
					K (%)	Th (ppm)	U (ppm)		K (%)	Th (ppm)	U (ppm)									
VC85 (5.10-5.30)	GL17076	5.20	125-180	19 ± 5	-	-	-	0.87 ± 0.12	1.96 ± 0.12	8.70 ± 0.54	1.91 ± 0.14	1.46 ± 0.17	0.09 ± 0.01	260	1.04 ± 0.02	1.06 ± 0.03	1.02 ± 0.02	1.08 ± 0.04	0.98 ± 0.02
VC85 (4.60-4.80)	GL17077	4.70	125-180	20 ± 5	-	-	-	0.78 ± 0.11	1.76 ± 0.11	7.80 ± 0.52	1.83 ± 0.14	1.31 ± 0.16	0.10 ± 0.01	240	1.02 ± 0.03	1.04 ± 0.03	1.01 ± 0.02	1.05 ± 0.04	0.94 ± 0.02
VC107 (1.00-1.25)	GL17078	1.08	90-125	20 ± 5	-	-	-	0.84 ± 0.12	1.75 ± 0.11	8.82 ± 0.56	2.06 ± 0.14	1.36 ± 0.17	0.17 ± 0.02	260	1.01 ± 0.03	1.03 ± 0.03	0.99 ± 0.03	1.02 ± 0.05	0.73 ± 0.02
VC79 (4.15-4.35)	GL17079	4.25	90-125	19 ± 5	-	-	-	0.87 ± 0.12	1.86 ± 0.12	9.14 ± 0.57	1.89 ± 0.14	1.44 ± 0.17	0.10 ± 0.01	240	1.05 ± 0.02	1.09 ± 0.03	1.03 ± 0.02	1.17 ± 0.07	0.99 ± 0.02
VC79 (0.75-1.00)	GL17080	0.90	90-125	19 ± 5	-	-	-	0.65 ± 0.10	1.49 ± 0.10	5.91 ± 0.46	1.56 ± 0.13	1.14 ± 0.14	0.18 ± 0.02	240	1.02 ± 0.02	1.04 ± 0.02	1.03 ± 0.02	1.07 ± 0.04	1.01 ± 0.02
VC74 (5.00-5.36)	GL17081	5.25	125-180	18 ± 4	-	-	-	0.62 ± 0.09	1.35 ± 0.09	5.64 ± 0.45	1.54 ± 0.13	1.04 ± 0.13	0.09 ± 0.01	240	1.01 ± 0.02	1.02 ± 0.02	1.01 ± 0.02	1.07 ± 0.04	0.99 ± 0.02

Field Code	Lab Code	Total D_r ($Gy.ka^{-1}$)	D_e (Gy)	Age (ka)
VC85 (5.10-5.30)	GL17076	2.43 ± 0.22	139.0 ± 8.7	57.2 ± 6.4 (5.7)
VC85 (4.60-4.80)	GL17077	2.19 ± 0.21	152.0 ± 8.7	69.5 ± 7.7 (6.9)
VC107 (1.00-1.25)	GL17078	2.37 ± 0.22	141.7 ± 6.6	59.8 ± 6.2 (5.5)
VC79 (4.15-4.35)	GL17079	2.42 ± 0.22	139.1 ± 6.3	57.6 ± 5.9 (5.1)
VC79 (0.75-1.00)	GL17080	1.96 ±0.18	131.2 ± 7.4	66.8 ± 7.1 (6.3)
VC74 (5.00-5.36)	GL17081	1.75 ± 0.16	144.3 ± 7.3	82.4 ± 8.5 (7.5)

Table 1 D_r, D_e and Age data of submitted samples located at c. 53°N, 2°E. Age estimates expressed relative to year of sampling. Uncertainties in age are quoted at 1σ confidence, are based on analytical errors and reflect combined systematic and experimental variability and (in parenthesis) experimental variability alone (see 6.0). **Blue** indicates samples with accepted age estimates, **red**, age estimates with caveats (see Table 2).

Generic considerations	Field Code	Lab Code	Sample specific considerations
Absence of *in situ* γ spectrometry data (see section 4.0)	VC85 (5.10-5.30)	GL17076	None
	VC85 (4.60-4.80)	GL17077	None
	VC107 (1.00-1.25)	GL17078	Significant feldspar contamination (see section 3.1.1, Table 1 & Fig. 1) Accept as minimum age estimate
	VC79 (4.15-4.35)	GL17079	Overdispersed interpolated to applied regenerative-dose ratio (see section 3.1.4 and Table 1) Accept tentatively
	VC79 (0.75-1.00)	GL17080	Potentially significant U disequilibrium (see section 4.0 & Fig. 5) Accept tentatively
	VC74 (5.00-5.36)	GL17081	None

Table 2 Analytical validity of sample suite age estimates and caveats for consideration

1.0 Mechanisms and principles

Upon exposure to ionising radiation, electrons within the crystal lattice of insulating minerals are displaced from their atomic orbits. Whilst this dislocation is momentary for most electrons, a portion of charge is redistributed to meta-stable sites (traps) within the crystal lattice. In the absence of significant optical and thermal stimuli, this charge can be stored for extensive periods. The quantity of charge relocation and storage relates to the magnitude and period of irradiation. When the lattice is optically or thermally stimulated, charge is evicted from traps and may return to a vacant orbit position (hole). Upon recombination with a hole, an electron's energy can be dissipated in the form of light generating crystal luminescence providing a measure of dose absorption.

Herein, quartz is segregated for dating. The utility of this minerogenic dosimeter lies in the stability of its datable signal over the mid to late Quaternary period, predicted through isothermal decay studies (e.g. Smith *et al*., 1990; retention lifetime 630 Ma at 20°C) and evidenced by optical age estimates concordant with independent chronological controls (e.g. Murray and Olley, 2002). This stability is in contrast to the anomalous fading of comparable signals commonly observed for other ubiquitous sedimentary minerals such as feldspar and zircon (Wintle, 1973; Templer, 1985; Spooner, 1993)

Optical age estimates of sedimentation (Huntley *et al*., 1985) are premised upon reduction of the minerogenic time dependent signal (Optically Stimulated Luminescence, OSL) to zero through exposure to sunlight and, once buried, signal reformulation by absorption of litho- and cosmogenic radiation. The signal accumulated post burial acts as a dosimeter recording total dose absorption, converting to a chronometer by estimating the rate of dose absorption quantified through the assay of radioactivity in the surrounding lithology and streaming from the cosmos.

$$\text{Age} = \frac{\text{Mean Equivalent Dose } (D_e, \text{ Gy})}{\text{Mean Dose Rate } (D_r, \text{ Gy.ka}^{-1})}$$

Aitken (1998) and Bøtter-Jensen *et al*. (2003) offer a detailed review of optical dating.

2.0 Sample Preparation

Six sediment cores were submitted for Optical dating. To preclude optical erosion of the datable signal prior to measurement, all samples were opened and prepared under controlled laboratory illumination provided by Encapsulite RB-10 (red) filters. To isolate that material potentially exposed to daylight during sampling, sediment located within 10 mm of each core face was removed.

The remaining sample was dried and then sieved. The fine sand fraction was segregated and subjected to acid and alkaline digestion (10% HCl, 15% H_2O_2) to attain removal of carbonate and organic components respectively. A further acid digestion in HF (40%, 60 mins) was used to etch the outer 10-15 μm layer affected by α radiation and degrade each samples' feldspar content. During HF treatment, continuous magnetic stirring was used to effect isotropic etching of grains. 10% HCl was then added to remove acid soluble fluorides. Each sample was dried, resieved and quartz isolated from the remaining heavy mineral fraction using a sodium polytungstate density separation at 2.68g.cm^{-3}. Twelve 8 mm multi-grain aliquots (*c*. 3-6 mg) of quartz from each sample were then mounted on aluminium discs for determination of D_e values.

All drying was conducted at 40°C to prevent thermal erosion of the signal. All acids and alkalis were Analar grade. All dilutions (removing toxic-corrosive and non-minerogenic luminescence-bearing substances) were conducted with distilled water to prevent signal contamination by extraneous particles.

3.0 Acquisition and accuracy of D_e value

All minerals naturally exhibit marked inter-sample variability in luminescence per unit dose (sensitivity). Therefore, the estimation of D_e acquired since burial requires calibration of the natural signal using known amounts of laboratory dose. D_e values were quantified using a single-aliquot regenerative-dose (SAR) protocol (Murray and Wintle 2000; 2003) facilitated by a Risø TL-DA-15 irradiation-stimulation-detection system (Markey *et al*., 1997; Bøtter-Jensen *et al*., 1999). Within this apparatus, optical signal stimulation is provided by an assembly of blue diodes (5 packs of 6 Nichia NSPB500S), filtered to 470±80 nm conveying 15 $mW.cm^{-2}$ using a 3 mm Schott GG420 positioned in front of each diode pack. Infrared (IR) stimulation, provided by 6 IR diodes (Telefunken TSHA 6203) stimulating at 875±80nm delivering ~5 $mW.cm^{-2}$, was used to indicate the presence of contaminant feldspars (Hütt *et al*., 1988). Stimulated photon emissions from quartz aliquots are in the ultraviolet (UV) range and were filtered from stimulating photons by 7.5 mm HOYA U-340 glass and detected by an EMI 9235QA photomultiplier fitted with a blue-green sensitive bialkali photocathode. Aliquot irradiation was conducted using a 1.48 GBq $^{90}Sr/^{90}Y$ β source calibrated for multi-grain aliquots of 90-125 μm and 125-180 μm quartz against the 'Hotspot 800' ^{60}Co γ source located at the National Physical Laboratory (NPL), UK.

SAR by definition evaluates D_e through measuring the natural signal (Fig. 1) of a single aliquot and then regenerating that aliquot's signal by using known laboratory doses to enable calibration. For each aliquot, five different regenerative-doses were administered so as to image dose response. D_e values for each aliquot were then interpolated, and associated counting and fitting errors calculated, by way of exponential plus linear regression (Fig. 1). Weighted (geometric) mean D_e values were calculated from 12 aliquots using the central age model outlined by Galbraith *et al*. (1999) and are quoted at 1σ confidence (Table 1). The accuracy with which D_e equates to total absorbed dose and that dose absorbed since burial was assessed. The former can be considered a function of laboratory factors, the latter, one of environmental issues. Diagnostics were deployed to estimate the influence of these factors and criteria instituted to optimise the accuracy of D_e values.

3.1 Laboratory Factors

3.1.1 Feldspar contamination

The propensity of feldspar signals to fade and underestimate age, coupled with their higher sensitivity relative to quartz makes it imperative to quantify feldspar contamination. At room temperature, feldspars generate a signal (IRSL; Fig. 1) upon exposure to IR whereas quartz does not. The signal from feldspars contributing to OSL can be depleted by prior exposure to IR. For all aliquots the contribution of any remaining feldspars was estimated from the OSL IR depletion ratio (Duller, 2003). The influence of IR depletion on the OSL signal can be illustrated by comparing the regenerated post-IR OSL D_e with the applied regenerative-dose. If the addition to OSL by feldspars is insignificant, then the repeat dose ratio of OSL to post-IR OSL should be statistically consistent with unity (Table 1). If any aliquots do not fulfil this criterion, then the sample age estimate should be accepted tentatively. The source of feldspar contamination is rarely rooted in sample preparation; it predominantly results from the occurrence of feldspars as inclusions within quartz.

3.1.2 Preheating

Preheating aliquots between irradiation and optical stimulation is necessary to ensure comparability between natural and laboratory-induced signals. However, the multiple irradiation and preheating steps that are required to define single-aliquot regenerative-dose response leads to signal sensitisation, rendering calibration of the natural signal inaccurate. The SAR protocol (Murray and Wintle, 2000; 2003) enables this sensitisation to be monitored and corrected using a test dose, here set at 5 Gy preheated to 220°C for 10s, to track signal sensitivity between irradiation-preheat steps. However, the accuracy of sensitisation correction for both natural and laboratory signals can be preheat dependent.

The Dose Recovery test was used to assess the optimal preheat temperature for accurate correction and calibration of the time dependent signal. Dose Recovery (Fig. 2) attempts to quantify the combined effects of thermal transfer and

sensitisation on the natural signal, using a precise lab dose to simulate natural dose. The ratio between the applied dose and recovered D_e value should be statistically concordant with unity. For this diagnostic, 6 aliquots were each assigned a 10 s preheat between 180°C and 280°C.

That preheat treatment fulfilling the criterion of accuracy within the Dose Recovery test was selected to generate the final D_e value from a further 12 aliquots. Further thermal treatments, prescribed by Murray and Wintle (2000; 2003), were applied to optimise accuracy and precision. Optical stimulation occurred at 125ºC in order to minimise effects associated with photo-transferred thermoluminescence and maximise signal to noise ratios. Inter-cycle optical stimulation was conducted at 280ºC to minimise recuperation.

3.1.3 Irradiation

For all samples having D_e values in excess of 100 Gy, matters of signal saturation and laboratory irradiation effects are of concern. With regards the former, the rate of signal accumulation generally adheres to a saturating exponential form and it is this that limits the precision and accuracy of D_e values for samples having absorbed large doses. For such samples, the functional range of D_e interpolation by SAR has been verified up to 600 Gy by Pawley *et al*. (2010). Age estimates based on D_e values exceeding this value should be accepted tentatively.

3.1.4 Internal consistency

Abanico plots (Dietze *et al*., 2016) are used to illustrate inter-aliquot D_e variability (Fig. 3). D_e values are standardised relative to the central D_e value for natural signals and are described as overdispersed when >5% lie beyond $\pm 2\sigma$ of the standardising value; resulting from a heterogeneous absorption of burial dose and/or response to the SAR protocol. For multi-grain aliquots, overdispersion of natural signals does not necessarily imply inaccuracy. However where overdispersion is observed for regenerated signals, the efficacy of sensitivity correction may be problematic. Murray and Wintle (2000; 2003) suggest repeat dose ratios (Table 1) offer a measure of SAR protocol success, whereby ratios ranging across 0.9-1.1 are acceptable. However, this variation of repeat dose ratios in the high-dose region can have a significant impact on D_e interpolation. The influence of this effect can be outlined by quantifying the ratio of interpolated to applied regenerative-dose ratio (Table 1). In this study, where both the repeat dose ratios and interpolated to applied regenerative-dose ratios range across 0.9-1.1, sensitivity-correction is considered effective.

3.2 Environmental factors

3.2.1 Incomplete zeroing

Post-burial OSL signals residual of pre-burial dose absorption can result where pre-burial sunlight exposure is limited in spectrum, intensity and/or period, leading to age overestimation. This effect is particularly acute for material eroded and redeposited sub-aqueously (Olley *et al*., 1998, 1999; Wallinga, 2002) and exposed to a burial dose of <20 Gy (e.g. Olley *et al*., 2004), has some influence in sub-aerial contexts but is rarely of consequence where aerial transport has occurred. Within single-aliquot regenerative-dose optical dating there are two diagnostics of partial resetting (or bleaching); signal analysis (Agersnap-Larsen *et al*., 2000; Bailey *et al*., 2003) and inter-aliquot D_e distribution studies (Murray *et al*., 1995).

Within this study, signal analysis was used to quantify the change in D_e value with respect to optical stimulation time for multi-grain aliquots. This exploits the existence of traps within minerogenic dosimeters that bleach with different efficiency for a given wavelength of light to verify partial bleaching. $D_e(t)$ plots (Fig. 4; Bailey *et al*., 2003) are constructed from separate integrals of signal decay as laboratory optical stimulation progresses. A statistically significant increase in natural $D_e(t)$ is indicative of partial bleaching assuming three conditions are fulfilled. Firstly, that a statistically significant increase in $D_e(t)$ is observed when partial bleaching is simulated within the laboratory. Secondly, that there is no significant rise in $D_e(t)$ when full bleaching is simulated. Finally, there should be no significant augmentation in $D_e(t)$ when zero dose is simulated. Where partial bleaching is detected, the age derived from the sample should be considered a maximum estimate only. However, the utility of signal analysis is strongly dependent upon a samples pre-burial

experience of sunlight's spectrum and its residual to post-burial signal ratio. Given in the majority of cases, the spectral exposure history of a deposit is uncertain, the absence of an increase in natural D_e (t) does not necessarily testify to the absence of partial bleaching.

Where requested and feasible, the insensitivities of multi-grain single-aliquot signal analysis may be circumvented by inter-aliquot D_e distribution studies. This analysis uses aliquots of single sand grains to quantify inter-grain D_e distribution. At present, it is contended that asymmetric inter-grain D_e distributions are symptomatic of partial bleaching and/or pedoturbation (Murray *et al*., 1995; Olley *et al*., 1999; Olley *et al*., 2004; Bateman *et al*., 2003). For partial bleaching at least, it is further contended that the D_e acquired during burial is located in the minimum region of such ranges. The mean and breadth of this minimum region is the subject of current debate, as it is additionally influenced by heterogeneity in microdosimetry, variable inter-grain response to SAR and residual to post-burial signal ratios.

3.2.2 Turbation

As noted in section 3.1.1, the accuracy of sedimentation ages can further be controlled by post-burial trans-strata grain movements forced by pedo- or cryoturbation. Berger (2003) contends pedogenesis prompts a reduction in the apparent sedimentation age of parent material through bioturbation and illuviation of younger material from above and/or by biological recycling and resetting of the datable signal of surface material. Berger (2003) proposes that the chronological products of this remobilisation are A-horizon age estimates reflecting the cessation of pedogenic activity, Bc/C-horizon ages delimiting the maximum age for the initiation of pedogenesis with estimates obtained from Bt-horizons providing an intermediate age 'close to the age of cessation of soil development'. Singhvi et al. (2001), in contrast, suggest that B and C-horizons closely approximate the age of the parent material, the A-horizon, that of the 'soil forming episode'. Recent analyses of inter-aliquot D_e distributions have reinforced this complexity of interpreting burial age from pedoturbated deposits (Lombard *et al*., 2011; Gliganic *et al*., 2015; Jacobs *et al*., 2008; Bateman *et al*., 2007; Gliganic *et al*., 2016). At present there is no definitive post-sampling mechanism for the direct detection of and correction for post-burial sediment remobilisation. However, intervals of palaeosol evolution can be delimited by a maximum age derived from parent material and a minimum age obtained from a unit overlying the palaeosol. Inaccuracy forced by cryoturbation may be bidirectional, heaving older material upwards or drawing younger material downwards into the level to be dated. Cryogenic deformation of matrix-supported material is, typically, visible; sampling of such cryogenically-disturbed sediments can be avoided.

4.0 Acquisition and accuracy of D_r value

Lithogenic D_r values were defined through measurement of U, Th and K radionuclide concentration and conversion of these quantities into β and γ D_r values (Table 1). α and β contributions were estimated from sub-samples by laboratory-based γ spectrometry using an Ortec GEM-S high purity Ge coaxial detector system, calibrated using certified reference materials supplied by CANMET. γ dose rates can be estimated from *in situ* NaI gamma spectrometry or, where direct measurements are unavailable as in the present case, from laboratory-based Ge γ spectrometry. *In situ* measurements reduce uncertainty relating to potential heterogeneity in the γ dose field surrounding each sample. The level of U disequilibrium was estimated by laboratory-based Ge γ spectrometry. Estimates of radionuclide concentration were converted into D_r values (Adamiec and Aitken, 1998), accounting for D_r modulation forced by grain size (Mejdahl, 1979) and present moisture content (Zimmerman, 1971). Cosmogenic D_r values were calculated on the basis of sample depth, geographical position and matrix density (Prescott and Hutton, 1994).

The spatiotemporal validity of D_r values can be considered a function of five variables. Firstly, age estimates devoid of *in situ* γ spectrometry data should be accepted tentatively if the sampled unit is heterogeneous in texture or if the sample is located within 300 mm of strata consisting of differing texture and/or mineralogy. However, where samples are obtained

throughout a vertical profile, consistent values of γ D_r based solely on laboratory measurements may evidence the homogeneity of the γ field and hence accuracy of γ D_r values. Secondly, disequilibrium can force temporal instability in U and Th emissions. The impact of this infrequent phenomenon (Olley *et al*., 1996) upon age estimates is usually insignificant given their associated margins of error. However, for samples where this effect is pronounced (>50% disequilibrium between ^{238}U and ^{226}Ra; Fig. 5), the resulting age estimates should be accepted tentatively. Thirdly, pedogenically-induced variations in matrix composition of B and C-horizons, such as radionuclide and/or mineral remobilisation, may alter the rate of energy emission and/or absorption. If D_r is invariant through a dated profile and samples encompass primary parent material, then element mobility is likely limited in effect. Fourthly, spatiotemporal detractions from present moisture content are difficult to assess directly, requiring knowledge of the magnitude and timing of differing contents. However, the maximum influence of moisture content variations can be delimited by recalculating D_r for minimum (zero) and maximum (saturation) content. Finally, temporal alteration in the thickness of overburden alters cosmic D_r values. Cosmic D_r often forms a negligible portion of total D_r. It is possible to quantify the maximum influence of overburden flux by recalculating D_r for minimum (zero) and maximum (surface sample) cosmic D_r.

5.0 Estimation of Age

Ages reported in Table 1 provide an estimate of sediment burial period based on mean D_e and D_r values and their associated analytical uncertainties. Uncertainty in age estimates is reported as a product of systematic and experimental errors, with the magnitude of experimental errors alone shown in parenthesis (Table 1). Cumulative frequency plots indicate the inter-aliquot variability in age (Fig. 6). The maximum influence of temporal variations in D_r forced by minima-maxima in moisture content and overburden thickness is also illustrated in Fig. 6. Where uncertainty in these parameters exists this age range may prove instructive, however the combined extremes represented should not be construed as preferred age estimates. The analytical validity of each sample is presented in Table 2.

6.0 Analytical uncertainty

All errors are based upon analytical uncertainty and quoted at 1σ confidence. Error calculations account for the propagation of systematic and/or experimental (random) errors associated with D_e and D_r values.

For D_e values, systematic errors are confined to laboratory β source calibration. Uncertainty in this respect is that combined from the delivery of the calibrating γ dose (1.2%; NPL, pers. comm.), the conversion of this dose for SiO_2 using the respective mass energy-absorption coefficient (2%; Hubbell, 1982) and experimental error, totalling 3.5%. Mass attenuation and bremsstrahlung losses during γ dose delivery are considered negligible. Experimental errors relate to D_e interpolation using sensitisation corrected dose responses. Natural and regenerated sensitisation corrected dose points (S_i) were quantified by,

$$S_i = (D_i - x.L_i) / (d_i - x.L_i) \qquad \textbf{Eq.1}$$

where D_i = Natural or regenerated OSL, initial 0.2 s
L_i = Background natural or regenerated OSL, final 5 s
d_i = Test dose OSL, initial 0.2 s
x = Scaling factor, 0.08

The error on each signal parameter is based on counting statistics, reflected by the square-root of measured values. The propagation of these errors within Eq. 1 generating σS_i follows the general formula given in Eq. 2. σS_i were then used to define fitting and interpolation errors within exponential plus linear regressions.

For D_r values, systematic errors accommodate uncertainty in radionuclide conversion factors (5%), β attenuation coefficients (5%), a-value (4%; derived from a systematic α source uncertainty of 3.5% and experimental error), matrix density (0.20 $g.cm^{-3}$), vertical thickness of sampled section (specific to sample collection device), saturation moisture content (3%), moisture content attenuation (2%), burial moisture content (25% relative, unless direct evidence exists of the magnitude and period of differing content) and NaI gamma spectrometer calibration (3%). Experimental errors are associated with radionuclide quantification for each sample by NaI and Ge gamma spectrometry.

The propagation of these errors through to age calculation was quantified using the expression,

$$\sigma y\ (\delta y/\delta x) = (\Sigma\ ((\delta y/\delta x_n).\sigma x_n)^2)^{1/2} \qquad \textbf{Eq. 2}$$

where y is a value equivalent to that function comprising terms x_n and where σy and σx_n are associated uncertainties.

Errors on age estimates are presented as combined systematic and experimental errors and experimental errors alone. The former (combined) error should be considered when comparing luminescence ages herein with independent chronometric controls. The latter assumes systematic errors are common to luminescence age estimates generated by means identical to those detailed herein and enable direct comparison with those estimates.

Fig. 1 Signal Calibration

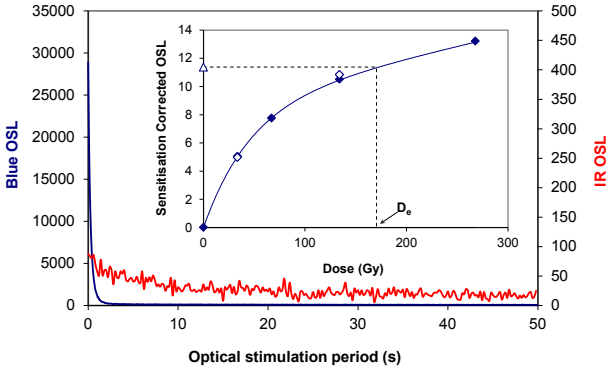

Fig. 2 Dose Recovery

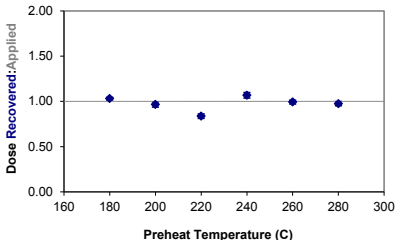

Fig. 3 Inter-aliquot D_e distribution

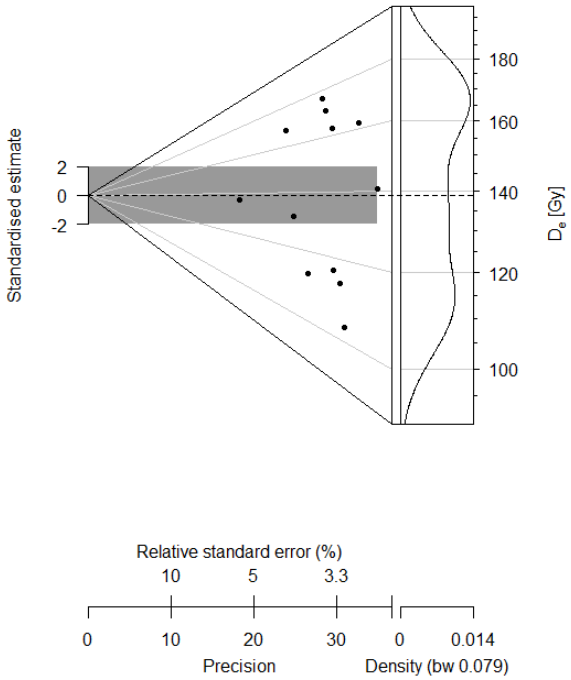

Fig. 4 Signal Analysis

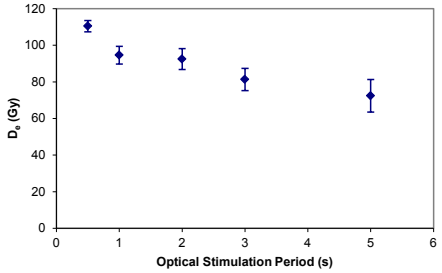

Fig. 5 U Decay Activity

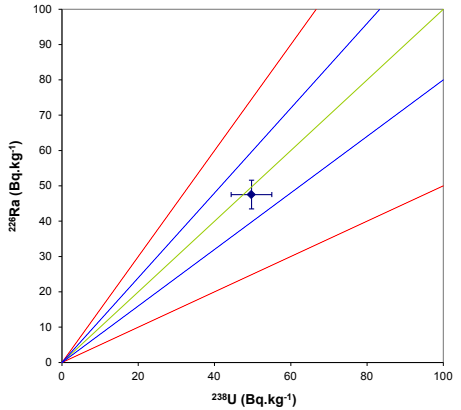

Fig. 6 Age Range

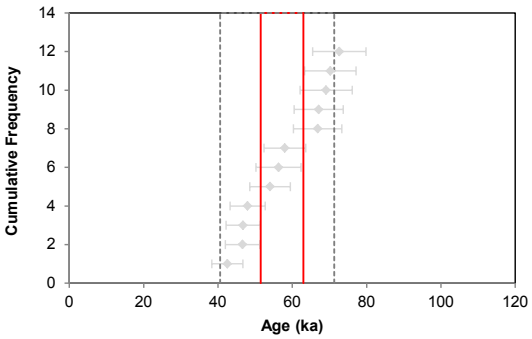

Fig. 1 Signal Calibration Natural blue and laboratory-induced infrared (IR) OSL signals. Detectable IR signal decays are diagnostic of feldspar contamination. Inset, the natural blue OSL signal (open triangle) of each aliquot is calibrated against known laboratory doses to yield equivalent dose (D_e) values. Repeats of low and high doses (open diamonds) illustrate the success of sensitivity correction.

Fig. 2 Dose Recovery The acquisition of D_e values is necessarily predicated upon thermal treatment of aliquots succeeding environmental and laboratory irradiation. The Dose Recovery test quantifies the combined effects of thermal transfer and sensitisation on the natural signal using a precise lab dose to simulate natural dose. Based on this an appropriate thermal treatment is selected to generate the final D_e value.

Fig. 3 Inter-aliquot D_e distribution Abanico plot of inter-aliquot statistical concordance in D_e values derived from **natural** irradiation. Discordant data (those points lying beyond **±2 standardised ln D_e**) reflect heterogeneous dose absorption and/or inaccuracies in calibration.

Fig. 4 Signal Analysis Statistically significant increase in **natural** D_e value with signal stimulation period is indicative of a partially-bleached signal, provided a significant increase in D_e results from **simulated partial bleaching** followed by insignificant adjustment in D_e for simulated **zero** and **full bleach** conditions. Ages from such samples are considered maximum estimates. In the absence of a significant rise in D_e with stimulation time, simulated partial bleaching and zero/full bleach tests are not assessed.

Fig. 5 U Activity Statistical concordance (equilibrium) in the activities of the daughter radioisotope ^{226}Ra with its parent ^{238}U may signify the temporal stability of D_r emissions from these chains. Significant differences (disequilibrium; >50%) in activity indicate addition or removal of isotopes creating a time-dependent shift in D_r values and increased uncertainty in the accuracy of age estimates. A 20% disequilibrium marker is also shown.

Fig. 6 Age Range The Cumulative frequency plot indicates the inter-aliquot variability in age. It also shows the **mean age range**; an estimate of sediment burial period based on mean D_e and D_r values with associated analytical uncertainties. The **maximum influence** of temporal variations in D_r forced by minima-maxima variation in moisture content and overburden thickness is outlined and may prove instructive where there is uncertainty in these parameters. However the combined extremes represented should not be construed as preferred age estimates.

Sample: GL17076

Fig. 1 Signal Calibration

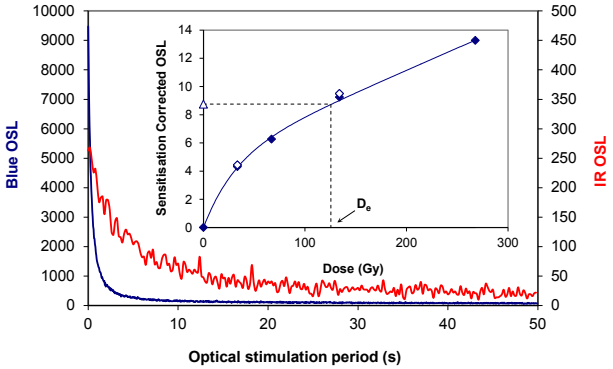

Fig. 2 Dose Recovery

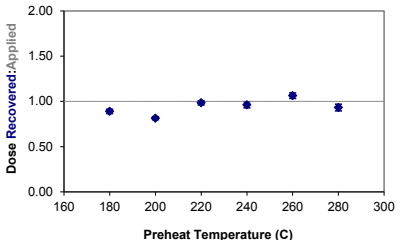

Fig. 3 Inter-aliquot D_e distribution

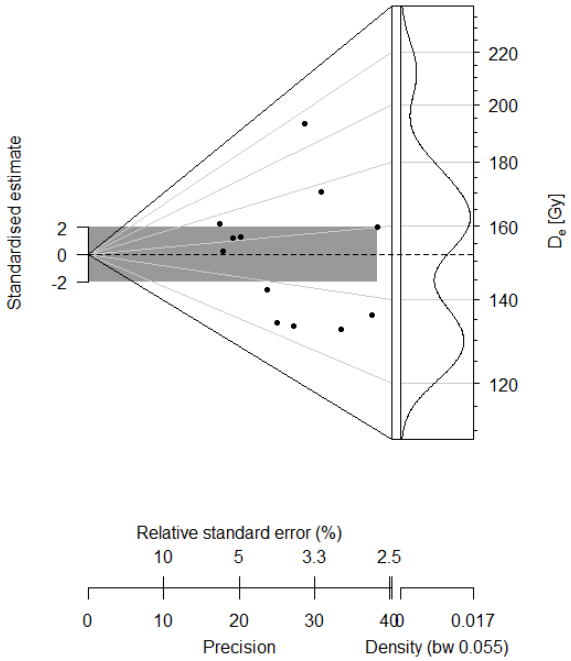

Fig. 4 Signal Analysis

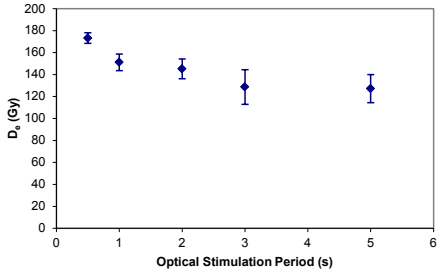

Fig. 5 U Decay Activity

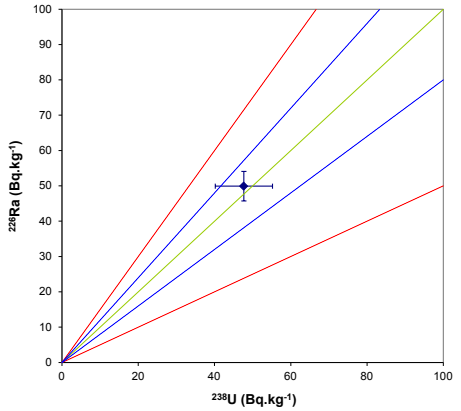

Fig. 6 Age Range

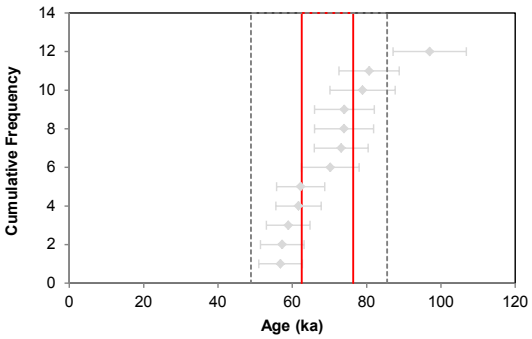

Fig. 1 Signal Calibration Natural blue and laboratory-induced infrared (IR) OSL signals. Detectable IR signal decays are diagnostic of feldspar contamination. Inset, the natural blue OSL signal (open triangle) of each aliquot is calibrated against known laboratory doses to yield equivalent dose (D_e) values. Repeats of low and high doses (open diamonds) illustrate the success of sensitivity correction.

Fig. 2 Dose Recovery The acquisition of D_e values is necessarily predicated upon thermal treatment of aliquots succeeding environmental and laboratory irradiation. The Dose Recovery test quantifies the combined effects of thermal transfer and sensitisation on the natural signal using a precise lab dose to simulate natural dose. Based on this an appropriate thermal treatment is selected to generate the final D_e value.

Fig. 3 Inter-aliquot D_e distribution Abanico plot of inter-aliquot statistical concordance in D_e values derived from **natural** irradiation. Discordant data (those points lying beyond ±2 standardised ln D_e) reflect heterogeneous dose absorption and/or inaccuracies in calibration.

Fig. 4 Signal Analysis Statistically significant increase in **natural** D_e value with signal stimulation period is indicative of a partially-bleached signal, provided a significant increase in D_e results from **simulated partial bleaching** followed by insignificant adjustment in D_e for simulated **zero** and **full bleach** conditions. Ages from such samples are considered maximum estimates. In the absence of a significant rise in D_e with stimulation time, simulated partial bleaching and zero/full bleach tests are not assessed.

Fig. 5 U Activity Statistical concordance (equilibrium) in the activities of the daughter radioisotope ^{226}Ra with its parent ^{238}U may signify the temporal stability of D_r emissions from these chains. Significant differences (disequilibrium; >50%) in activity indicate addition or removal of isotopes creating a time-dependent shift in D_r values and increased uncertainty in the accuracy of age estimates. A 20% disequilibrium marker is also shown.

Fig. 6 Age Range The Cumulative frequency plot indicates the inter-aliquot variability in age. It also shows the **mean age range**; an estimate of sediment burial period based on mean D_e and D_r values with associated analytical uncertainties. The **maximum influence** of temporal variations in D_r forced by minima-maxima variation in moisture content and overburden thickness is outlined and may prove instructive where there is uncertainty in these parameters. However the combined extremes represented should not be construed as preferred age estimates.

Sample: GL17077

Fig. 1 Signal Calibration

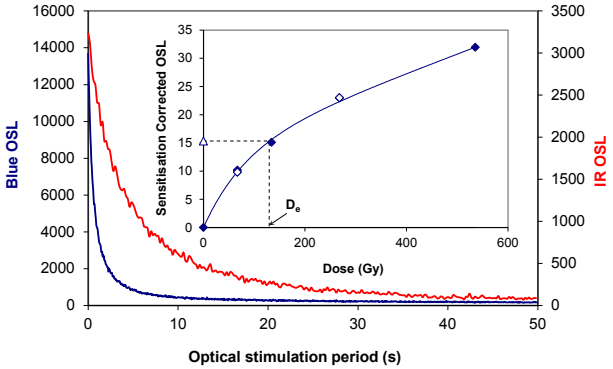

Fig. 1 Signal Calibration Natural blue and laboratory-induced infrared (IR) OSL signals. Detectable IR signal decays are diagnostic of feldspar contamination. Inset, the natural blue OSL signal (open triangle) of each aliquot is calibrated against known laboratory doses to yield equivalent dose (D_e) values. Repeats of low and high doses (open diamonds) illustrate the success of sensitivity correction.

Fig. 2 Dose Recovery The acquisition of D_e values is necessarily predicated upon thermal treatment of aliquots succeeding environmental and laboratory irradiation. The Dose Recovery test quantifies the combined effects of thermal transfer and sensitisation on the natural signal using a precise lab dose to simulate natural dose. Based on this an appropriate thermal treatment is selected to generate the final D_e value.

Fig. 3 Inter-aliquot D_e distribution Abanico plot of inter-aliquot statistical concordance in D_e values derived from **natural** irradiation. Discordant data (those points lying beyond **±2 standardised ln D_e**) reflect heterogeneous dose absorption and/or inaccuracies in calibration.

Fig. 4 Signal Analysis Statistically significant increase in **natural** D_e value with signal stimulation period is indicative of a partially-bleached signal, provided a significant increase in D_e results from **simulated partial bleaching** followed by insignificant adjustment in D_e for simulated **zero** and **full bleach** conditions. Ages from such samples are considered maximum estimates. In the absence of a significant rise in D_e with stimulation time, simulated partial bleaching and zero/full bleach tests are not assessed.

Fig. 5 U Activity Statistical concordance (equilibrium) in the activities of the daughter radioisotope ^{226}Ra with its parent ^{238}U may signify the temporal stability of D_r emissions from these chains. Significant differences (disequilibrium; >50%) in activity indicate addition or removal of isotopes creating a time-dependent shift in D_r values and increased uncertainty in the accuracy of age estimates. A 20% disequilibrium marker is also shown.

Fig. 6 Age Range The Cumulative frequency plot indicates the inter-aliquot variability in age. It also shows the **mean age range**; an estimate of sediment burial period based on mean D_e and D_r values with associated analytical uncertainties. The **maximum influence** of temporal variations in D_r forced by minima-maxima variation in moisture content and overburden thickness is outlined and may prove instructive where there is uncertainty in these parameters. However the combined extremes represented should not be construed as preferred age estimates.

Fig. 2 Dose Recovery

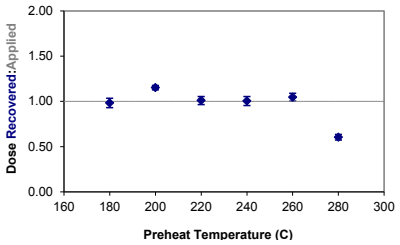

Fig. 3 Inter-aliquot D_e distribution

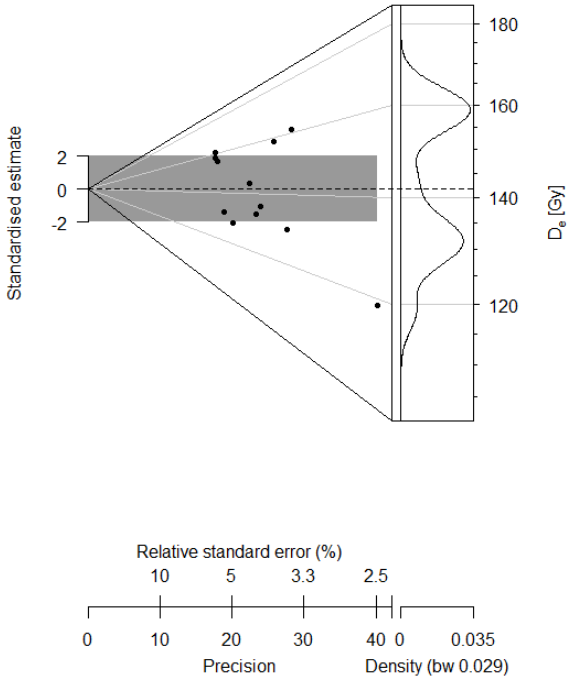

Fig. 4 Signal Analysis

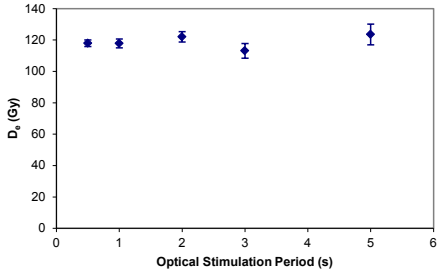

Fig. 5 U Decay Activity

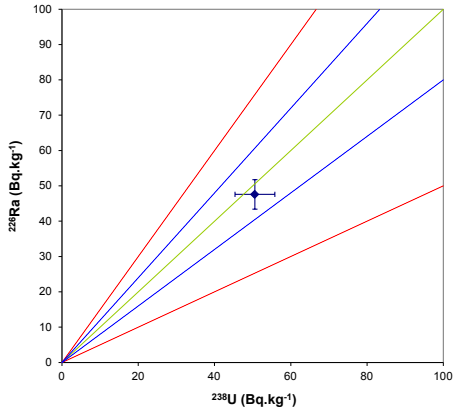

Fig. 6 Age Range

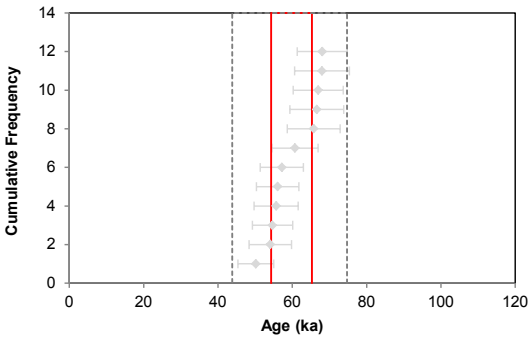

Sample: GL17078

Fig. 1 Signal Calibration

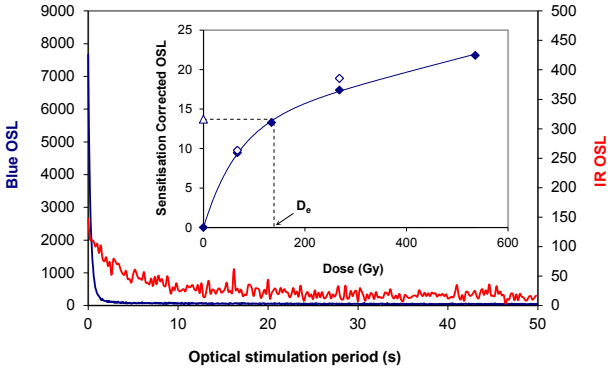

Fig. 2 Dose Recovery

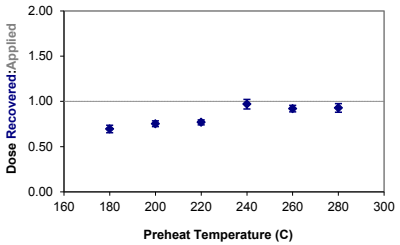

Fig. 3 Inter-aliquot D_e distribution

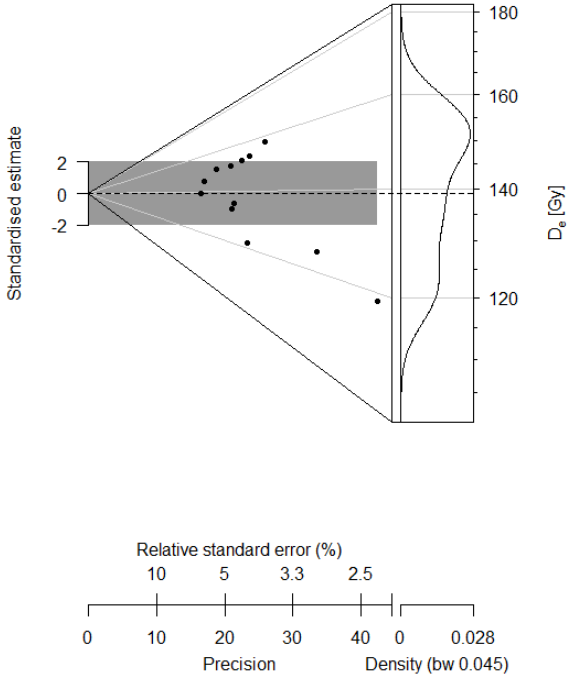

Fig. 4 Signal Analysis

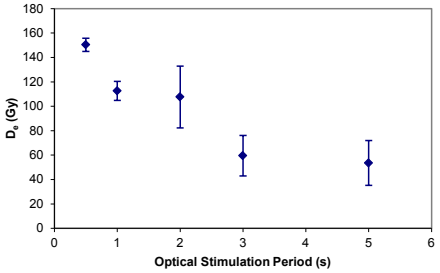

Fig. 5 U Decay Activity

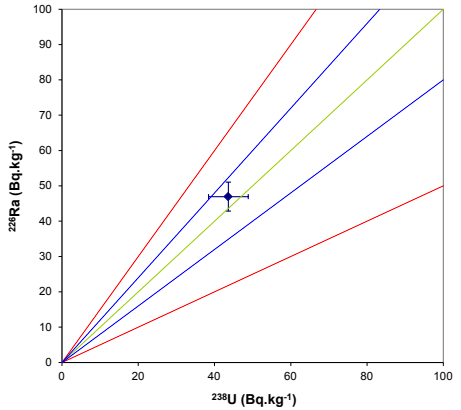

Fig. 6 Age Range

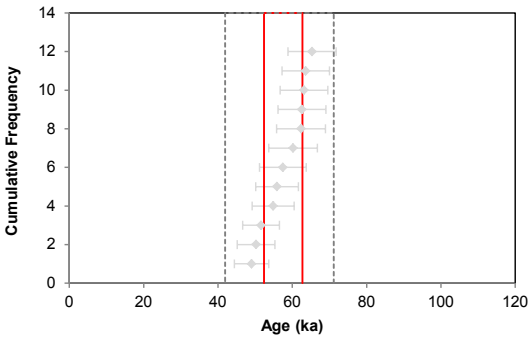

Fig. 1 Signal Calibration Natural blue and laboratory-induced infrared (IR) OSL signals. Detectable IR signal decays are diagnostic of feldspar contamination. Inset, the natural blue OSL signal (open triangle) of each aliquot is calibrated against known laboratory doses to yield equivalent dose (D_e) values. Repeats of low and high doses (open diamonds) illustrate the success of sensitivity correction.

Fig. 2 Dose Recovery The acquisition of D_e values is necessarily predicated upon thermal treatment of aliquots succeeding environmental and laboratory irradiation. The Dose Recovery test quantifies the combined effects of thermal transfer and sensitisation on the natural signal using a precise lab dose to simulate natural dose. Based on this an appropriate thermal treatment is selected to generate the final D_e value.

Fig. 3 Inter-aliquot D_e distribution Abanico plot of inter-aliquot statistical concordance in D_e values derived from **natural** irradiation. Discordant data (those points lying beyond **±2 standardised ln D_e**) reflect heterogeneous dose absorption and/or inaccuracies in calibration.

Fig. 4 Signal Analysis Statistically significant increase in **natural** D_e value with signal stimulation period is indicative of a partially-bleached signal, provided a significant increase in D_e results from **simulated partial bleaching** followed by insignificant adjustment in D_e for simulated **zero** and **full bleach** conditions. Ages from such samples are considered maximum estimates. In the absence of a significant rise in D_e with stimulation time, simulated partial bleaching and zero/full bleach tests are not assessed.

Fig. 5 U Activity Statistical concordance (equilibrium) in the activities of the daughter radioisotope ^{226}Ra with its parent ^{238}U may signify the temporal stability of D_r emissions from these chains. Significant differences (disequilibrium; >50%) in activity indicate addition or removal of isotopes creating a time-dependent shift in D_r values and increased uncertainty in the accuracy of age estimates. A 20% disequilibrium marker is also shown.

Fig. 6 Age Range The Cumulative frequency plot indicates the inter-aliquot variability in age. It also shows the **mean age range**; an estimate of sediment burial period based on mean D_e and D_r values with associated analytical uncertainties. The **maximum influence** of temporal variations in D_r forced by minima-maxima variation in moisture content and overburden thickness is outlined and may prove instructive where there is uncertainty in these parameters. However the combined extremes represented should not be construed as preferred age estimates.

Sample: GL17079

Fig. 1 Signal Calibration

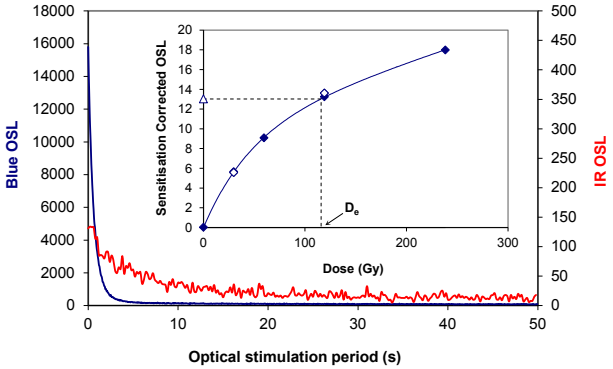

Fig. 2 Dose Recovery

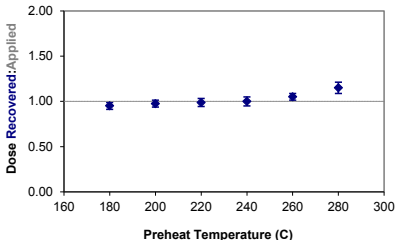

Fig. 3 Inter-aliquot D_e distribution

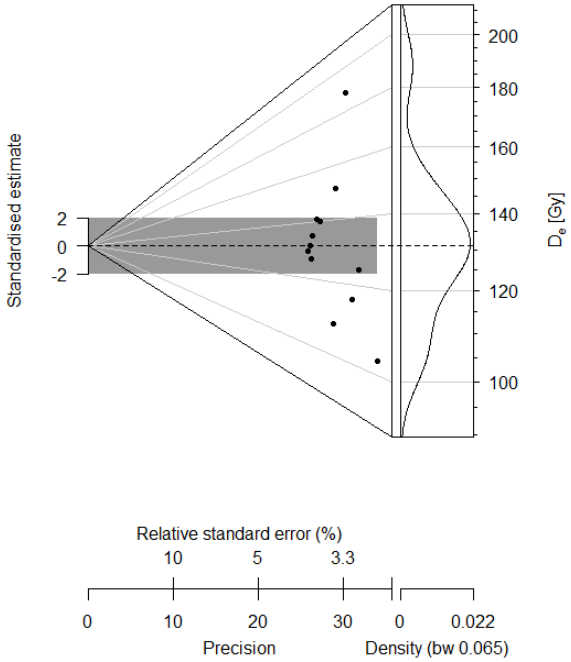

Fig. 4 Signal Analysis

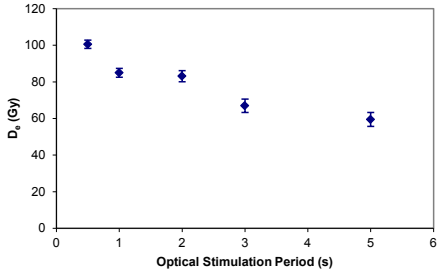

Fig. 5 U Decay Activity

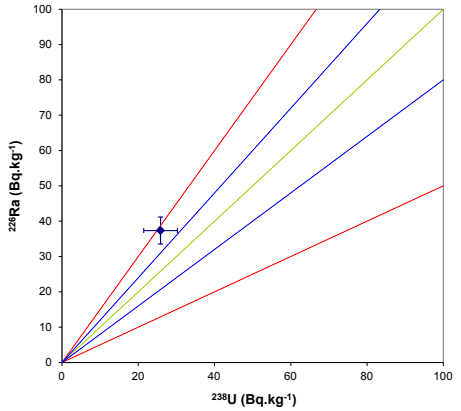

Fig. 6 Age Range

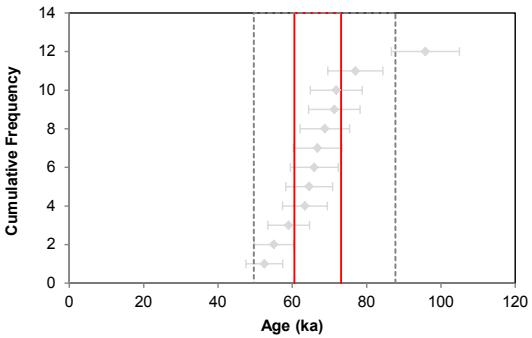

Fig. 1 Signal Calibration Natural blue and laboratory-induced infrared (IR) OSL signals. Detectable IR signal decays are diagnostic of feldspar contamination. Inset, the natural blue OSL signal (open triangle) of each aliquot is calibrated against known laboratory doses to yield equivalent dose (D_e) values. Repeats of low and high doses (open diamonds) illustrate the success of sensitivity correction.

Fig. 2 Dose Recovery The acquisition of D_e values is necessarily predicated upon thermal treatment of aliquots succeeding environmental and laboratory irradiation. The Dose Recovery test quantifies the combined effects of thermal transfer and sensitisation on the natural signal using a precise lab dose to simulate natural dose. Based on this an appropriate thermal treatment is selected to generate the final D_e value.

Fig. 3 Inter-aliquot D_e distribution Abanico plot of inter-aliquot statistical concordance in D_e values derived from **natural** irradiation. Discordant data (those points lying beyond ±2 standardised ln D_e) reflect heterogeneous dose absorption and/or inaccuracies in calibration.

Fig. 4 Signal Analysis Statistically significant increase in **natural** D_e value with signal stimulation period is indicative of a partially-bleached signal, provided a significant increase in D_e results from **simulated partial bleaching** followed by insignificant adjustment in D_e for simulated **zero** and **full bleach** conditions. Ages from such samples are considered maximum estimates. In the absence of a significant rise in D_e with stimulation time, simulated partial bleaching and zero/full bleach tests are not assessed.

Fig. 5 U Activity Statistical concordance (equilibrium) in the activities of the daughter radioisotope ^{226}Ra with its parent ^{238}U may signify the temporal stability of D_r emissions from these chains. Significant differences (disequilibrium; >50%) in activity indicate addition or removal of isotopes creating a time-dependent shift in D_r values and increased uncertainty in the accuracy of age estimates. A 20% disequilibrium marker is also shown.

Fig. 6 Age Range The Cumulative frequency plot indicates the inter-aliquot variability in age. It also shows the **mean age range**; an estimate of sediment burial period based on mean D_e and D_r values with associated analytical uncertainties. The **maximum influence** of temporal variations in D_r forced by minima-maxima variation in moisture content and overburden thickness is outlined and may prove instructive where there is uncertainty in these parameters. However the combined extremes represented should not be construed as preferred age estimates.

Sample: GL17080

Fig. 1 Signal Calibration

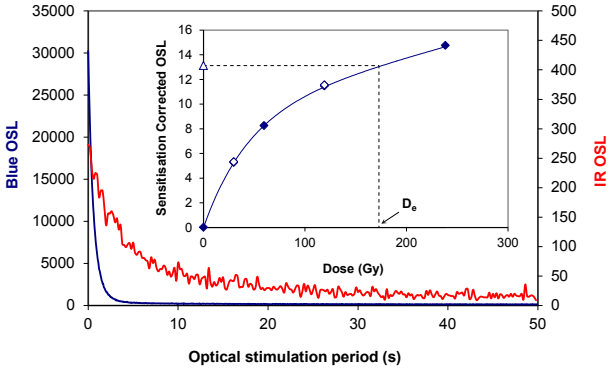

Fig. 2 Dose Recovery

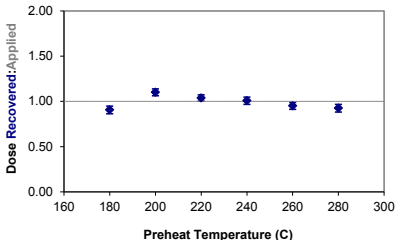

Fig. 3 Inter-aliquot D_e distribution

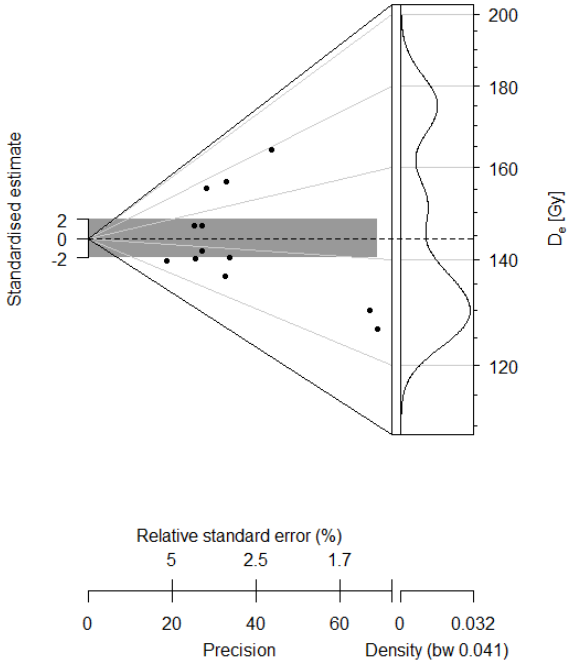

Fig. 4 Signal Analysis

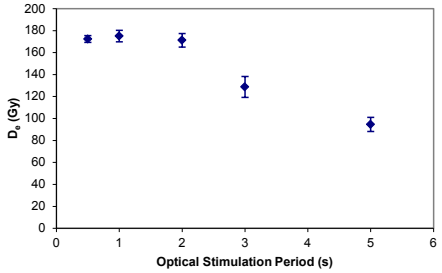

Fig. 5 U Decay Activity

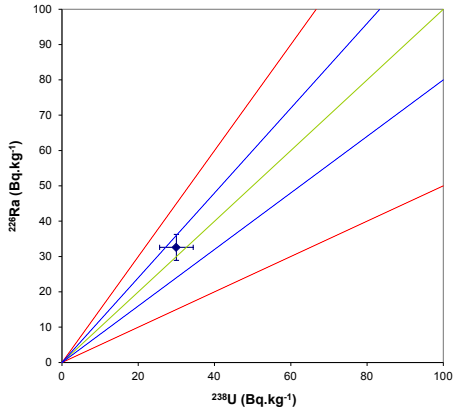

Fig. 6 Age Range

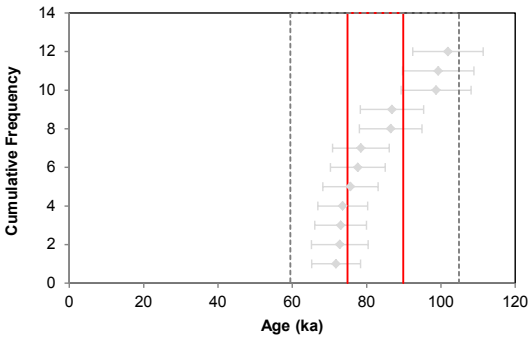

Fig. 1 Signal Calibration Natural blue and laboratory-induced infrared (IR) OSL signals. Detectable IR signal decays are diagnostic of feldspar contamination. Inset, the natural blue OSL signal (open triangle) of each aliquot is calibrated against known laboratory doses to yield equivalent dose (D_e) values. Repeats of low and high doses (open diamonds) illustrate the success of sensitivity correction.

Fig. 2 Dose Recovery The acquisition of D_e values is necessarily predicated upon thermal treatment of aliquots succeeding environmental and laboratory irradiation. The Dose Recovery test quantifies the combined effects of thermal transfer and sensitisation on the natural signal using a precise lab dose to simulate natural dose. Based on this an appropriate thermal treatment is selected to generate the final D_e value.

Fig. 3 Inter-aliquot D_e distribution Abanico plot of inter-aliquot statistical concordance in D_e values derived from **natural** irradiation. Discordant data (those points lying beyond **±2 standardised ln D_e**) reflect heterogeneous dose absorption and/or inaccuracies in calibration.

Fig. 4 Signal Analysis Statistically significant increase in **natural** D_e value with signal stimulation period is indicative of a partially-bleached signal, provided a significant increase in D_e results from **simulated partial bleaching** followed by insignificant adjustment in D_e for simulated **zero** and **full bleach** conditions. Ages from such samples are considered maximum estimates. In the absence of a significant rise in D_e with stimulation time, simulated partial bleaching and zero/full bleach tests are not assessed.

Fig. 5 U Activity Statistical concordance (equilibrium) in the activities of the daughter radioisotope ^{226}Ra with its parent ^{238}U may signify the temporal stability of D_r emissions from these chains. Significant differences (disequilibrium; >50%) in activity indicate addition or removal of isotopes creating a time-dependent shift in D_r values and increased uncertainty in the accuracy of age estimates. A 20% disequilibrium marker is also shown.

Fig. 6 Age Range The Cumulative frequency plot indicates the inter-aliquot variability in age. It also shows the **mean age range**; an estimate of sediment burial period based on mean D_e and D_r values with associated analytical uncertainties. The **maximum influence** of temporal variations in D_r forced by minima-maxima variation in moisture content and overburden thickness is outlined and may prove instructive where there is uncertainty in these parameters. However the combined extremes represented should not be construed as preferred age estimates.

Sample: GL17081

References

Adamiec, G. and Aitken, M.J. (1998) Dose-rate conversion factors: new data. *Ancient TL*, 16, 37-50.

Agersnap-Larsen, N., Bulur, E., Bøtter-Jensen, L. and McKeever, S.W.S. (2000) Use of the LM-OSL technique for the detection of partial bleaching in quartz. *Radiation Measurements*, 32, 419-425.

Aitken, M. J. (1998) An introduction to optical dating: the dating of Quaternary sediments by the use of photon-stimulated luminescence. Oxford University Press.

Bailey, R.M., Singarayer, J.S. , Ward, S. and Stokes, S. (2003) Identification of partial resetting using D_e as a function of illumination time. *Radiation Measurements*, 37, 511-518.

Bateman, M.D., Frederick, C.D., Jaiswal, M.K., Singhvi, A.K. (2003) Investigations into the potential effects of pedoturbation on luminescence dating. *Quaternary Science Reviews*, 22, 1169-1176.

Bateman, M.D., Boulter, C.H., Carr, A.S., Frederick, C.D., Peter, D. and Wilder, M. (2007) Detecting post-depositional sediment disturbance in sandy deposits using optical luminescence. *Quaternary Geochronology*, 2, 57-64.

Berger, G.W. (2003). Luminescence chronology of late Pleistocene loess-paleosol and tephra sequences near Fairbanks, Alaska. *Quaternary Research*, 60, 70-83.

Bøtter-Jensen, L., Mejdahl, V. and Murray, A.S. (1999) New light on OSL. *Quaternary Science Reviews*, 18, 303-310.

Bøtter-Jensen, L., McKeever, S.W.S. and Wintle, A.G. (2003) Optically Stimulated Luminescence Dosimetry. Elsevier, Amsterdam.

Dietze, M., Kreutzer, S., Burow, C., Fuchs, M.C., Fischer, M., Schmidt, C. (2016) The abanico plot: visualising chronometric data with individual standard errors. *Quaternary Geochronology*, 31, 1-7.

Duller, G.A.T (2003) Distinguishing quartz and feldspar in single grain luminescence measurements. *Radiation Measurements*, 37, 161-165.

Galbraith, R. F., Roberts, R. G., Laslett, G. M., Yoshida, H. and Olley, J. M. (1999) Optical dating of single and multiple grains of quartz from Jinmium rock shelter (northern Australia): Part I, Experimental design and statistical models. *Archaeometry*, 41, 339-364.

Gliganic, L.A., May, J.-H. and Cohen, T.J. (2015). All mixed up: using single-grain equivalent dose distribution sto identify phases of pedogenic mixing on a dryland alluvial fan. *Quaternary International*, 362, 23-33.

Gliganic, L.A., Cohen, T.J., Slack, M. and Feathers, J.K. (2016) Sediment mixing in Aeolian sandsheets identified and quantified using single-grain optically stimulated luminescence. *Quaternary Geochronology*, 32, 53-66.

Huntley, D.J., Godfrey-Smith, D.I. and Thewalt, M.L.W. (1985) Optical dating of sediments. *Nature*, 313, 105-107.

Hubbell, J.H. (1982) Photon mass attenuation and energy-absorption coefficients from 1keV to 20MeV. *International Journal of Applied Radioisotopes*, 33, 1269-1290.

Hütt, G., Jaek, I. and Tchonka, J. (1988) Optical dating: K-feldspars optical response stimulation spectra. *Quaternary Science Reviews*, 7, 381-386.

Jacobs, A., Wintle, A.G., Duller, G.A.T, Roberts, R.G. and Wadley, L. (2008) New ages for the post-Howiesons Poort, late and finale middle stone age at Sibdu, South Africa. *Journal of Archaeological Science*, 35, 1790-1807.

Lombard, M., Wadley, L., Jacobs, Z., Mohapi, M. and Roberts, R.G. (2011) Still Bay and serrated points from the Umhlatuzana rock shelter, Kwazulu-Natal, South Africa. *Journal of Archaeological Science*, 37, 1773-1784.

Markey, B.G., Bøtter-Jensen, L., and Duller, G.A.T. (1997) A new flexible system for measuring thermally and optically stimulated luminescence. *Radiation Measurements*, 27, 83-89.

Mejdahl, V. (1979) Thermoluminescence dating: beta-dose attenuation in quartz grains. *Archaeometry*, 21, 61-72.

Murray, A.S. and Olley, J.M. (2002) Precision and accuracy in the Optically Stimulated Luminescence dating of sedimentary quartz: a status review. *Geochronometria*, 21, 1-16.

Murray, A.S. and Wintle, A.G. (2000) Luminescence dating of quartz using an improved single-aliquot regenerative-dose protocol. *Radiation Measurements*, 32, 57-73.

Murray, A.S. and Wintle, A.G. (2003) The single aliquot regenerative dose protocol: potential for improvements in reliability. *Radiation Measurements*, 37, 377-381.

Murray, A.S., Olley, J.M. and Caitcheon, G.G. (1995) Measurement of equivalent doses in quartz from contemporary water-lain sediments using optically stimulated luminescence. *Quaternary Science Reviews*, 14, 365-371.

Olley, J.M., Murray, A.S. and Roberts, R.G. (1996) The effects of disequilibria in the Uranium and Thorium decay chains on burial dose rates in fluvial sediments. *Quaternary Science Reviews*, 15, 751-760.

Olley, J.M., Caitcheon, G.G. and Murray, A.S. (1998) The distribution of apparent dose as determined by optically stimulated luminescence in small aliquots of fluvial quartz: implications for dating young sediments. *Quaternary Science Reviews*, 17, 1033-1040.

Olley, J.M., Caitcheon, G.G. and Roberts R.G. (1999) The origin of dose distributions in fluvial sediments, and the prospect of dating single grains from fluvial deposits using -optically stimulated luminescence. *Radiation Measurements,* 30**,** 207-217.

Olley, J.M., Pietsch, T. and Roberts, R.G. (2004) Optical dating of Holocene sediments from a variety of geomorphic settings using single grains of quartz. *Geomorphology*, 60, 337-358.

Pawley, S.M., Toms, P.S., Armitage, S.J., Rose, J. (2010) Quartz luminescence dating of Anglian Stage fluvial sediments: Comparison of SAR age estimates to the terrace chronology of the Middle Thames valley, UK. *Quaternary Geochronology*, 5, 569-582.

Prescott, J.R. and Hutton, J.T. (1994) Cosmic ray contributions to dose rates for luminescence and ESR dating: large depths and long-term time variations. *Radiation Measurements*, 23, 497-500.

Singhvi, A.K., Bluszcz, A.., Bateman, M.D., Someshwar Rao, M. (2001). Luminescence dating of loess-palaeosol sequences and coversands: methodological aspects and palaeoclimatic implications. *Earth Science Reviews*, 54, 193-211.

Smith, B.W., Rhodes, E.J., Stokes, S., Spooner, N.A. (1990) The optical dating of sediments using quartz. *Radiation Protection Dosimetry*, 34, 75-78.

Spooner, N.A. (1993) The validity of optical dating based on feldspar. Unpublished D.Phil. thesis, Oxford University.

Templer, R.H. (1985) The removal of anomalous fading in zircons. *Nuclear Tracks and Radiation Measurements*, 10, 531-537.

Wallinga, J. (2002) Optically stimulated luminescence dating of fluvial deposits: a review. *Boreas* 31, 303-322.

Wintle, A.G. (1973) Anomalous fading of thermoluminescence in mineral samples. *Nature*, 245, 143-144.

Zimmerman, D. W. (1971) Thermoluminescent dating using fine grains from pottery. *Archaeometry*, 13, 29-52.

APPENDIX 3

Core	VC074								VC079			VC085				
Depth (mbsf)	0.80	0.85	1.24	1.30	1.40	1.50	1.61	1.76	0.40	0.70	1.40	1.58	1.70	2.26	2.38	2.50
Sample id	D1	D2	D3	D4	D5	D6	D7	D8	D13	D14	D15	D23	D24	D26	D27	D28
Taxon & Salinity Group																
Polyhalobous																
Coscinodiscus sp.										cf						
Grammatophora sp.	1									1	1					
Paralia sulcata	1								2	2	1		cf			
Rhaphoneis sp.										1	cf					
Rhaphoneis surirella										2						
Polyhalobous to Mesohalobous																
Pseudopodosira westii	cf															
Mesohalobous																
Campylodiscus echeneis				cf												
Cyclotella striata	1															
Synedra pulchella							cf									
Halophilous to Oligohal. Indif.																
Diploneis ovalis			1													
Epithemia turgida			1			1									1	
Oligohalobous Indifferent																
Achnanthes clevei			1													

Core	VC074								VC079			VC085				
Depth (mbsf)	0.80	0.85	1.24	1.30	1.40	1.50	1.61	1.76	0.40	0.70	1.40	1.58	1.70	2.26	2.38	2.50
Sample id	D1	D2	D3	D4	D5	D6	D7	D8	D13	D14	D15	D23	D24	D26	D27	D28
Achnanthes kolbei							1									
Amphora libyca			1				1									
Amphora pediculus		1	1				2									
Aulacoseira ambigua	2	3	3	2	2											
Aulacoseira granulata	3	2	2													
Aulacoseira sp.	1		1	1	1		1									
Caloneis bacillum					1											
Campylodiscus hibernicus						1										
Cocconeis disculus			1													
Cocconeis placentula							2	1								
Cymbella cistula								1								
Epithemia adnata			1													
Epithemia sp.					1	cf	1									1
Fragilaria brevistriata			2		1											
Fragilaria construens		1	1													
Fragilaria construens var.binodis		1														
Fragilaria construens var.venter		1	1													
Fragilaria lapponica			1													
Fragilaria pinnata			1				1	1					cf			
Gyrosigma attenuatum		1						cf								
Navicula (Sellaphora) pupula			1													

Core	VC074								VC079			VC085				
Depth (mbsf)	0.80	0.85	1.24	1.30	1.40	1.50	1.61	1.76	0.40	0.70	1.40	1.58	1.70	2.26	2.38	2.50
Sample id	D1	D2	D3	D4	D5	D6	D7	D8	D13	D14	D15	D23	D24	D26	D27	D28
Navicula cari					1											
Navicula elginensis					1											
Navicula laterostrata					1											
Navicula scutelloides	1		1													
Pinnularia major						cf								cf	1	
Pinnularia microstauron								1								
Synedra parasitica		1	1		1											
Synedra ulna				1		1	1	1								
Halophobous																
Brachysira brebissonii						1										
Unknown Salinity Group																
Achnanthes sp.			1				1									
Amphora sp.			1				1									
Campylodiscus sp.						1										
Cocconeis sp.							1									
Cyclotella sp.	1															
Cymbella sp.																1
Diploneis sp.								1					1			
Fragilaria sp.					1											
Gomphonema sp.				1												
Gyrosigma sp.																1
Inderminate centric sp.				1						1						

Core	VC074								VC079			VC085				
Depth (mbsf)	0.80	0.85	1.24	1.30	1.40	1.50	1.61	1.76	0.40	0.70	1.40	1.58	1.70	2.26	2.38	2.50
Sample id	D1	D2	D3	D4	D5	D6	D7	D8	D13	D14	D15	D23	D24	D26	D27	D28
Inderminate pennate sp.	1							1								
Navicula sp.							1	1								
Surirella sp.																1
Unknown diatom								1		1	1	1	1		1	
Unknown naviculaceae	1		1		1	1	1	1			1				1	1

APPENDIX 4

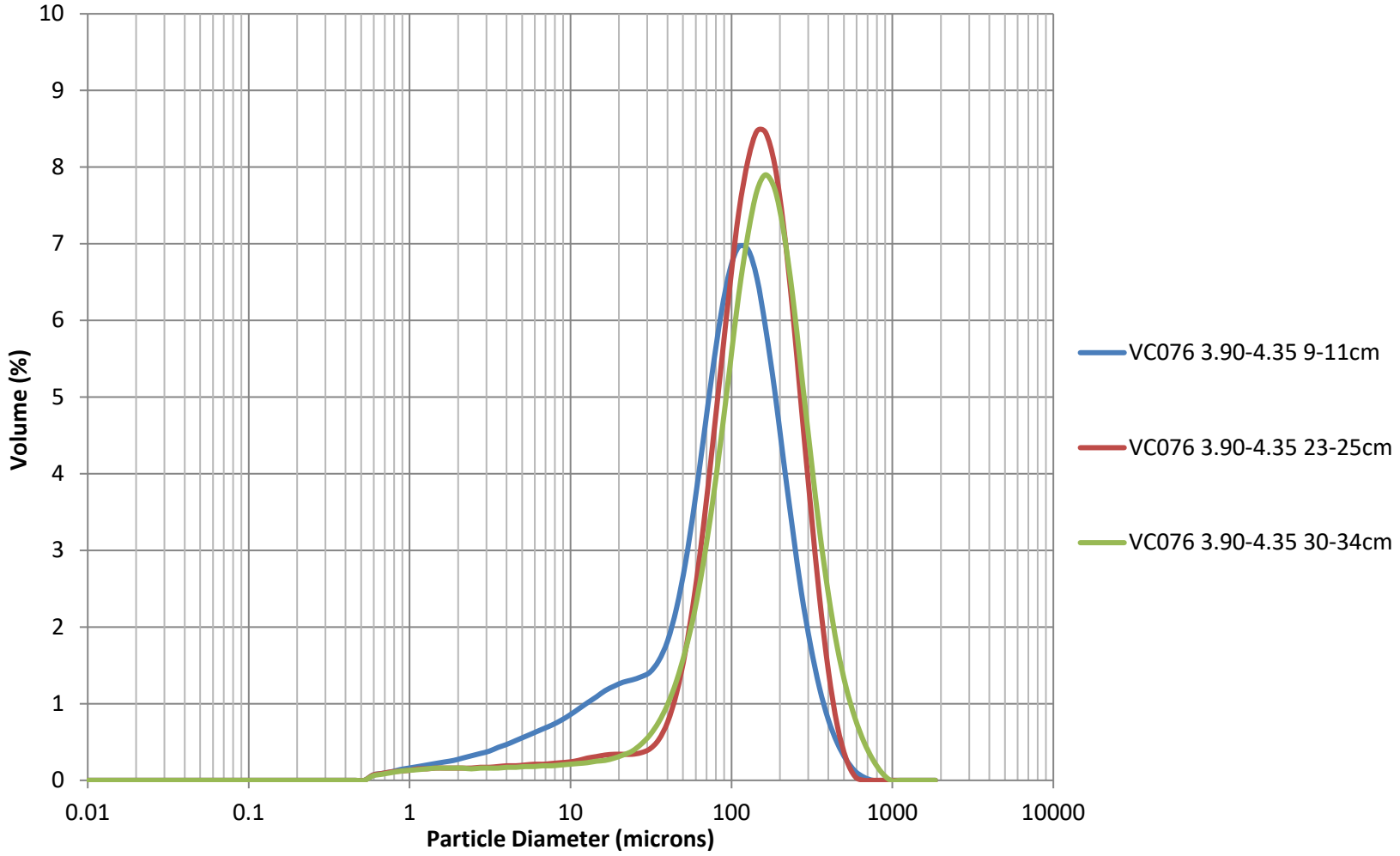
10
9
8
7
6
5
4
3
2
1
0
Volume (%)
0.01
0.1
1
10
100
1000
10000
Particle Diameter (microns)
VC076 3.90-4.35 9-11cm
VC076 3.90-4.35 23-25cm
VC076 3.90-4.35 30-34cm

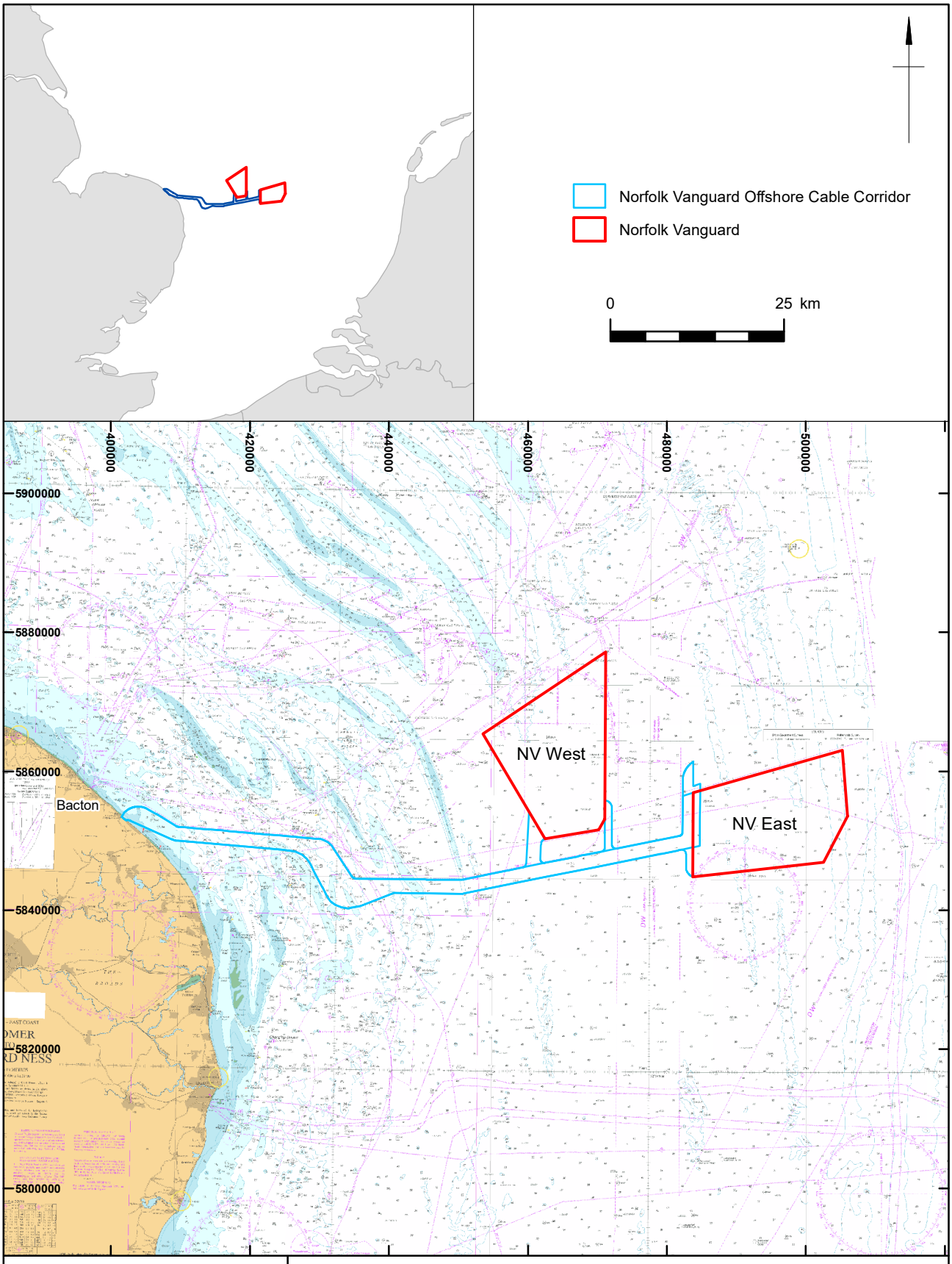

Date:	20/04/2018	Revision Number:	0
Scale:	1:800,000 at A4	Illustrator:	KJF
Path:	X:\PROJECTS\114843\GIS\FigsMXD\2018_04_20\114843_Geoarch_Fig01.mxd		

Coordinate system:
ETRS1989 UTM Z31N

Location of Norfolk Vanguard Offshore Wind Farm

Figure 1

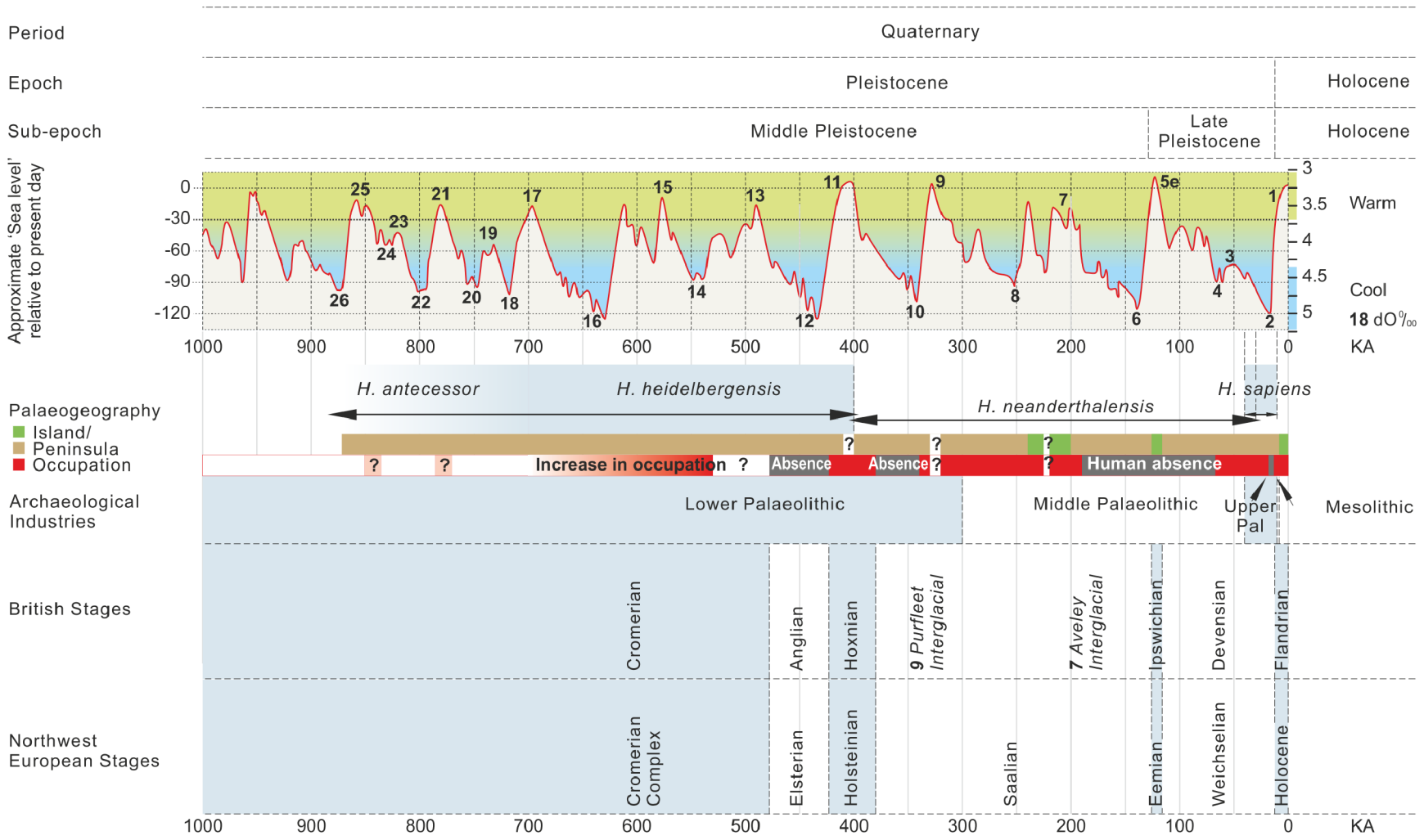

The figure presents information derived from several references: the global sea-level curve is from Lisiecki and Raymo (2005) and Jelgersma (1979). Details on the geology and archaeology were provided by Dix and Westley (2004); Funnel (1995); Gibbard and van Kolfschoten (2004); Kukla et al. (2002); Lee et al. (2006); Lowe and Walker (1997) and Wymer (1999).

Date:	21/03/2018	Revision Number:	0
Scale:	N/A	Illustrator:	RAM
Path:	X:\PROJECTS\114843\GIS\FigsMXD\2018_03_21\114843_Fig02.mxd		

Chronostratigraphic timeline for the last 1 million years

Figure 2

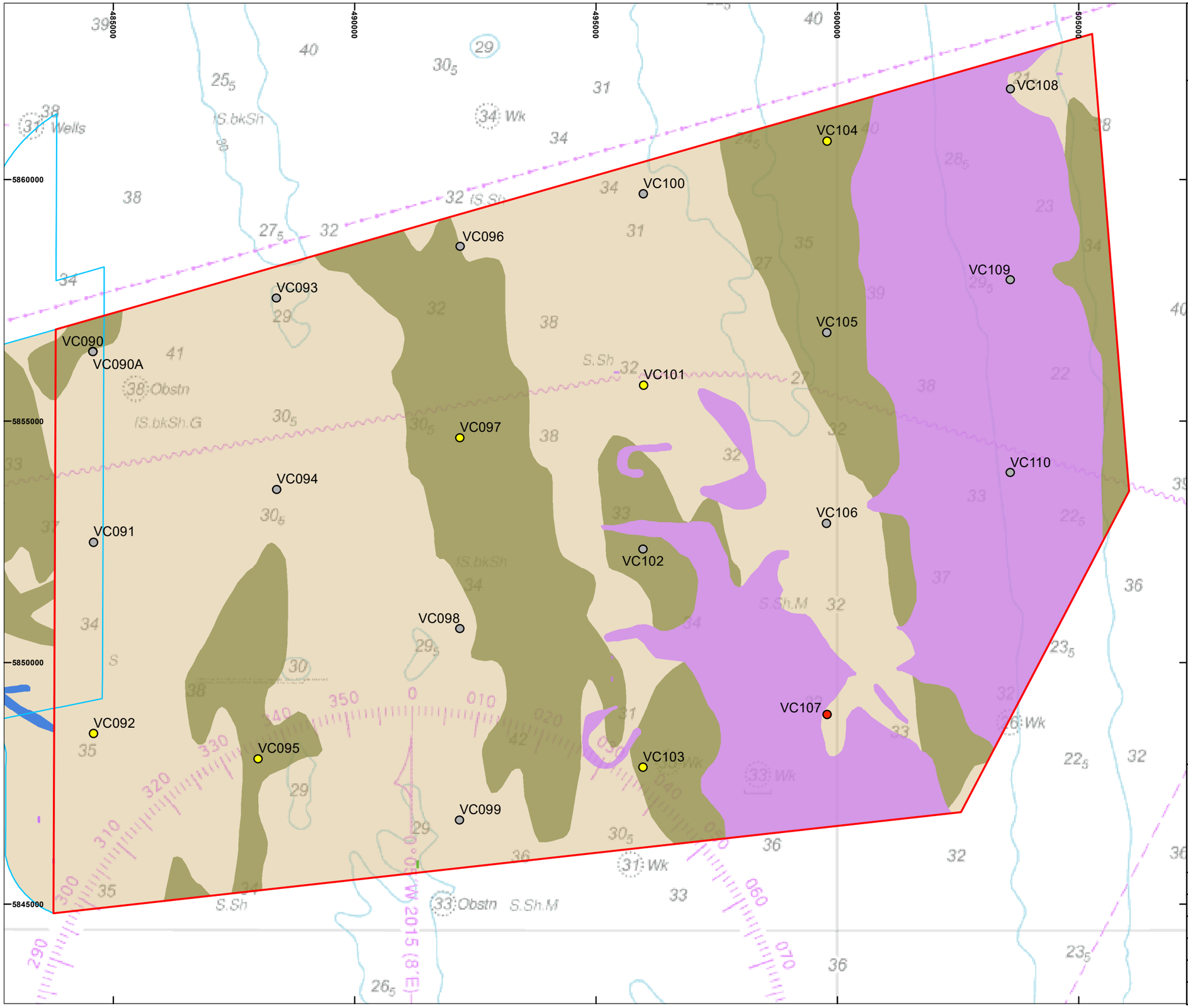

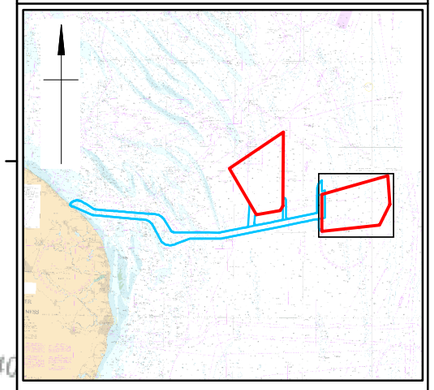

Geoarchaeology assessment stage of vibrocores

- 1
- 2
- 3

Norfolk Vanguard Offshore Cable Corridor

Norfolk Vanguard

Deposits of archaeological interest

- Holocene (Pre-Transgression), Channel
- Devensian, Acoustic Blanking
- Ipswichian or Devensian, Infilled Depression
- Pre-Anglian, High Amplitude Reflector
- Brown Bank Formation extents

0 2.5 km

Coordinate system:
ETRS1989 UTM Z31N

Date:	20/04/2018
Revision Number:	0
Scale:	1:80,000 at A3
Illustrator:	KJF/ND
Path:	X:\PROJECTS\114843\GIS\
FigsMXD\2018_04_20\114843_Geoarch_Fig03.mxd	

Norfolk Vanguard East, geophysics and borehole location (interpretative geophysics after Wessex Archaeology, 2017b)

Figure 3

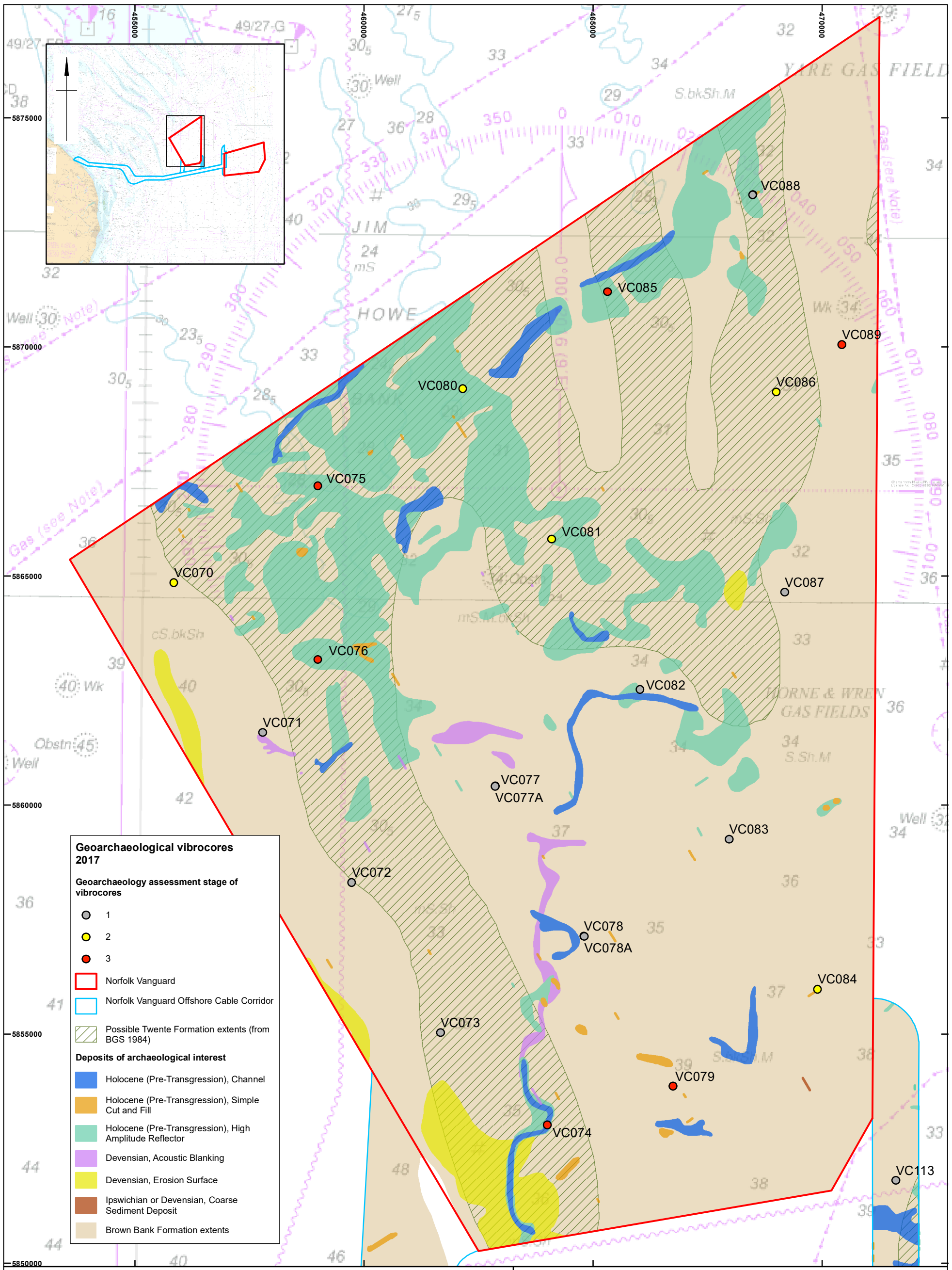

Date:	20/04/2018	Revision Number:	0
Scale:	1:80,000 at A3	Illustrator:	KJF/ND
Path:	X:\PROJECTS\114843\GIS\FigsMXD\2018_04_20\114843_Geoarch_Fig04.mxd		

Norfolk Vanguard West, geophysics and borehole location (interpretative geophysics after Wessex Archaeology, 2017b)

Figure 4

Wessex Archaeology Ltd registered office Portway House, Old Sarum Park, Salisbury, Wiltshire SP4 6EB
Tel: 01722 326867 Fax: 01722 337562 info@wessexarch.co.uk www.wessexarch.co.uk

FS 606559